

Distribution Agreement

In presenting this thesis or dissertation as a partial fulfillment of the requirements for an advanced degree from Emory University, I hereby grant to Emory University and its agents the non-exclusive license to archive, make accessible, and display my thesis or dissertation in whole or in part in all forms of media, now or hereafter known, including display on the world wide web. I understand that I may select some access restrictions as part of the online submission of this thesis or dissertation. I retain all ownership rights to the copyright of the thesis or dissertation. I also retain the right to use in future works (such as articles or books) all or part of this thesis or dissertation.

Signature :

Jamie A.G. Hamilton

Date

Delineating How Aging- and Obesity-Associated Chronic Inflammation Impacts B-cell
Acute Lymphoblastic Leukemia Progression

By

Jamie A.G. Hamilton
Doctor of Philosophy

Graduate Division of Biological and Biomedical Sciences
Cancer Biology

Curtis J. Henry, PhD
Advisor

Christopher C. Porter, M.D.
Committee Member

Malathy Shanmugam, PhD, MS
Committee Member

Jessica Alvarez, PhD, RD
Committee Member

Gregory B. Lesinski, PhD, MPH
Committee Member

Accepted:

Kimberly Jacob Arriola, Ph.D. MPH
Dean of the James T. Laney School of Graduate Studies

Date

Delineating How Aging- and Obesity-Associated Chronic Inflammation Impacts B-cell
Acute Lymphoblastic Leukemia Progression

By

Jamie A.G. Hamilton
BS, Florida A&M University, 2017

Advisor: Curtis J. Henry, PhD

An abstract of

A dissertation submitted to the faculty of the
James T. Laney School of Graduate Studies of Emory University
in partial fulfillment of the requirements for the degree of
Doctor of Philosophy
in
Graduate Division of Biological and Biomedical Sciences
Cancer Biology
2022

Abstract

Delineating how Aging- and Obesity-associated Chronic Inflammation Impacts B-cell acute lymphoblastic leukemia Progression
By Jamie A.G. Hamilton

Acute lymphoblastic leukemia (**ALL**) is a blood cancer derived from an overabundance of immature lymphocytes. Leukemia is classified based on the lymphocyte that transforms, such as B-cells or T-cells. B-cell malignancies are the most common cancer in children, with B-cell acute lymphoblastic leukemia (**B-ALL**) **accounting for 80% of all ALL**. Currently, survival outcomes for patients with B-ALL exceed 80%; however, in patients with relapsed or refractory disease, survival outcomes are significantly lower. Furthermore, comorbidities, like advanced age or obesity, are reported to decrease survival outcomes. Both conditions are associated with a loss of immunological homeostasis with the hallmark induction of chronic inflammation. In this dissertation, I present my results demonstrating that targeting the inflammatory microenvironment improves the efficacy of chemotherapies and immunotherapies in aged and obese settings of B-ALL.

In the context of obesity, I discovered that the cytokine interleukin-9 (**IL-9**), **which has mainly been studied in the context of allergic reactions**, is secreted by murine and human adipocytes. Furthermore, as reported in other hematological malignancies, I discovered that IL-9 drives B-ALL progression by decreasing the pro-apoptotic mediator BIM. Notably, I also discovered that circulating IL-9 levels positively correlates with BMI in pediatric patients with B-ALL. In addition to IL-9 impacting B-ALL progression, in the context of aging, I found that aging-associated reductions in interleukin-37 (**IL-37**) levels were associated with reduced T-cell mediated immunosurveillance of B-ALL cells. Furthermore, I found that elevating IL-37 levels in aged backgrounds, improved T-cell. Mechanistically, this effect was achieved by decreasing elevated homeostatic NF- κ B levels in aged T-cells. In xenograft models of B-ALL, in which aged mice were treated with aged chimeric antigen receptor (**CAR**) T-cells generated from a 67-year-old donor; aged mice with the longest survival outcomes were those that received the combination of recombinant IL-37 and CAR T-cell therapy.

Collectively, my studies demonstrate that aging and obesity impacts B-ALL progression, in part, by altering immunological homeostasis. Furthermore, I present data demonstrating that targeting or resupplying pro-inflammatory or anti-inflammatory cytokines, respectively, has therapeutic potential and should be considered for further exploration as novel therapeutic option for hematological malignancies in patients with underlying comorbidities.

Delineating How Aging- and Obesity-Associated Chronic Inflammation Impacts B-cell
Acute Lymphoblastic Leukemia Progression

By

Jamie A.G. Hamilton
BS, Florida A&M University, 2017

Advisor: Curtis J. Henry, PhD

A dissertation submitted to the faculty of the
James T. Laney School of Graduate Studies of Emory University
in partial fulfillment of the requirements for the degree of
Doctor of Philosophy
in
Graduate Division of Biological and Biomedical Sciences
Cancer Biology
2022

Acknowledgments

“Remember where you came from and remember who you represent.”

-William Willard Brown, Beloved Grandfather

Firstly, I would like to thank God for guiding me to complete this PhD program.

Thank you to my parents, Jamie Lavelle Hamilton, and Krista Brown Hamilton, for your constant love, support, and encouragement in the face of challenging odds. From little puddles in parking lots to school science fairs, you both have always championed curiosity and hard work. The person I am today, stands on a foundation built with your help and guidance.

Thank you to my grandparents, Verna Hamilton, Jessie Hamilton, Ora Haynes Brown and the late William Brown. There is no love like a grandparent's love- and through the highs and lows of my life you have always been there. Thank you, I will always love you.

Thank you to my little sisters, Alexis Hamilton & Kennedy Hamilton, who inspire me every day with their fearless determination and passion for growth. Throughout this process, the two of you were always there, and I am forever grateful to be your big brother.

Thank you to my family both near and extended. Auntie Chris, Auntie Kim, Aunt Estella, Uncle Zach, Uncle Richard, Uncle Kirk and every one of my beloved cousins. Your countless kind words and actions have culminated in a deep well of loving support that I pulled from in the darkest times of pursuing this PhD. I felt the love in every card, text, and thoughtful voicemail.

Thank you to Jadia Bullock, who's ambition, drive and determination are a constant source of inspiration. Your love, support and kindness are a clear light in a murky path.

A sincere thank you to my advisor, Curtis J. Henry who over the years has shown me how to grow as a scientist, as an individual and as a student. One of the best choices I made in the pursuit of my doctorate was to choose the Henry Lab to conduct my research.

Thank you to my beloved friends from childhood, Florida A&M University, and Emory University. The memories and bonds we created will always have a place in my heart.

I would also like to thank my dissertation committee, the Emory University Cancer Biology program, The American Society of Hematology, Laney EDGE, Emory Biotech Consulting Club and FGLSAMP whose feedback, financial support and career guidance made the research presented in this dissertation possible.

Your words, actions, support will not be forgotten, thank you from the bottom of my heart.

<u>Table of Contents</u>	Page Number
<u>Chapter 1: Introduction</u>	1
1.1 Overview	2
a. Aging	4
b. Obesity	
c. Aging, Obesity & Cancer Progression	6
1.2 B-ALL Overview	9
a. Patient Demographics	
b. Disease Mechanism	10
c. Chemotherapy Treatments	12
1.3 Immunotherapy in B-ALL	13
a. Blinatumomab	13
b. CAR-T cell therapy	15
c. Neutralizing Antibodies	18
d. Checkpoint Inhibitors	19
1.4 Challenges to B-cell Immunotherapy	21
a. Immunosuppressive tumor microenvironment	21
b. T-cell exhaustion & Summary of Introduction	23
<u>Chapter 2: Utilizing Interleukin-37 treatment to boost anti-leukemia mediated immunity in aged background</u>	25
2.1 Abstract	26
2.2 Introduction	27
2.3 Materials & Methods	30
2.4 Results	34
2.5 Discussion	45
2.6 Figures, Supplemental Figures & Tables	51
<u>Chapter 3: Adipocyte-secreted Interleukin-9 Promotes B-cell Acute Lymphoblastic Leukemia Progression</u>	68
3.1 Abstract	69
3.2 Introduction	70
3.3 Materials & Methods	72
3.4 Results	77
3.5 Discussion	84
3.6 Figures, Supplemental Figures & Tables	87
<u>Chapter 4: Discussion</u>	98
4.1 Summary and implications of results	99
4.2 Limitations and Future Directions	101

<u>Figures</u>	<u>Page Number</u>
Figure 1: Aging is associated with a loss of immune homeostasis that contributes to various aging-associated pathologies	3
Figure 2: Obesity is associated with an increase in adipose tissue that contributes to chronic inflammation, poor immune cell function, and increased risk of cancer development.	5
Figure 3: 13 Cancers that are associated with being overweight and obese.	7
Figure 4: Mechanisms leading to development of B-ALL.	11
Figure 5: Mechanism of action of Blinatumomab in CD19+ B-ALL	14
Figure 6: Overview on workflow for CAR T-cell therapy	16
Figure 7: Mechanism's cancer cells utilize to evade CAR T-cells	17
Figure 8: Mechanism of action of anti PD-1 antibody, an immune checkpoint inhibitor	20
Figure 9: Major cell types contributing to the immunosuppressive tumor microenvironment	22
Figure 10: Mechanisms that can drive T cells to the exhausted phenotype	24
Figure 11: Interleukin-37 suppresses inflammaging, and decreased levels are observed in aged human monocytes	51
Figure 12: Interleukin-37 restores a youthful gene expression profile in aged T-cells.	52

Figure 13: Recombinant IL-37 treatment reduces PD-1 surface expression and improves the function of aged T-cells	53
Figure 14: Recombinant IL-37 treatment opposes TNF- α signaling in aged T-cells.	54
Figure 15: Recombinant IL-37 treatment protects aged mice from B-ALL pathogenesis in a T-cell dependent manner.	55
Figure 16: Recombinant IL-37 Treatment Improves the Efficacy of Aged CAR T-cells.	56
Figure 17: Interleukin-9 is secreted by adipocytes and is elevated in obese mice.	87
Figure 18: Interleukin-9 Receptor is expressed on human B-ALL cells and is upregulated in adipocyte secretome.	88
Figure 19: Interleukin-9 induces proliferation in human B-ALL cells.	89
Figure 20: Interleukin-9 protects human B-ALL cells from chemotherapy-mediated cytotoxicity.	90
Figure 21: Interleukin-9 promotes B-ALL progression.	91
Figure 22: Interleukin-9 plasma levels are positively correlated with BMI in patients with B-ALL	92

Chapter 1: Introduction

Portions of this chapter are published in **Hamilton J**, Henry C, Aging and immunotherapies: New horizons for the golden ages. *Aging and Cancer*. 2020 September 30. PMID 35874875

1.1 Overview of Aging & Obesity

a. Aging

The world's elderly population, those older than 65, is projected to grow to 1.6 billion individuals in the next three decades[1]. By 2035, a “silver tsunami” is expected to occur in the United States, with the number of Americans 65 and older predicted to surpass those 18 and younger[2]. This exceptional feat is in part attributed to the development of vaccines and antibiotics, which has increased the number of children surviving deadly childhood diseases such as polio, smallpox, measles, and pneumonia[3, 4] converging with declining birth rates. Other modern advances, such as a better understanding of nutrition, the implementation of routine exercise, more stringent clean water standards, and improvements in sewage treatment have also significantly contributed to extending the global life expectancy[5, 6].

One hallmark of aging is immunological decline, known as immunosenescence, which is documented in most vertebrates including mice and humans (**Figure 1**). This change in the immunological landscape is pleiotropic, marked by attenuated immune responses in T cells (CD4⁺ T-helper cells and CD8⁺ cytotoxic T cells), B cells, and innate immune cells such as dendritic cells (DCs), macrophages, and neutrophils[7]. The decline in immunological integrity in elderly individuals increases their risk of infection, attenuates vaccine responses, and compromises tumor surveillance mechanisms, which increases their chances of developing cancer[7-10]. In this thesis we define novel roles for cytokines deregulated in the aged microenvironment and demonstrate how targeting these factors improve the efficacy of immunotherapies imaged models of B-ALL.

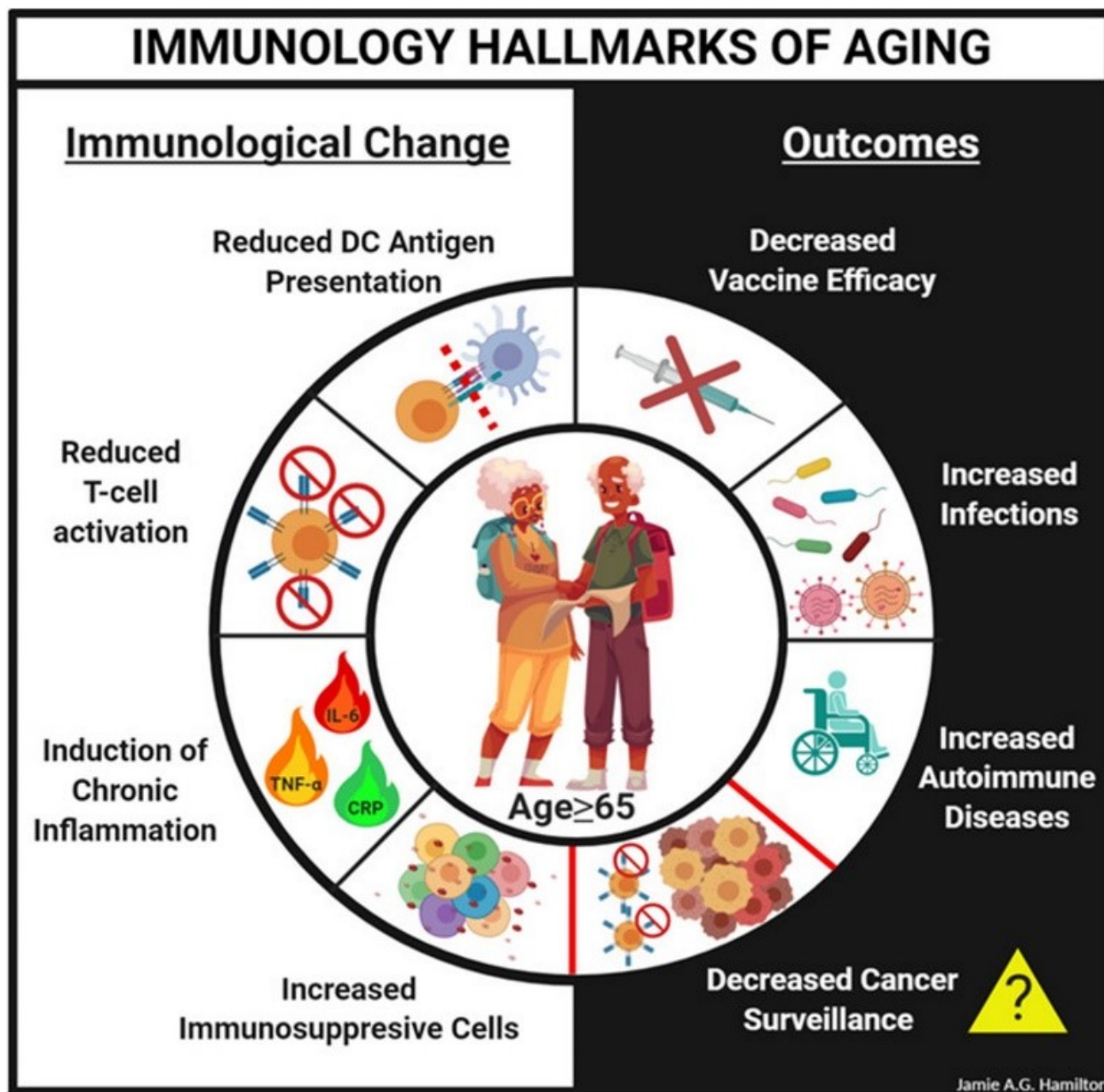


FIGURE 1: Aging is associated with a loss of immune homeostasis that contributes to various aging-associated pathologies

b. Obesity

The Center for Disease Control and Prevention (CDC) reports that obesity rates in children and adolescents have more than tripled since the 1970's [11] By 2030, adult obesity rates are projected to rise to 38% globally and 85% of the United States[12]. Obesity is associated with an increased risk for coronary heart disease, high blood pressure, insulin resistance and cancer development[13, 14]. Considering the consistent growth of this demographic in children and adults, delineating the molecular phenotypes that drive and impact obesity is of vital importance.

Obesity is broadly characterized by a global increase in adipose tissue, chronic inflammation, insulin resistance and immune dysfunction (**Figure 2**)[15, 16]. Adipose tissue, once considered an inert tissue, is now studied as an endocrine organ responsible for secreting several pro-inflammatory cytokines and chemokines including IL-1, IL-6, TNF- α , and CXCL5[15, 17]. Furthermore, adipocytes can recruit proinflammatory macrophages(M1), plasmacytoid dendritic cells and B-cells[18-20]. Given these findings, one aim of this thesis was to delineate the relationship between obesity, adipokines, and B-ALL progression.

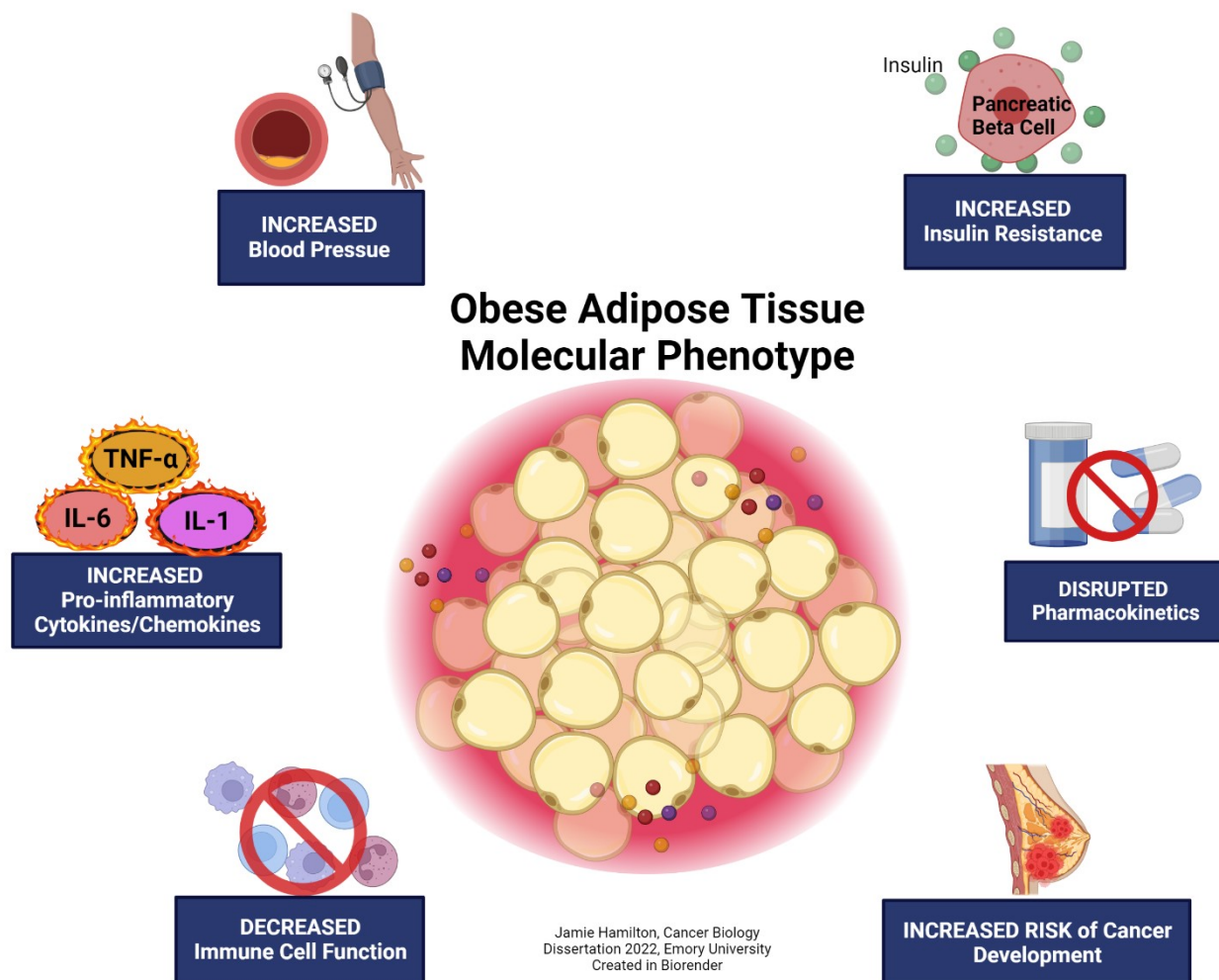


FIGURE 2: Obesity is associated with an increase in adipose tissue that contributes to chronic inflammation, poor immune cell function, and increased risk of cancer development.

c. Aging, Obesity & Cancer Progression

Aging is the greatest prognostic factor for developing cancer with 60% of new cancer diagnoses being made in adults aged 65 and older, and 70% of cancer deaths occurring in this population[21-23]. The failure to achieve durable responses in elderly patients is multifactorial, and one of the barriers to success is the lack of aging-related research and clinical trials that include aged patients[24, 25]. For instance, between 2007 and 2018, an average of 40% of patients 65 and older were enrolled in clinical trials, despite constituting 60% of all patients with cancer[26, 27]. Additionally, safety and efficacy information were only reported in 42% and 45% of initial approval documents available in the FDA database for approved drugs [26]. Furthermore, the inconsistent recruitment of elderly patients in clinical trials has led to the development of treatments mainly in younger, healthier patients who typically have different biological and physiological responses[26].

In addition to poor enrollment in clinical trials, the lack of preclinical studies conducted in aged animal models have further hampered the development of efficacious and safe drugs for aged patients[28, 29]. In the limited studies that have been conducted using aged mice and humans, it is consistently documented that aging alters the pharmacodynamics and pharmacokinetics of chemotherapies[30, 31]. A common manifestation of altered drug metabolism in aged patients is increased drug-induced toxicity, which often limits the dosage of chemotherapies that can be safely administered to elderly patients[32-34]. Due to the reduced efficacy of chemotherapies in aged patients, there is increased interest in identifying novel therapies that can be used to effectively treat aging-associated cancers without accompanying toxicities.

13 cancers are associated with overweight and obesity

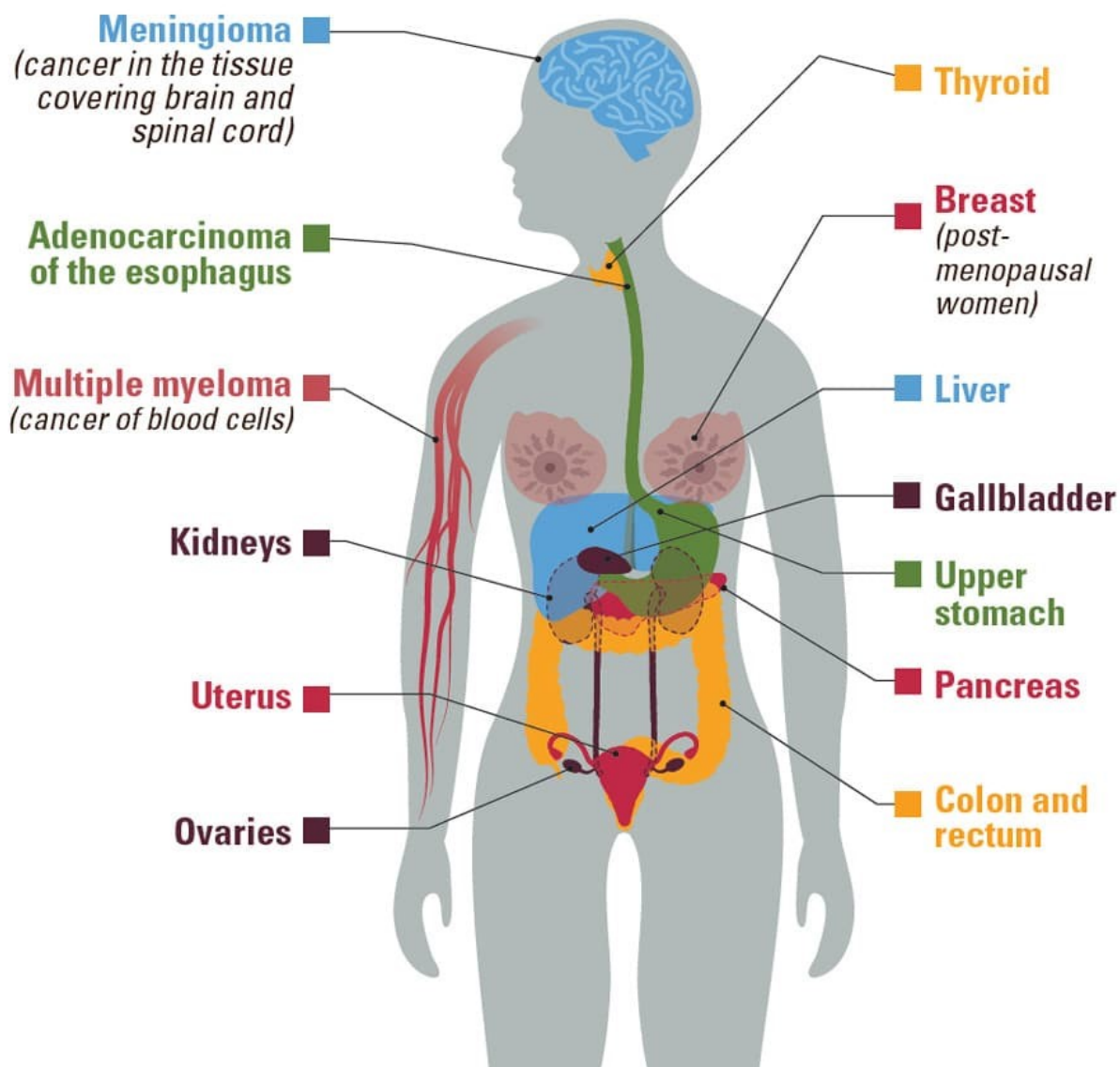


FIGURE 3: 13 Cancers that are associated with being overweight and obese.
 (Image from Center for Disease Control, <https://www.cdc.gov/cancer/obesity/index.htm>, Site visited August 2022)

Aging, Obesity & Cancer Progression Continued:

Obesity is associated with several cancer types, thought to be related to the high levels of chronic inflammation and hormonal imbalances in patients with obesity (**Figure 3**). The high levels of chronic inflammation found in patients with obesity have been correlated with high levels of reactive oxidative species and this oxidative stress oxidative radicals can damage DNA and promote oncogenesis [35, 36]. The source of this inflammatory environment are the pro-inflammatory adipocytes, which are found at significantly higher levels in obese individuals compared to lean individuals [37, 38] The molecular understanding of how adipocytes promote cancer progression follows three current theories: adipocytes are feeding the cancer cells with lipids and proliferation inducing cytokines, adipocytes are limiting chemotherapy uptake in cancer cells, and adipocytes are initiating oncogenesis. Future studies in the coming decades will seek to delineate the precise mechanisms by which obesity is able to promote cancer.

1.2 B-cell acute lymphoblastic leukemia

a. Patient Demographics

Acute lymphoblastic leukemia (ALL) is the most common cancer in children, making up 28% of all pediatric cancers[39]. In 2022, the estimated new cases of adult acute lymphoblastic leukemia comprised 3-4% of adult cancer cases[39]. According to the U.S. Center for Disease Control (CDC) pediatric ALL has an incidence of 75.2 in 1million. ALL is classified based on the malignant lymphocytes population that has transformed, T-cells or B-cells [40].

Within this dissertation we will focus on B-cell acute lymphoblastic leukemia (B-ALL), which is the most common of the ALL subtypes within both pediatric and adult populations [41, 42]. B-ALL can be further classified based on the mutational status of the lymphocytes, which will be explored in the next section, the expression of each subtype varies widely[42, 43]. The global annual incidence of B-ALL is estimated to be 1-5 per of 100,000 individuals[44]. The most common subtypes of pediatric B-ALL include several chromosomal abnormalities (ETV6-RUNX1, Hyperdiploidy, TCF3-PBX1 and BCR-ABL1-like)[45, 46].

b. Disease mechanisms/Driver mutations

The symptoms of ALL can include frequent infections, fever, spontaneous bruising, fatigue and weight loss [40]. Diagnosis of ALL occurs through blood smears to deduce morphology, immunophenotyping, cytogenetics and PCR for driver mutations[47]. The primary causes of death from leukemia, if the disease is not successfully treated include infection, hemorrhage, and organ failure [48]. It should be noted that leukemia has an increased rate of survival compared to most other cancer types, however there are aggressive subtypes that require further study to develop effective treatments given that event free survival rates for Ph-like and Infant-ALL, are 63% and 47% respectively [41, 49-51].

B-cell acute lymphoblastic leukemia is characterized by an abundance of malignant B-cells, which contain a variety of driver mutations. The evidence of what initiates oncogenesis of B-ALL is limited, currently it is theorized to begin in a germline mutation or exogenous oncogenic insult such as ionizing radiation, pesticides, and cigarette smoking [52-55]. **Figure 4** highlights the different mechanisms that can lead to the development of B-ALL. The common driver mutations of ALL include Hyperdiploid, TCF-PBX1, ETV6-RUNX1, Ph-like, Ph positive, DUX4/ERG and MLL rearrangement[41, 53]. These mutations promote constitutive signaling of RAS, JAK-STAT, ABL, PI3K/mTOR and other proliferation and survival factors [46, 53].

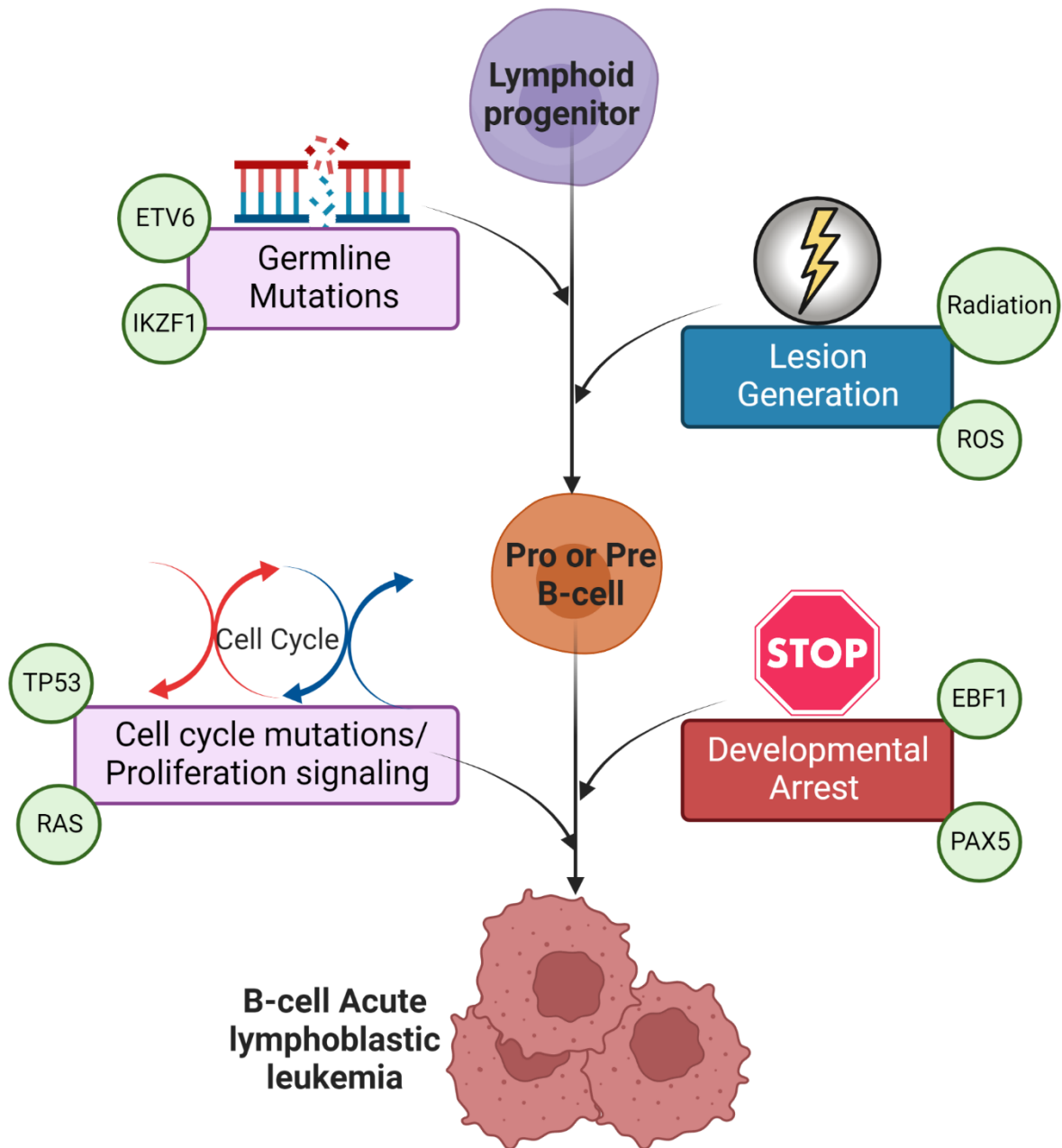


FIGURE 4: Mechanisms leading to development of B-ALL.

c. Chemotherapy treatments

Treatment of B-ALL consist of three stages: induction, consolidation, and maintenance. The current frontline therapies include methotrexate, doxorubicin or daunorubicin, vincristine, L-asparaginase, and corticosteroids[41]. These cytotoxic therapies are used at different stages of treatment depending on response, cancer stage and dosing schedule. These therapies are effective during induction stages and consolidation however less than 50% of adult patients can achieve long term remission [41, 56].

Methotrexate, a folate antagonist directly targets rapidly proliferating cells by inhibiting the enzyme dihydrofolate reductase from synthesizing folate, a necessary component for DNA synthesis [57]. Methotrexate treatment is utilized throughout the consolidation, and maintenance phases of B-ALL [58-60]. Doxorubicin, an anthracycline drug that intercalates into DNA- thereby disrupting DNA replication [61]. Vincristine, a vinca alkaloid that obstructs the microtubules during the M-phase of the cell cycle thereby inducing mitotic catastrophe [62]. These treatments, while often effective in initiating the remission of B-ALL, should be noted to have numerous toxicities. Notably, vincristine induces severe side effects including cardiovascular toxicity, bone marrow depression and peripheral neuropathy [63, 64]. Considering these complications, the field of immunotherapy has seen a significant rise in interest, with the hopes of developing a less toxic and more personalized treatment.

1.3 Immunotherapy in B-ALL

a. Blinatumomab

The immunotherapy Blinatumomab was the first in class bispecific T-cell engager approved to treatment in the United States. This therapy has been found to be efficacious for B-ALL patients, inducing those with minimal residual disease[65]. This bispecific antibody binds to both CD19 on B-cells and CD3 on T-cells, creating a cytolytic synapse resulting in T-cell activation, proliferation and release of cytotoxic granules eliminating the bound CD19+ cell (**Figure 5**) [66, 67] A major advantage of this therapy includes the ability to have low doses still be effective leading to less toxic side effects, however if a cancer cell has reduced levels of CD19 this therapy will not be as effective [68, 69].

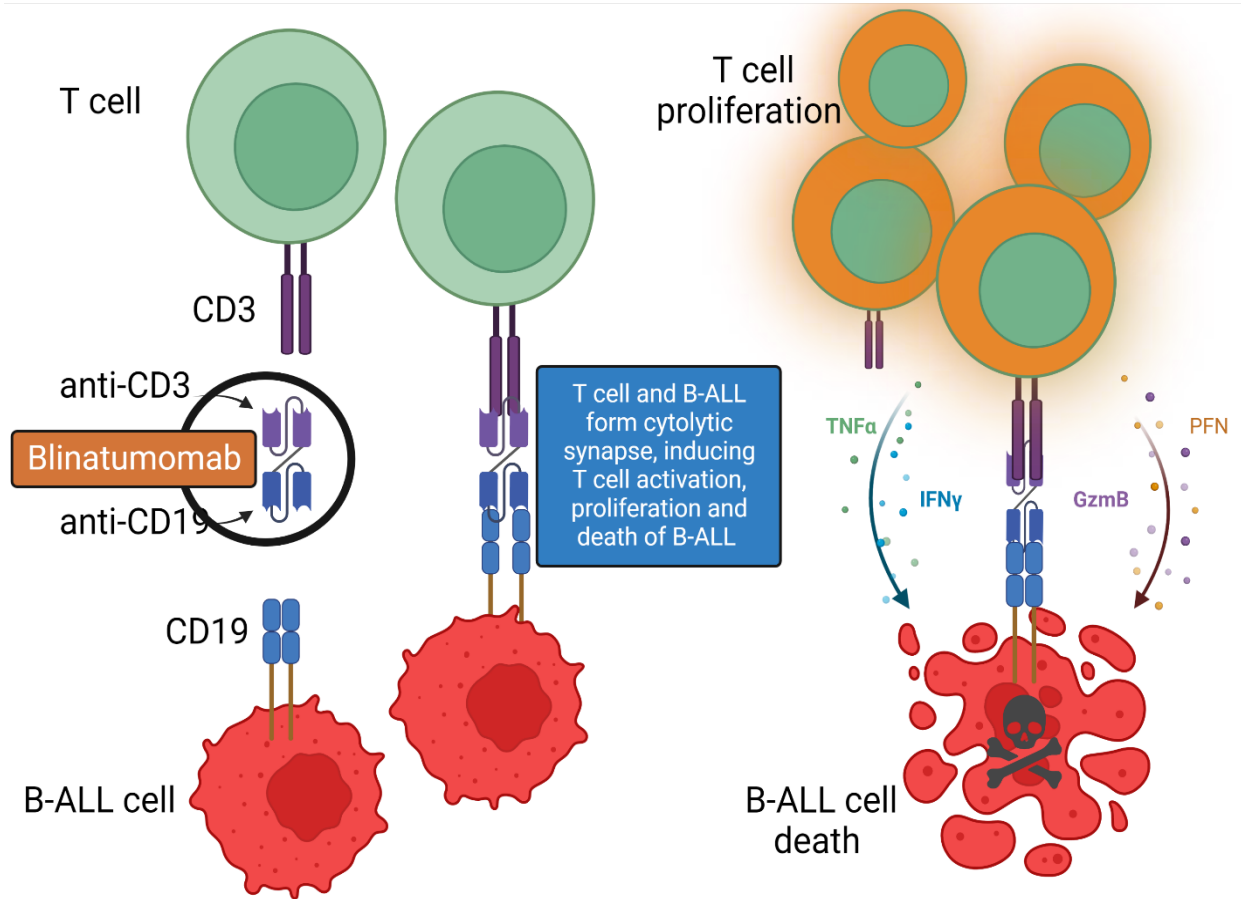


Figure 5: Mechanism of action of Blinatumomab in CD19+ B-ALL

b. CAR T-cell therapy

CAR T-cell therapy is viewed as one of the largest revolutions in the field of immunotherapy to date[70, 71]. Chimeric antigen receptor (CAR) therapy operates on the following principle: removal of patient T-cells, insertion of the CAR gene into the exogenous T-cells, grow these engineered CAR T-cells and inject them back in the patient with the ability to recognize and fight the cancer (**Figure 6**)[70, 72]. The greatest benefit to this system is the interchangeability of the gene that inserted, CD-19 CARs were the first developed and approved in 2017, however every year new targets are being developed in order to get around the different known evasion mechanisms (**Figure 7**)[73]. There are several limitations of CAR T-cell therapy: the process of growing exogenous CAR T-cells is a novel challenge for the biomanufacturing industry, low surface target expression, cytokine release syndrome and the current price of production[73, 74]. While this therapy has potential to revolutionize the field of immunotherapy, these are significant barriers that must be overcome to realize the potential of CAR T-cell therapy.

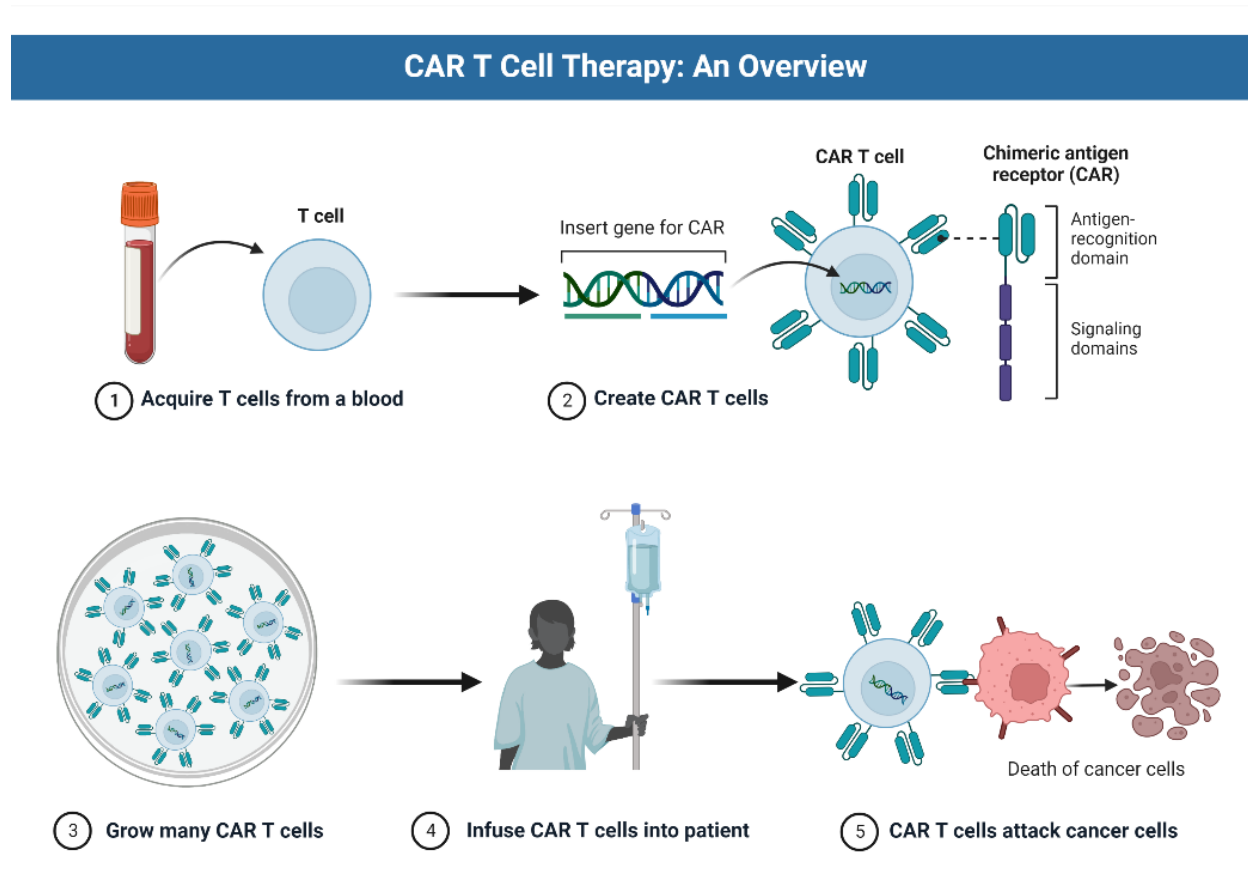


Figure 6: Overview on workflow for CAR T-cell therapy (Created by Biorender)

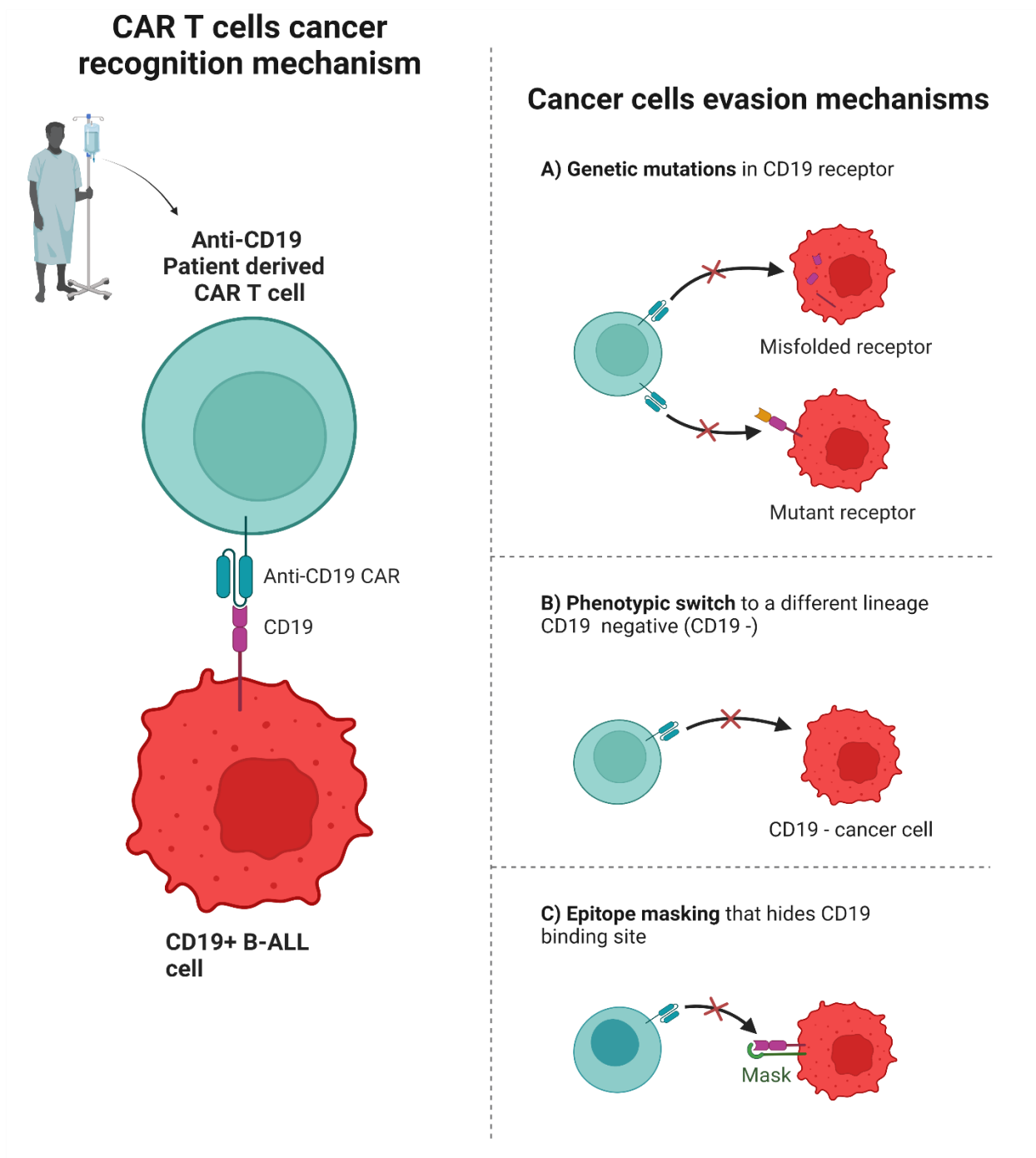


Figure 7: Mechanism's cancer cells utilize to evade CAR T-cells
(Based on Biorender Template)

c. Neutralizing Antibodies

The utilization of antibodies against leukemia surface targets can induce cell death via a variety of pathways[75]. In acute lymphoblastic leukemia, among the most frequent targets are CD19, CD20 and CD52 [76, 77] Antibodies targeting these markers are sometimes used in combination (antibody-drug conjugates, ADCs) with the aforementioned chemotherapies in B-ALL treatment. The use of high-throughput screens has made finding the optimal ADC for B-cell malignancies a distinct possibility in the coming years[78].

Rituximab, an anti-CD20 monoclonal antibody has been proven to be effective alone and in combination with chemotherapy protocols for B-cell malignancies, including Ph-negative B-ALL [79-81]. Rituximab mediated cell death is thought to be driven by two broad pathways: initiation of complement cascade, natural killer cells binding to induce antibody dependent cellular cytotoxicity (ADCC), or crosslinking of rituximab and CD20 in a lipid raft leading to apoptosis [80].

Inotuzumab, is a humanized anti-CD22 directed monoclonal antibody conjugated with a cytotoxic agent such as calicheamicin[82]. Upon binding the antibody-drug conjugate will enter the lysosome, activate, and bind to DNA where it will induce cell death. This therapy is effective across B-cell malignancies, notably B-ALL, due to greater than 90% of B-ALL cells expressing CD22 but low expression in non-malignant B-cells[83, 84].

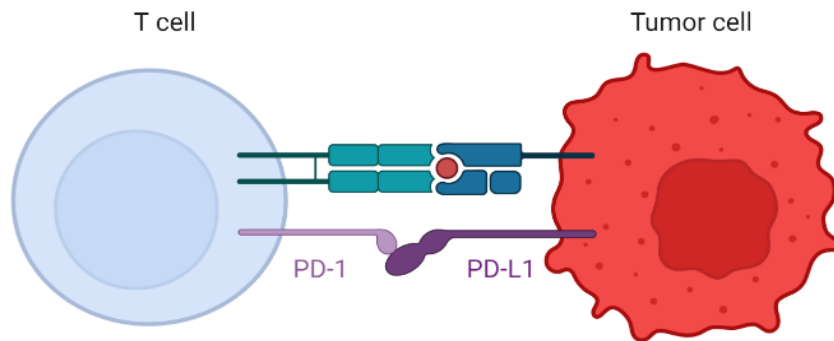
Neutralizing antibodies remain a cost-effective, and biologically effective method to treat many cancers. Further development of novel antibody-drug conjugates will allow for this form of immunotherapy to continue to develop and grow.

d. Checkpoint inhibitors

An immune checkpoint is a molecule that acts to prevent an immune response from being so strong that it begins to destroy the body[85]. These surface proteins will interact with T-cells to deactivate the cytotoxic T-cells, thereby preventing the T-cell from harming the body[86, 87]. Cancer cells commonly utilize immune checkpoint proteins in order to prevent the cytotoxic T-cells from destroying the cancer[88, 89]. This immune evasion is a common pathway to resurgence of disease after the initial rounds of chemotherapy treatment[85, 86].

In order to inhibit the immune evasion of cancer cells, immune checkpoint inhibitors (ICI) were developed[90]. PD-1, PDL-1, and CTLA-4 inhibitors are the current targets of most approved immune checkpoint inhibitors for solid cancers. Upon binding of an inhibitor, the T-cell is now free to engage the cancer cell inducing cell death (**Figure 8**).

Immune checkpoint inhibits T-cell activation



Anti-PD-1 antibodies permit T cell activation

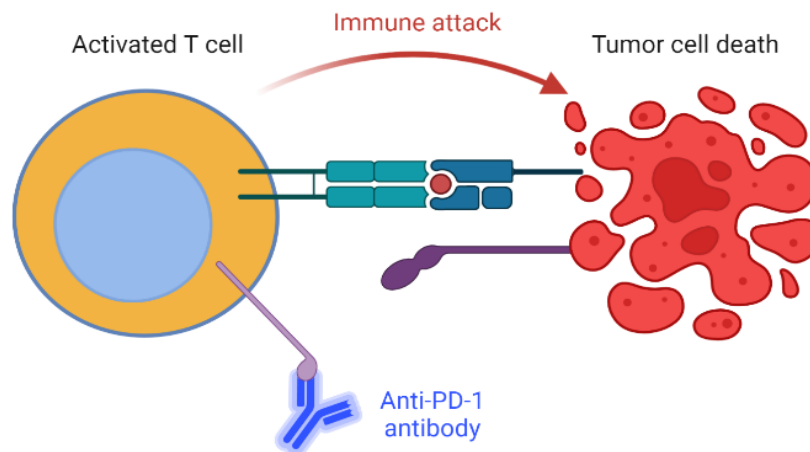


Figure 8: Mechanism of action of anti PD-1 antibody, an immune checkpoint inhibitor. (Created using a Biorender Template)

1.4 Challenges to B-cell Immunotherapy

a. Immunosuppressive tumor microenvironment

In the past, tumors were studied in isolation or in the context of one or two cell types. However, recent studies have highlighted the ability of the tumor microenvironment to promote cancer progression and to inhibit anti-tumor immunity[91]. This immunosuppressive tumor microenvironment serves as a challenging barrier for immunotherapies to overcome. This microenvironment is comprised of immune cells, tumor cells and stromal cells that all work to inhibit the immune response and shift the immune axis towards the survival of the cancer cells (**Figure 9**). This environment disrupts the ability of immune checkpoint inhibitors and cell therapies from reaching the cancer and being effective against the cancer cells[92-96]. Overcoming the immunosuppressive environment, is important for the development of the next generation of immunotherapies.

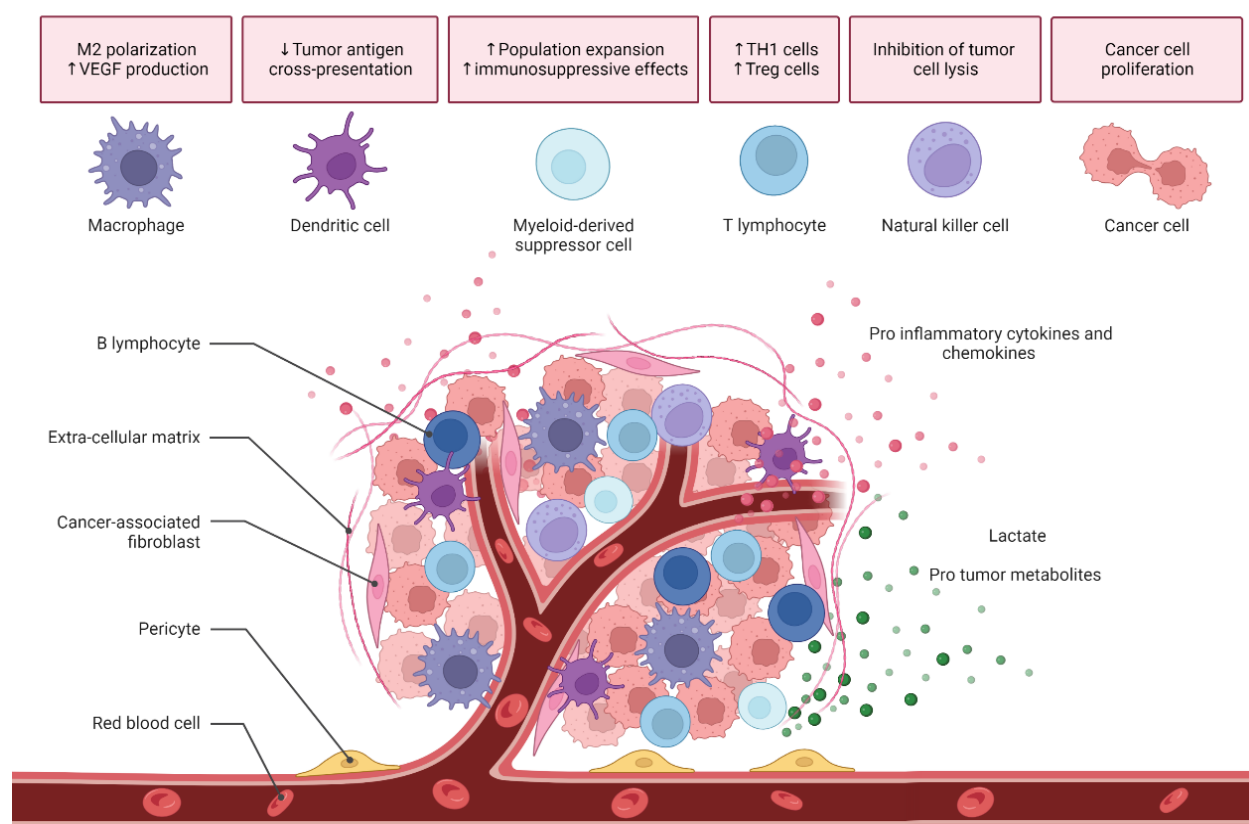


Figure 9: Major cell types contributing to the immunosuppressive tumor microenvironment. (Based on Biorender Template)

b. T-cell exhaustion

T-cells in cancer patients are in a biologically hostile environment, such as chronic infection or cancer, leading many of these cells to enter an exhausted state[97, 98]. This represents a challenge to the efficacy of immunotherapies. A chronically inflamed microenvironment can promote T-cell exhaustion, this state is a hallmark of aging and obesity[99, 100]. Furthermore, T-cell exhaustion can be induced by excessive antigen stimulation and coinhibitory signaling (**Figure10**) [97].

Summary of Introduction:

In summary, this information highlights the importance of our need to understand the impact of the microenvironment on cancer progression. This will be particularly important for susceptible populations, such as those with obesity or aged patients, given their poor outcomes to chemotherapy treatment and developing data for responses to immunotherapies. In the following chapter we will discuss results from my dissertation work which describes the role of IL-9 and IL-37 in B-ALL progression.

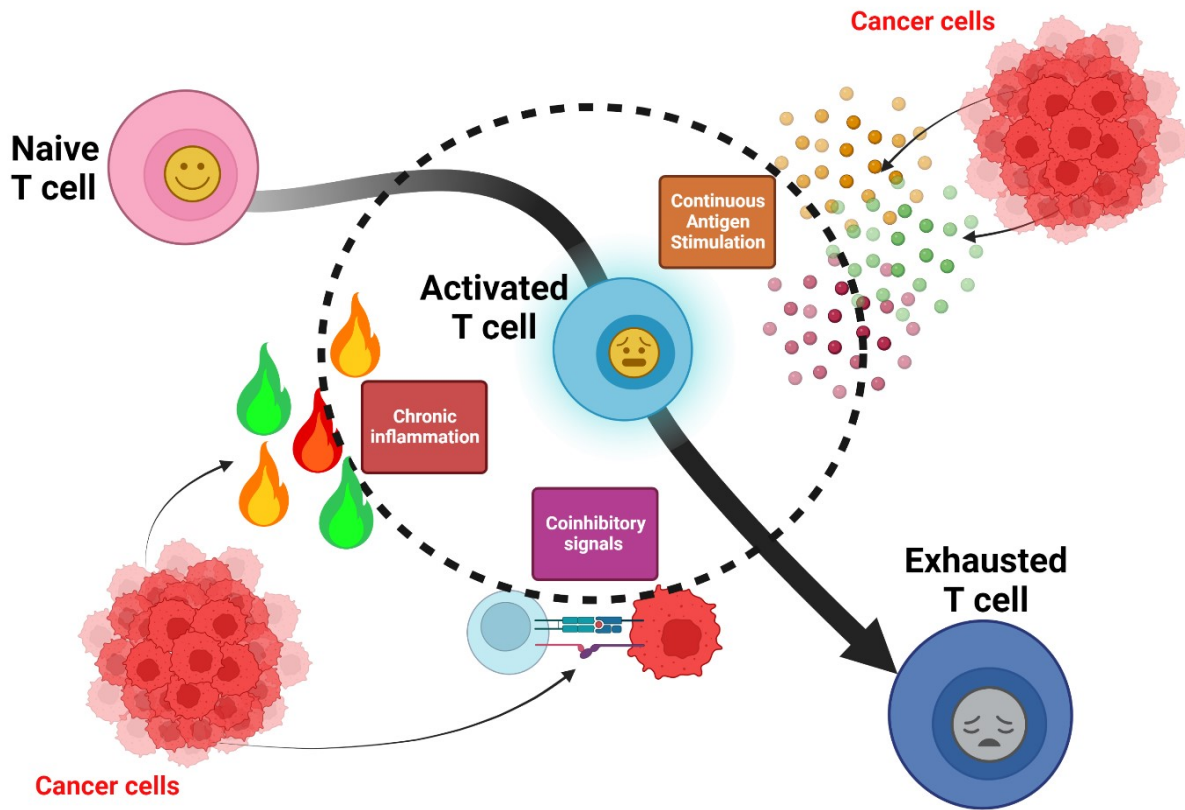


Figure 10: Mechanisms that can drive T cells to the exhausted phenotype

**Chapter 2: Utilizing IL-37 treatment to
boost anti-leukemia immunity in aged
backgrounds**

2.1 Abstract

Aging-associated declines in innate and adaptive immune responses are well documented and pose a risk for the growing aging population, which is predicted to comprise greater than 40 percent of the world's population by 2050. Efforts have been made to improve immunity in aged populations; however, safe, and effective protocols to accomplish this goal have not been universally established. Aging-associated chronic inflammation is postulated to compromise immunity in aged mice and humans. Interleukin-37 (IL-37) is a potent anti-inflammatory cytokine, and we present data demonstrating that IL-37 gene expression levels in human monocytes significantly decline with age. Furthermore, we demonstrate that transgenic expression of interleukin-37 (IL-37) in aged mice reduces or prevents aging-associated chronic inflammation, splenomegaly, and accumulation of myeloid cells (macrophages and dendritic cells) in the bone marrow and spleen. Additionally, we show that IL-37 expression decreases the surface expression of programmed cell death protein 1 (PD-1) and augments cytokine production from aged T-cells. Improved T-cell function coincided with a youthful restoration of *Pdcd1*, *Lat*, and *Stat4* gene expression levels in CD4⁺ T-cells and *Lat* in CD8⁺ T-cells when aged mice were treated with recombinant IL-37 (rIL-37) but not control immunoglobulin (Control Ig). Importantly, IL-37-mediated rejuvenation of aged endogenous T-cells was also observed in aged chimeric antigen receptor (CAR) T-cells, where improved function significantly extended the survival of mice transplanted with leukemia cells. Collectively, these data demonstrate the potency of IL-37 in boosting the function of aged T-cells and highlight its therapeutic potential to overcome aging-associated immunosenescence.

2.2 Introduction

Declining immunity is a hallmark of aging in mice and humans (Dorshkind et al., 2009; Henry et al., 2011). The effect of a waning immune response with age is thought to contribute to increased infection-related mortalities in the elderly, higher cancer incidence, and decreased vaccination efficacy, which all pose major obstacles for maintaining a healthy aged population (Dorshkind et al., 2009; Henry et al., 2011).

The causes underlying aging-associated immune impairments are under investigation with chronic inflammation being postulated as a major culprit responsible for compromising immunity and promoting aging-associated diseases (Ahmad et al., 2009; Franceschi & Campisi, 2014; Licastro et al., 2005; Lin & Karin, 2007). “Inflammaging” in mice and humans is characterized by a subclinical, systemic increase in pro-inflammatory cytokines including tumor necrosis factor-alpha (TNF- α), interleukin-6 (IL-6), interleukin-1 beta (IL-1 β), and C-reactive protein (CRP) (Franceschi & Campisi, 2014; Frasca & Blomberg, 2016; Meijas et al., 2018; Olivieri et al., 2018). Elevated levels of these inflammatory mediators have been shown to regulate the homeostasis and function of hematopoietic stem, progenitor, and mature immune cells, which express cytokine receptors that regulate their steady and activated states (de Bruin et al., 2013; Passegue & Ernst, 2009; Pronk et al., 2011; Qin et al., 2019; Sato et al., 2009; Schuettpelz & Link, 2013; Yamashita & Passegue, 2019). The impact of aging-associated immune senescence and chronic inflammation on the safety and efficacy of immune-based therapies has not been thoroughly investigated. Immunotherapies have revolutionized our ability to treat refractory and relapsed diseases (Bayraktar et al., 2019; Boettcher et al., 2019; Riker et al., 2007; Zhang & Chen, 2018). Antibody-mediated and chimeric antigen receptor (CAR) T-cell therapies have shown remarkable success in treating previously intractable

diseases such as melanoma (Riker et al., 2007). Immunotherapies are also frequently used to treat relapsed and refractory hematological malignancies including B-cell acute lymphoblastic leukemia (B-ALL) and diffuse large B-cell lymphoma (DLBCL) (Barsan et al., 2020; Davila & Brentjens, 2016; Jacoby et al., 2019; Pehlivan et al., 2018). Despite the success of immunotherapies in patients with terminal disease, over 50% of patients receiving CD19-directed CAR T-cell therapy will relapse within the first 2 years of receiving treatment, which is attributed, in part, to the loss of the target antigen on malignant cells (Cao et al., 2018; Cheng et al., 2019; Gardner et al., 2017; Lee et al., 2015; Li, Zhang, et al., 2018; Maude, Frey, et al., 2014; Maude et al., 2018; O'Donnell et al., 2019; Park et al., 2018; Song et al., 2019; Turtle et al., 2016). Other factors that may contribute to the efficacy of immunotherapies include the inflammatory status of the patient and inherent quality of the immune system, including T-cells.

We have previously demonstrated that the anti-inflammatory cytokine interleukin-37 (IL-37) reduces aging-associated inflammation and improves hematopoiesis in aged mice (Henry et al., 2015). There are over a dozen interleukin-1 (IL-1) family members that mainly act to promote inflammation (e.g., IL-1 α , IL-1 β , and IL-18). However, interleukin-37 (IL-37) is a relatively new family member capable of blocking the pro-inflammatory actions of IL-18 by competing for the IL-18 receptor (IL-18R α subunit) and attenuating MyD88 activity when it binds to the Ig-like Toll/IL-1R (TIR) receptor known as TIR8 (Dinarello et al., 2016; Eisenmesser et al., 2019; Nold et al., 2010). There are five different IL-37 splice variants encoded by humans (denoted IL-37a-e); however, IL-37b is the predominant form found in humans (Dinarello & Bufler, 2013; Dinarello et al., 2016). Thus, IL-37b is commonly referred to simply as IL-37 (Dinarello & Bufler, 2013). Messenger RNA (mRNA) for IL-37 has been found in various human tissues including the

bone marrow, lung, thymus, and lymph nodes and is produced by activated dendritic cells (DCs), natural killer (NK) cells, monocytes, and B-cells (Dinarello & Bufler, 2013). Studies performed in IL-37 transgenic (IL-37tg) mice reveal that IL-37 potently suppresses IL-6, IL-1 β , and TNF- α production in response to various TLR agonists or diseases driven by chronic inflammation including atherosclerosis, hepatocellular carcinoma, and colitis (Ji et al., 2017; Liu et al., 2016; Liu et al., 2018; McNamee et al., 2011; Nold et al., 2010; Zhao et al., 2014).

Given the close association of aging, declining immunity, and cancer development, in this study we determined how IL-37 impacted the function of aged endogenous and CAR T-cells. We demonstrate that transgenic expression of IL-37 in aged mice and treating aged mice with recombinant human IL-37 (rIL-37) improves the function of non-engineered and CAR T-cells. To the best of our knowledge, our results are the first to demonstrate that treating aged mice with rIL-37 restores the expression of key genes involved in T-cell activation which decline with normal aging and reduces the surface expression of multiple immunoinhibitory proteins on aged CD4⁺ and CD8⁺ T-cells to youthful levels. Furthermore, we demonstrate that IL-37 signaling directly opposes TNF- α signaling and downregulates PD-1 surface expression on aged T-cells. Additionally, rIL-37 treatment of aged mice augments cytokine production by endogenous T-cells, and when combined with CAR T-cell therapy, improves their therapeutic capacity in a murine model of B-ALL. Given our findings that the expression of the IL-37 gene decreases in an age-dependent manner in human monocytes, our results demonstrate that increasing circulating IL-37 levels in aged backgrounds may represent a novel strategy to overcome aging-associated T-cell senescence.

2.3 Materials & Methods

a. Mice

BALB/c and C57BL/6 mice of different ages were purchased from the National Institute of Aging (NIA) or the National Cancer Institute (NCI) and were used for all experiments in this study with the expectation of data presented in Figure 6c,d. Interleukin-37 (IL-37) transgenic mice were backcrossed onto a C57BL/6 background for more than 10 generations (Nold et al., 2010), and both transgene-positive and transgene-negative littermates were aged in-house. CIEA NOG immunodeficient mice (nomenclature: NOD.Cg- Prkdc^{scid}Il2rg^{tm1Sug}/ JicTac) were purchased from Taconic Biosciences and maintained inhouse. These mice were used for xenograft experiments presented in Figure 6 C, D. Female and male mice were used in these studies.

b. Cell lines

Human and murine B-cell acute lymphoblastic leukemia (B-ALL) cell lines were gifted from the laboratories of Dr. Douglas Graham and Dr. Christopher Porter (Department of Pediatrics; Emory University School of Medicine). Human B-ALL cells (REH) and murine B-ALL cells (GFP-expressing, BCR-ABL1+ /Arf-null) were grown in RPMI 1640 media supplemented with 20% FBS.

c. Construction of CD19-CAR

The sequence for the CD19-directed single chain variable fragment (scFv) was generated using the published anti-CD19 murine immunoglobulin protein sequence (FMC63) (Nicholson et al., 1997), and the cDNA sequence designed to express the scFv was codon optimized for optimal expression in human cells using the codon optimization tool from IDT (Coralville, IA). The C-terminus of VH was joined with the N-terminus of VL using a 15 bp linker encoding a glycine and serine pentapeptide

repeat (G4S)₃ (Huston et al., 1993). The gene block for the CD19 scFv cDNA sequence was created by Genewiz (South Plainfield, NJ). The CD19 scFv sequence was then cloned into the CAR of our cassette, which is a second-generation CAR consisting of the transmembrane and intracellular domains of CD28, and the intracellular signaling domain of CD3 ζ (Raikar et al., 2018). A CD8 hinge region connects the CD19 scFv to the CD28 domain. A bicistronic vector coexpressing eGFP and the CD19-CAR via a self-cleaving 2A peptide sequence (P2A) was used to enable identification of positively transduced cells by flow cytometry.

d. Endogenous T-cell assays

CD4⁺ or CD8⁺ T-cells were purified from aged mice using Magnetic-activated cell sorting (MACs) as described above. T-cells were stimulated ($10^4 - 5 \times 10^4$ cells/well) in 96-well flat bottom plates (Millipore Sigma; cat. no. CLS3997) coated with α CD3 (10 μ g/ml; BD Biosciences; cat. no. 553057) and α CD28 (2 μ g/ml; BD Biosciences; cat. no. 553294) antibodies in RPMI 1640 media supplemented with 10% FBS. On day 3 of culture, T-cells were harvested, and intracellular cytokine staining was performed as previously described (Henry et al., 2008, 2010) to determine interleukin-2 (α IL-2 PE; Biolegend; cat. no. 503808) and interferon-gamma (α IFN- γ APC; Biolegend; cat. No. 505810) production using flow cytometry (% positive and mean fluorescence intensity [MFI]). To determine CD44 and PD-1 surface expression on murine T-cells, cells were surface stained with α PD-1 PE (Biolegend, cat. no. 135205) and α CD44 APC (Biolegend; cat. no. 103012) for 1 h (covered on ice) and the MFI for each marker was determined using flow cytometry. All flow cytometry data were analyzed using the FlowJo software (BD Biosciences).

e. CAR T-cell assays

GFP-expressing murine CD19-directed CAR T-cells were harvested from aged mice after adoptive transfer using Fluorescence-activated cell sorting (FACs). Murine CAR T-cells were stimulated *ex vivo* with murine CD19-expressing BCR-ABL1+ /Arf-null B-ALL cells. On day 3 of culture, cells were harvested, and surface stained for 1 h (covered on ice) with α CD4 Pacific Blue (Biolegend, cat. no. 100428) or α CD8 Pacific Blue (Biolegend; cat. no. 100725). Following surface staining, intracellular cytokine staining for IL-2 and IFN- γ production was performed as described above.

f. T-cell depletion experiments

T-cells were depleted from aged (24 months) C57BL/6 mice using CD4 (anti-CD4; clone GK1.5; purchased from Bio X Cell) and CD8 (anti-CD8 α ; clone 53-6.72 and anti-CD8 β ; clone 53-5.8; purchased from Bio X Cell) T-cell depleting antibodies (i.p.; 0.5 mg/mouse/each antibody for two consecutive days). One day after the administration of T-cell depleting antibodies, mice were treated with Control Ig (i.v.; 100 μ g/mouse) or rIL-37 (i.v.; 100 μ g/mouse), and these treatments continued once weekly for the duration of the experiment. Two days after the administration of T-cell depleting antibodies, mice were transplanted with murine B-ALL (GFP-expressing, BCRABL1+ /Arfnull) cells (i.v.; 2×10^4 B-ALL cells/ mouse) and survival was monitored for >3 months. Once signs of leukemia manifested (the detection of GFP+ cells in the peripheral blood, lethargy, ruffled fur, labored breathing, or greater than 7% weight loss), mice were removed from the study.

g. CAR T-cell adoptive transfer experiments

Aged mice were conditioned with busulfan (i.v.; 25 mg/kg; (Henry et al., 2015)) and injected with GFP-expressing, murine CD19- directed CAR T-cells (i.v.; 106

cells/mouse) on day 2 post-conditioning. Mice were treated with Control Ig (i.v.; 100 µg/mouse) or rIL-37 (i.v.; 100 µg/mouse) beginning on day 2 post-adoptive transfer of CAR T-cells and continued receiving treatment once weekly for 2 weeks. After the 2-week treatment period, GFP-expressing CAR T-cells were harvested for functional analysis as described above.

h. Xenograft studies

Male and Female CIEA NOG Mice (immunodeficient mice lacking T-, B-, and NK cells) were transplanted intravenously (i.v.) with 5×10^4 CD19-expressing human B-ALL cells (REH cells). After signs of morbidity were observed (day 7), mice were treated with human CD19-directed CAR T-cells (i.v.; 10^6 /mouse) from a 67-year-old donor beginning on day 10 post-transplantation of human B-ALL cells. Mice were simultaneously treated with Control Ig or rIL-37 (i.v.; 100 µg/mouse/each group), and this treatment was continued (without co-administration of additional CAR T-cells) once weekly for the duration of the experiment in surviving mice. Mice were removed from the study when leukemia-induced signs of morbidity manifested (lethargy, ruffled fur, or labored breathing). All animal experiments were approved by and performed in accordance with guidelines of the IACUC of the University of Colorado Anschutz Medical Campus and Emory University School of Medicine.

i. Statistics

Unpaired t tests, Cox proportional hazards tests, and one-way ANOVA were used to analyze the data, with a p-value of less than 0.05 considered statistically significant. All error bars represent biological replicates, not technical replicates. Statistical analyses were performed with GraphPad Prism software, version 8.4.2 (GraphPad Software). All results are expressed as the mean \pm SEM.

2.4 Results

Interleukin-37 suppresses inflammaging, and decreased levels are observed in aged human monocytes

One hallmark of aging is the onset of chronic inflammation in mice and humans (Frasca & Blomberg, 2016). This manifestation is postulated to contribute to numerous aging-associated pathologies including cancer (Ferrucci & Balducci, 2008; Frasca & Blomberg, 2016; Furman et al., 2019; Leonardi et al., 2018). The underlying mechanisms governing aging-associated chronic inflammation are being investigated, with data supporting reduced gut barrier function and microbiome dysbiosis emerging as plausible explanations (Biragyn & Ferrucci, 2018; Fernandes et al., 2019; Fransen et al., 2017). Furthermore, studies performed on aged monocytes and macrophages demonstrated more robust and durable inflammatory responses when myeloid cells were stimulated (Biragyn & Ferrucci, 2018; Kovtonyuk et al., 2016; Puchta et al., 2016); however, the reasons behind these heightened responses are unclear.

Our group has previously demonstrated that transgenic expression of the anti-inflammatory cytokine IL-37 improves hematopoiesis and the function of B-progenitor cells in aged mice, which was largely driven by reducing aging-associated inflammation (Henry et al., 2015). We next wanted to determine how treating aged mice (≥ 24 months old) with rIL-37 impacted systemic inflammation relative to levels observed in IL-37 transgenic (IL-37 Tg) mice. Aged (24 months old) wild-type mice were treated with control immunoglobulin (Control Ig) or rIL-37 every 2 days for 2 weeks. We found that rIL-37 treatment significantly decreased circulating tumor necrosis factor-alpha (TNF- α ; Figure S1A), interleukin-1 beta (IL1 β ; Figure S1B), and interleukin-6 (IL-6; Figure S1C) levels in aged mice which were comparable to observations in aged IL-37tg mice (Figure

S1D–F). Given the ability of IL-37 to mitigate inflamm-aging in aged mice, we next asked whether IL-37 levels declined in humans with age. We mined the R2 database for studies where *IL-37* gene expression profiles were available for healthy donors. Based on this criterion, we analyzed a repository submitted by Tompkins et al. The age range of donors in this database was 15–55 years old, reflective of young to middle-aged healthy humans (Figure S2). We arbitrarily set the cutoff for young donors as those between 15 and 39 years of age and middle-aged as donors between 40–55 years of age (Figure S2). When the data were binned into these groups, we found a slight decrease in *IL-37* gene expression levels in leukocytes recovered from middle-aged (n = 7) relative to young donors (n = 30) (Figure 1a). To assess the impact of advanced age on *IL-37* expression levels, we obtained peripheral blood mononuclear cells (PBMCs) from healthy donors of various ages, including those over 65 years of age. Monocytes, which are major producers of IL-37 (Cavalli & Dinarello, 2018; Li et al., 2019; Rudloff et al., 2017), were purified from PBMCs, and IL-37 and actin gene expression levels were compared. Similar to data provided in the Tompkins et al. study, we found a decreased trend in *IL-37* gene expression levels in monocytes isolated from donors between 10 and 30 and those 31–64 years of age (Figure 1b). In donors 65 and older, *IL-37* gene expression levels in monocytes were significantly lower than those observed in monocytes isolated from donors between 10 and 30 years of age. In all, these data demonstrate the potent ability of IL-37 to suppress aging-associated chronic inflammation and suggest that reduced *IL-37* levels in aged monocytes may contribute to the onset of inflammaging in humans.

Interleukin-37 abrogates splenomegaly and restores a youthful T-cell distribution in aged mice

Given these observations and our groups previous studies demonstrating improved B-progenitor cell function in IL-37 transgenic (IL-37 Tg) mice (Henry et al., 2015), we next determined whether recombinant IL-37 (rIL-37) treatment of aged mice mitigated aging-associated changes in hematopoiesis. Aged (24 months old) wild-type mice were treated with control immunoglobulin (Control Ig) or rIL-37 every 2 days for two weeks (Figure S3A). We found that rIL-37 treatment in aged mice prevented the aging-associated accumulation of myeloid progenitor cells in the bone marrow (Figure S3D) and macrophages in the spleen (Figure S3E). Despite altering the relative distribution of myeloid cells, rIL-37 treatment did not change the absolute number of hematopoietic stem cells (Figure S3B), B-progenitor cells (Figure S3C), splenic-derived B-cells (Figure S3E), or splenic-derived T-cells (Figure S3E) in aged mice.

Aging is associated with extensive microarchitectural changes in the spleen including the onset of splenomegaly as a result of prolonged stimulation mediated by chronic inflammation or neoplastic lesions (Aw et al., 2016; Pettan-Brewer & Treuting, 2011). In addition to abrogating aging-associated chronic inflammation, we found that transgenic expression of IL-37 also significantly reduced splenomegaly in aged mice (Figure 1c). Similar to its impact on hematopoiesis, treating aged mice with rIL-37 also mitigated splenomegaly (data not shown). Given this observation, we next determined how rIL-37 treatment of aged, naïve mice impacted the distribution of splenic-derived immune cells and their basal activation state. Young (2 months old) and aged (24 months old) mice were treated with control immunoglobulin (Control Ig) or rIL37 using the protocol described above. In these experiments, we found similar percentages of splenic-

derived CD4⁺ T-cells in young, naïve mice treated with Control Ig and rIL-37 (Figure S4A, B). In aged mice treated with Control Ig, we observed a slight decrease in the percentage of splenic-derived CD4⁺ T-cells relative to all treatment groups, whereas rIL-37 treatment led to a noticeable, although not statistically significant ($p = 0.059$), increase in the representation of T-helper cells (Figure S4A, B). Similarly, equivalent percentages of splenic-derived CD8⁺ T-cells were observed in young, naïve mice treated with Control Ig and those treated with rIL-37 (Figure S5A, B). In contrast to the slight decrease in the representation of CD4⁺ T-cells observed in aged mice treated with Control Ig, the percentage of CD8⁺ T-cells was noticeably, yet insignificantly ($p = 0.084$), higher than those observed in all treatment groups (Figure S5A, B). Interestingly, the trend toward increased representation of splenic-derived CD8⁺ T-cells in aged mice was mitigated by rIL-37 treatment (Figure S5A, B). Overall, these data demonstrate that treating aged mice with rIL-37 abrogates aging-associated splenomegaly and restores the representation of CD4⁺ and CD8⁺ T-cells to youthful levels (Figure 1d), whereas treating young mice with this anti-inflammatory cytokine does not impact the distribution of splenic-derived T-cells.

IL-37 promotes youthful gene expression profiles in aged T-cells and reduces the surface expression of immunoinhibitory proteins

Given the ability of rIL-37 treatment to restore a youthful CD4⁺ to CD8⁺ T-cell distribution in aged mice, we next determined how treatment with this anti-inflammatory cytokine impacted the gene and surface expression of regulators of T-cell activation. After 2 weeks of treatment, CD4⁺ T-cells isolated from aged mice treated with rIL-37 exhibited gene expression profiles that phenocopied CD4⁺ T-cells isolated from young mice (Figure

2a–c). When aged mice were treated with Control Ig, CD4⁺ T-cells exhibited a trend toward higher gene expression levels of *Pdcd1* (the gene encoding programmed cell death protein 1 [PD-1]) and significantly lower levels of *Lat* and *Stat4* (Figure 2b, c). Treatment of aged mice with rIL-37 reversed these phenotypes in CD4⁺ T-cells to youthful levels, which was comparable to young mice treated with Control Ig and rIL-37 (Figure 2b, c). Furthermore, we observed a significant increase in *Prf1* (the gene encoding perforin) expression levels in CD4⁺ T-cells isolated from aged mice treated with rIL-37. Unlike rIL-37-mediated gene expression alterations in aged CD4⁺ T-cells, treating young mice with rIL-37 did not alter *Cd3e*, *Cd28*, *Prf1*, *Pdcd1*, *Lat*, *Il12rb1*, or *Stat4* gene expression levels in CD4⁺ T-cells (Figure 2a–c). In addition to altering gene expression profiles in aged CD4⁺ T-cells, treating aged mice with rIL-37 also decreased the surface expression of the immunoinhibitory proteins Tim-3 and TIGIT on aged T-cells, whereas CD28 surface levels remained unchanged (Figure S4C–F). Despite the aging-associated increase in *Pdcd1* gene expression levels in aged CD4⁺ T-cells (Figure 2b), PD-1 surface expression on naïve CD4⁺ T-cells was negligible and not impacted by rIL-37 treatment (Figure S4C), which is consistent with PD-1 expression being induced on activated T-cells (Riley, 2009).

Unlike, changes observed in CD4⁺ T-cells in aged mice receiving rIL-37 treatment, aging-associated gene expression changes in CD8⁺ T-cells were largely unchanged with rIL-37 treatment with the exception of restoring youthful levels of *Lat* (Figure 2d–f). Similarly, to CD4⁺ T-cells, treating aged mice with rIL-37 also significantly decreased TIGIT surface levels on naïve CD8⁺ T-cells (Figure S5C, E), whereas Tim3 (Figure S5C, D) and CD28 (Figure S5C, F) surface expression was not impacted by rIL-37 treatment in young or aged mice. In addition to assessing the impact of rIL-37 treatment on aged T-lymphocytes, we also determined its impact on aged myeloid cells. Treating aged mice

with rIL-37 also led to a reduction (albeit insignificant) in splenic dendritic cells (Figure S6A, B) and macrophages (Figure S6C, D), consistent with an abrogation of splenomegaly (Figure 1c and Figure S3D, E). Despite decreasing the percentages of splenic-derived dendritic cells, which are the principal activators of naïve T-cells (Henry et al., 2008, 2010), rIL-37 treated did not rejuvenate their upregulation of the costimulatory molecules CD40, CD80, and CD86 to youthful levels after ex vivo stimulation with LPS (data not shown).

In all, these data demonstrate that treating aged mice with rIL-37 alters the activation threshold of naïve CD4⁺ and CD8⁺ T-cells, by increasing the expression of genes involved in T-cell activation (Stat4 and Lat) and decreasing the surface expression of immunoinhibitory proteins (Tim-3 and TIGIT).

Recombinant IL-37 treatment improves T-cell function in aged mice

Given that IL-37 treatment rejuvenated gene expression profiles and suppressed the surface expression of immunoinhibitory proteins, we next assessed how T-cell function was impacted. We purified CD4⁺ and CD8⁺ T-cells from aged (24 months old) wild-type mice treated every other day for 2 weeks with Control Ig or rIL-37 and stimulated them in vitro with α CD3/ α CD28 for 3 days. We found that rIL-37 treatment significantly mitigated T-cell exhaustion indicative of similar T-cell expansion observed between T-cell isolated from aged mice treated with rIL-37 and young mice treated with Control Ig or rIL37 (Figure S7A, B). In contrast, T-cell proliferative defects were observed in aged T-cell isolated from aged mice treated with Control Ig, where significant difference were apparent by Day 2 of culture and became more pronounced by Day 4 post-stimulation (Figure S7A, B). Furthermore, treating aged mice with rIL-37 significantly

reduced the surface expression of PD-1 on effector CD4⁺ and CD8⁺ T-cells, whereas CD44 surface levels remain unchanged (Figure 3a–c). We found that T-cells stimulated from aged mice treated with rIL-37 were more functional than T-cells activated from aged mice treated with Control Ig (Figure 3d). We observed significant increases in interleukin-2 (IL-2) and interferon-gamma (IFN- γ) production at the population (percentage; Figure 3e) and per cell (mean fluorescence intensity; Figure 3f, g) levels when T-cells were stimulated *ex vivo* from rIL-37-treated but not Control Ig-treated aged mice. In summary, these data demonstrate that treating aged mice with recombinant IL-37 effectively improves T-cell responses.

Pro-inflammatory cytokines, such as TNF- α , are potent inducers of PD-1/PD-L1 surface expression on immune cells (Bally et al., 2015; Lu et al., 2019). Given that treating aged mice with rIL-37 significantly reduced chronic inflammation and was particularly effective at lowering circulating TNF- α levels (Figure S1A, D), we next determined if rIL-37 directly counteracted TNF- α signaling and its ability to induce PD-1 surface expression on aged T-cells. In immune cells, TNF- α is a potent inducer of NF- κ B activation (Liu et al., 2017) and NF- κ B binding sites are in the PD-1 promoter (Redd et al., 2018). In these studies, we found that treating aged CD4⁺ and CD8⁺ T-cells with recombinant TNF α (rTNF- α) significantly augmented NF- κ B activation in T-cells (Figure 4a and Figure S8A) which correlated with increased PD-1 surface expression on effector T-cells (Figure 4b). We next determined whether rIL-37 stimulation could reduce NF- κ B activation in TNF- α stimulated aged T-cells. Interestingly, we found that rIL-37 abrogated the TNF- α induced NF- κ B activation in aged T-cells (Figure 4c and Figure S8B) and significantly decreased PD-1 surface expression (Figure 4d).

To determine whether IL-37 altered T-cell homeostasis prior to stimulation, we next performed gene expression profiling of targets induced (TMEM16F, GM130, PD-1, and SHP2) and suppressed (IFN γ , TBK1, and IRF3) by TNF- α and PD-1 signaling in aged naïve T-cells treated with Control Ig or rIL-37. In young naïve T-cells, we observed low basal expression of genes induced and suppressed by TNF- α and PD-1 signaling (Figure S8C). Furthermore, rIL-37 treatment did not impact the expression of these genes in young naïve T-cells (Figure S8D). In contrast, aged naïve T-cells exhibited high gene expression levels of TMEM16F, GM130, PD1, and SHP2 suggesting that these programs are primed for induction in aged T-cells (Figure 4e). Furthermore, treating aged naïve T-cells with rIL-37 significantly increased the homeostatic expression of genes suppressed by TNF- α and PD-1 signaling, particularly those involved in interferon production (Figure 4f). Taken together, these data demonstrate that rIL-37 improves the function of aged T-cells which is mediated, in part, by the ability of rIL37 treatment to directly oppose TNF- α -induced programs in aged T-cells.

Recombinant IL-37 treatment protects aged mice from B-ALL pathogenesis in a T-cell dependent manner

Two hallmarks of aging are the onset of chronic inflammation and compromised immunity, which are postulated to contribute to numerous aging-associated pathologies including cancer (Ferrucci & Balducci, 2008; Furman et al., 2019; Leonardi et al., 2018). We have previously demonstrated that transgenic expression of IL-37 improves hematopoiesis and the function of B-progenitor cells in aged mice, which was largely driven by reducing aging-associated inflammation (Henry et al., 2015). To determine how reducing aging-associated chronic inflammation impacts leukemia development, aged

wild-type, and IL-37 transgenic (IL-37tg) mice were transplanted with BCR-ABL1+ /Arf-null B-ALL cells (Figure S9A). Due to the presence of a strong driver mutation (BCR-ABL1) and the lack of a potent tumor suppressor (Arf), these cells can establish leukemia in mice without myeloablation, which leaves the immune system unperturbed (Boulos et al., 2011; Manlove et al., 2015; Rabe et al., 2019; Williams et al., 2006, 2007). After transplantation into aged wild-type mice, all mice succumbed to disease within 2 months post-injection of B-ALL cells (Figure S9B). The transgenic expression of IL-37 in aged mice resulted in a significant extension of survival, such that almost half of the mice injected with B-ALL cells survived for over 2 months (Figure S9B). In summary, these data demonstrate that IL37 expression in aged mice protects against B-ALL progression.

Recent studies have demonstrated that T-cells are required for the control of B-ALL development, which is in part regulated by the pro-inflammatory microenvironment (Rabe et al., 2019). Given these observations, we next determined whether treating aged mice with rIL-37 could improve T-cell-mediated anti-leukemia responses. To this end, aged mice were treated with Control Ig or T-cell depleting antibodies followed by treatment with Control Ig or rIL-37 prior to injection with BCR-ABL1+ /Arf-null B-ALL cells (Figure 5a). Mice were treated with control Ig or rIL-37 for the duration of this experiment.

Given the aggressive nature of this leukemia, all mice succumbed to disease within 42 days post-injection if left untreated (Figure 5b). Impressively, 60% of mice treated continuously with rIL-37 exhibited survival for greater than 3 months post-injection of B-ALL cells (Figure 5b). This protective effect was abrogated when CD4⁺ and CD8⁺ T-cells were depleted, suggesting that both T-cell populations are essential for immunity against B-ALL cells. In line with recent studies (Rabe et al., 2019), these data confirm the

importance of T-cells in the protection against B-ALL pathogenesis. Importantly, these data demonstrate that treating aged mice with recombinant IL-37 significantly boosts anti-leukemia T-cell-mediated immune responses.

Recombinant IL-37 treatment improves the efficacy of aged chimeric antigen receptor (CAR) T-cells

Given the ability of recombinant IL-37 to boost the function of aged T-cells, we next determined how rIL-37 treatment altered the efficacy of aged CAR T-cells. To this end, CD19-expressing CAR T-cells were engineered from T-cells isolated from aged (24 months old) mice and injected into aged (24 months old) recipient mice. On day 2 post-transplantation, mice were treated once weekly for 2 weeks with Control Ig or rIL-37. CAR T-cells were then purified from the spleen and stimulated with murine CD19-expressing B-ALL cells to determine the ex vivo production of IL-2 and IFN- γ (Figure 6a). Consistent with the improvements in the function of aged endogenous T-cells, rIL-37 treatment also increased IL-2 and IFN- γ production from aged CD4⁺ and CD8⁺ CAR T-cells (Figure 6b).

Given the ability of rIL-37 treatment to augment the function of aged murine CAR T-cells, we next determined how rIL-37 treatment impacted the efficacy of aged human CAR T-cells in vivo. Immunocompromised mice (6 months old) were transplanted with human B-ALL cells, and all mice injected with B-ALL cells exhibited signs of morbidity by day 7 post-transplantation (data not shown). On day 10 post-transplantation of B-ALL cells, mice began receiving treatment with human CD19-directed CAR T-cells (generated from a 67-year-old donor; Figure S10) with or without the coadministration of rIL-37 (which continued weekly for the duration of the experiment; Figure 6c). In these experiments, we found that treating mice with human CAR T-cells and control Ig resulted

in 20% of mice surviving for greater than 3 months (Figure 6d). When CAR T-cell therapy was combined with rIL-37 treatment, the 3-month survival of mice significantly increased to 60% (Figure 6d). Overall, the results of our study demonstrate that IL-37 can rejuvenate the function of aged endogenous T-cells and boost the efficacy of aged CAR T-cells resulting in attenuated B-ALL pathogenesis.

2.5 Discussion

Our team has previously reported that transgenic IL-37 expression in aged mice rejuvenated the function of aged B-progenitor cells and abrogated the selection of B-cells harboring oncogenic mutations; thereby, preventing leukemogenesis (Henry et al., 2015). In this study, we delineated how IL-37 impacted the function of mature immune cells.

Notably, we found that the IL-37 gene expression levels were significantly lower in monocytes isolated from donors 65 years of age or older relative to their younger counterparts, suggesting that inflammaging is accompanied by lower levels of IL-37 production from innate immune cells. This observation is consistent with published data suggesting that IL-37 gene expression levels are lower in the diseased synovia of patients with rheumatoid arthritis and other inflammatory diseases including allergic rhinitis, asthma, and non-small cell lung cancer (Cavalli et al., 2016).

Furthermore, we demonstrate for the first time, to our knowledge, that treating aged mice with recombinant IL-37 abrogates aging-associated splenomegaly. This change was accompanied by restoring a youthful balance of CD4⁺ to CD8⁺ T-cells and evoking youthful gene expression programs in T-lymphocytes. Of particular interest, the gene expression levels of the linker for the activation of T-cells (Lat) were found to be increased to youthful levels in aged CD4⁺ and CD8⁺ T-cells recovered from old mice receiving rIL-37 treatment. This observation suggests that rIL-37 treatment augments TCR-mediated signaling in aged T-cells. Indeed, T-cells isolated from aged mice receiving rIL-37 responded more robustly to α CD3/ α CD28 stimulation which mimics peptide-MHC/TCR activation. Indeed, both T-helper cells and cytotoxic lymphocytes exhibited significantly enhanced IL-2 and IFN- γ production with this mode of stimulation. Recombinant IL37 treatment of aged mice also significantly reduced Pdc1 (the gene encoding for PD-1) and

significantly increased Stat4 gene expression levels in T-helper cells, suggesting an attenuation of T-cell exhaustion and enhanced IL-12-mediated signaling (which may play a role in augmenting IFN- γ production from aged T-cells). In addition to modifying gene expression profiles, rIL-37 treatment of aged mice resulted in decreased surface expression of the immunosuppressive molecules PD-1, Tim-3, and TIGIT on activated T-cells coincident with increased proliferation after *in vitro* stimulation. The increase in the proliferation in aged T-cell is notable, because aged microenvironments are capable of potently suppressing the proliferation of young and aged T-cells (Quinn et al., 2018). Given that aging-associated T-cell dysfunction has been attributed to increased levels of PD-1, Tim-3, and TIGIT (Lee et al., 2016; Song et al., 2018), our results suggest that IL-37-mediated rejuvenation of aged T-cells is partially attributed to its ability to downregulate the surface expression of these immunoinhibitory proteins on T-lymphocytes. In all, these results demonstrate that IL-37 treatment reprograms gene expression profiles in aged T-cells resulting in more robust effector functions and an increased threshold for T-cell exhaustion post-stimulation.

The ability of IL-37 to restore youthful gene expression profiles, mitigate immunosuppressive mechanisms, and enhance effector T-cell function is attributed to both direct effects on T-cells and modulation of the immune environment. We found that transgenic expression of IL-37 and rIL-37 treatment attenuated aging-associated increases in circulating IL-1 β , IL-6, and TNF- α levels. Given that chronic TNF- α exposure suppresses T-cell receptor signaling (Cope et al., 1997), blocking TNF- α enhances CD8+ T-cell responses in murine models of melanoma (Bertrand et al., 2015), and TNF- α /PD-1 gene expression levels are positively correlated in patients with melanoma (Bertrand et al., 2017), we determined whether IL-37 antagonized TNF- α signaling in aged T-cells. In

immune cells, TNF- α stimulation potently activates NF- κ B, which has multiple binding sites in the T-cell PD-1 promoter region (Redd et al., 2018). We found rIL-37 directly antagonized TNF- α -mediated NF- κ B activation, which is consistent with published observations demonstrating similar effects in other pathological settings (Cavalli & Dinarello, 2018; Li et al., 2017; Nold et al., 2010; Xie et al., 2016). Furthermore, IL-37 treatment significantly reduced PD-1 surface expression and genes activated downstream of both PD1 and TNF- α signaling pathways (TMEM16F, GM130, PD-1, and SHP2). Directly stimulating aged T-cells with rIL-37 also augmented the expression levels of genes which promote interferon production (IFN- γ , TBK1, and IRF3), coincident with increased IFN- γ production from aged T-cells after α CD3/ α CD28 stimulation. Our observations support recent studies demonstrating that IL-37 treatment restores normal T-cell function (reduction in IL-17 production) in the chronic inflammatory setting of allergic rhinitis (Li, Shen, et al., 2018).

In addition to IL-37-mediated cell autonomous changes in aged T-cells, aging-associated increases in myelopoiesis were abrogated after treating aged mice with rIL-37. Similarly, splenic DC and macrophage populations were also decreased to youthful levels after aged mice received rIL-37 treatment. The reduction in myeloid cells in the bone marrow and spleens of aged mice treated with rIL-37 likely contributed to the significantly lower levels of circulating pro-inflammatory cytokines and more robust T-cell effector functions. Mechanistically, IL-37 binds the IL-18R α and IL-1R8 receptors, which are expressed on myeloid cells and T-cells and attenuates the production of pro-inflammatory cytokines by inhibiting transforming growth-factor- β -activated protein kinase 1 (TAK1), NF- κ B, and MAPK activity (Cavalli & Dinarello, 2018; Lunding et al., 2015; Nold et al., 2010). The “renormalization” of the inflammatory microenvironment in

aged mice which we demonstrate in this study is consistent with reported protective effects of IL-37 in other pathological inflammatory settings including endotoxin shock syndrome, lung and spinal cord injury, colitis, coronary artery disease, and arthritis (Cavalli & Dinarello, 2018).

Aging in mice and humans is associated with extensive immunological change including the onset of chronic inflammation and the development of compromised T-cell-mediated immunity (Henry et al., 2011; Ponnappan & Ponnappan, 2011; Ventura et al., 2017). Augmented immunosuppressive mechanisms in aged individuals are postulated to contribute to increased pathogenic infections and higher cancer incidence which are hallmarks of aging (Ladomersky et al., 2019; Rea et al., 2018). In addition to elevated cancer incidence, cancer-related mortality rates are significantly higher in older patients (White et al., 2014; Yancik, 2005). The failure to achieve similar survival outcomes in younger and older patients with cancer has been partially attributed to the inability to achieve effective chemotherapy dosages in older patients due to toxicity complications (Repetto, 2003). Given that chemotherapies are less effective in older patients (Kim & Hurria, 2013; Repetto, 2003), other therapeutic options, such as treatments using immunotherapies, are beginning to be used to treat older patients with solid and hematological malignancies. Indeed, CAR T-cell therapy is currently being used to treat relapsed and refractory B-ALL and DLBCL with new clinical trials open to test the efficacy of this cell-based therapy as a frontline option (Chavez et al., 2019; Hay & Turtle, 2017). Despite the success of CAR T-cell therapy, between 20 and 50 percent of the pediatric and adult patients receiving this form of immunotherapy will relapse within 2 years of treatment (Cao et al., 2018; Gardner et al., 2017; Lee et al., 2015; Li, Zhang, et al., 2018; Maude, Frey, et al., 2014; Maude et al., 2018; Park et al., 2018; Turtle et al., 2016; Xu et

al., 2019). The failure to achieve durable responses in patients receiving CAR T-cell therapy has resulted from receiving low potency CAR T-cells and the loss of target antigens on cancer cells (Xu et al., 2019). Additional studies in animal models and patients will be required to identify additional mechanisms of immune evasion.

In laboratory settings, the importance of using appropriate model systems for the pre-clinical development and validation of immunotherapies is paramount for efficacy and safety testing prior to clinical trials (Bouchlaka & Murphy, 2013; Repetto & Balducci, 2002). The incidence of most leukemias rises dramatically in individuals over 65, and mortality rates are higher in geriatric patients (Repetto & Balducci, 2002). Despite the strong association between aging and leukemia development, most of the pre-clinical studies of immunotherapies are conducted in young mice (Bouchlaka & Murphy, 2013; Repetto & Balducci, 2002). This is concerning given that a major hallmark of aging in mice and humans is attenuated immune function (Fane & Weeraratna, 2020). The immune microenvironment “edits” cancer cells, and these changes dictate tumor cell eradication, equilibrium, or immune escape (Gonzalez et al., 2018). Given the impact of the immune microenvironment on cancer progression and the immunological decline associated with aging (Gonzalez et al., 2018), there is a growing need to study how immunotherapies behave (efficacy and toxicity) in aged recipients.

Given the lack of preclinical studies and scant clinical data regarding the efficacy of CAR T-cell therapy in patients over 65 (van Holstein et al., 2019), our study is the first to demonstrate that functional defects in aged endogenous T-cells are transferable to engineered T-cells and are not completely overcome by the introduction of a CAR. Our findings corroborate a recent study demonstrating age-dependent functional defects in CAR T-cells engineered from old (>65 years old) relative to young (18–45 years old)

donors (Guha et al., 2017). In murine studies, we demonstrate that aging-associated increases in chronic inflammation, the onset of splenomegaly, and the accumulation of myeloid populations in the bone marrow and spleen can be prevented by the anti-inflammatory cytokine IL37. Importantly, we demonstrate that treating aged mice with rIL37 reduces TNF- α signaling and significantly decreased the surface expression of PD-1 on naïve CD4⁺ and CD8⁺ T-cells. This effect was not limited to endogenous T-cells, as demonstrated by the results that rIL-37 treatment also prevented high PD-1 surface expression on aged CAR T-cells. Impressively, the function of endogenous and CAR T-cells was improved by rIL-37 treatment, leading to increased cytokine production *ex vivo* and the augmented protection of mice with B-ALL.

Our study highlights the potency of recombinant IL-37 treatment in boosting T-cell-mediated immunity in aged backgrounds and its ability to increase the efficacy of aged CAR T-cells. Importantly, our results demonstrate that components of aging-associated immune senescence are reversible and further support emerging literature demonstrating the utility of targeting the inflammatory microenvironment as a viable option to improve the efficacy of immunotherapies (Bouchlaka et al., 2013; Maude, Barrett, et al., 2014).

2.6 Figures, Supplemental Figures, Tables

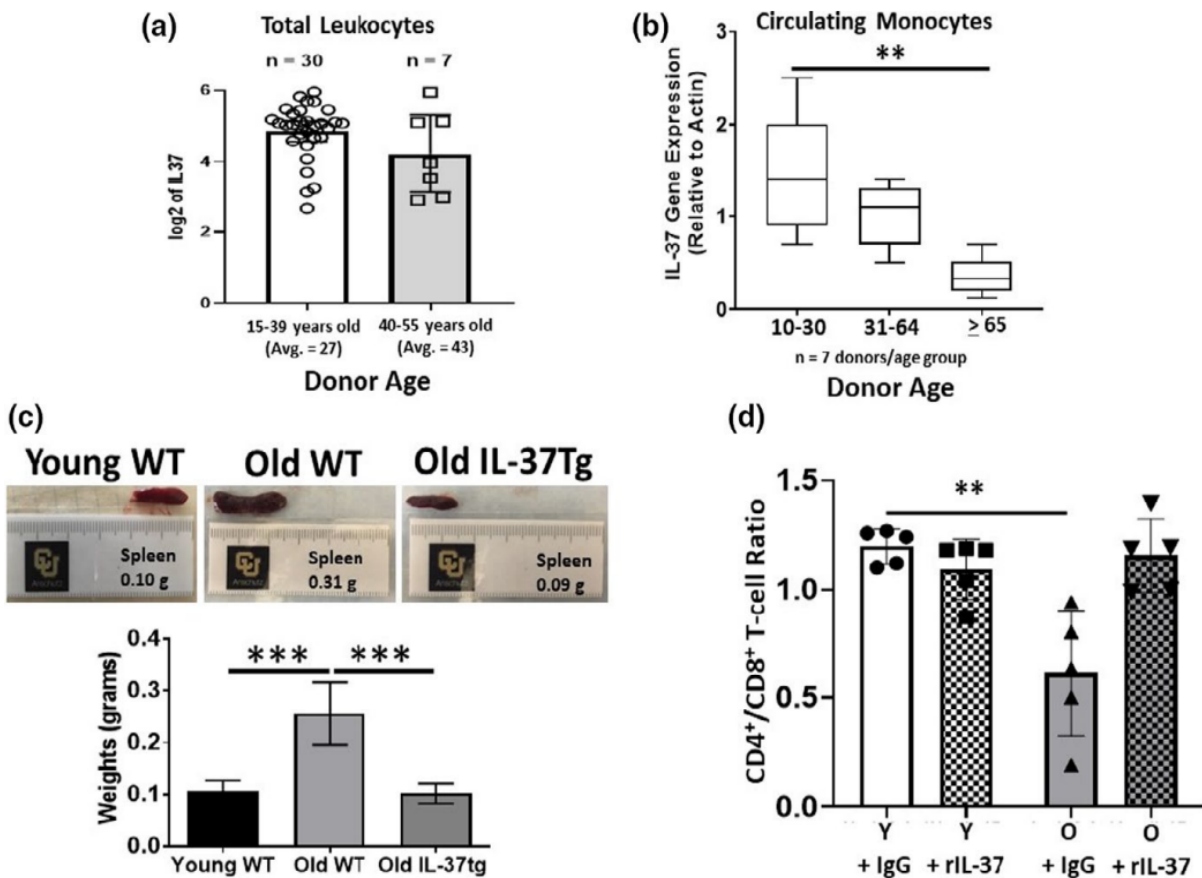


FIGURE 1 Interleukin-37 suppresses inflammation, and decreased levels are observed in aged human monocytes.

(a) The R2 Database was mined to determine IL-37 gene expression levels in healthy donors between the ages of 15-55 years of age. The gene expression levels are shown for young and middle-aged donors. (b) Monocytes were purified from PBMCs of healthy donors using MACs selection. The gene expression levels are shown for young, middle-aged, and old donors. (c) C57BL/6 wild-type and IL-37 transgenic mice were aged for 24 months and dissected to observe potential anatomical changes. The spleen appearance and weight are shown. (d) Young (2 months) and old (24 months) C57BL/6 mice were treated every other day for 2 weeks with control Ig or rIL-37, and the ratio of CD4⁺ to CD8⁺ T-cells was determined via flow cytometric analysis. Means \pm SD are shown with ** $p < 0.01$ and *** $p < 0.001$ determined using a Student's t

test relative to young donors in B or young Control Ig-treated mice in (d). A one-way ANOVA with Tukey's post-test was used to determine significance in (c). For results presented in (c), 3 independent experiments were conducted (n = 9 mice/group). In (d), data represent 5 mice/group

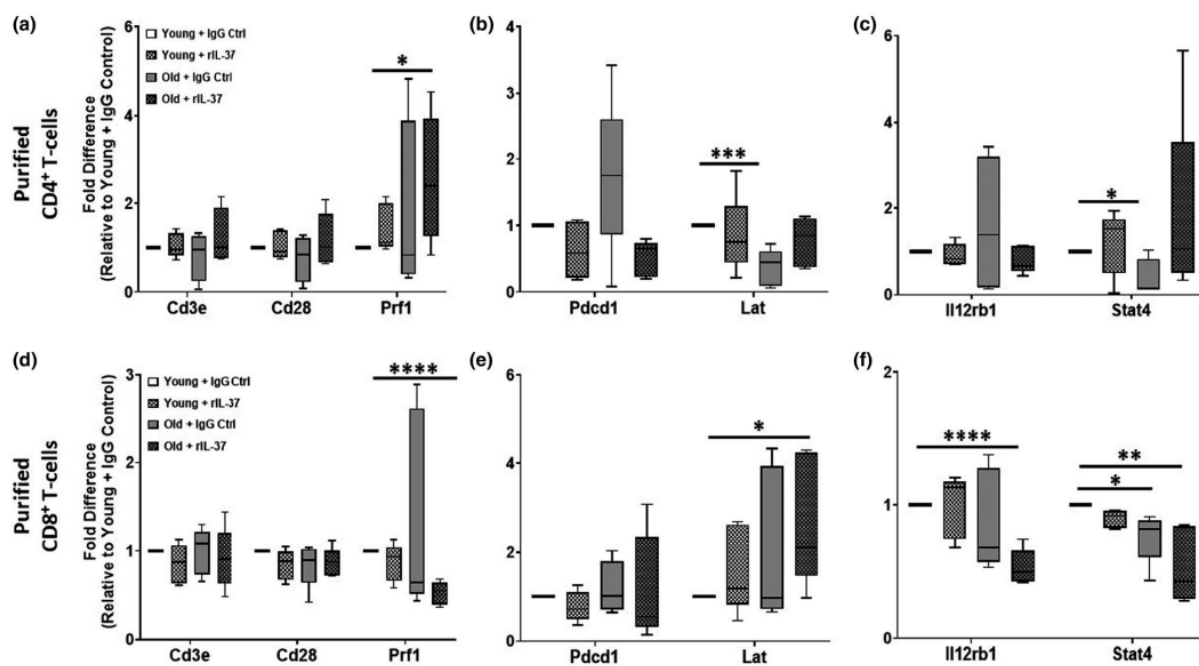


FIGURE 2 Interleukin-37 restores a youthful gene expression profile in aged T-cells. (a-f) Young (2 months) and old (24 months) C57BL/6 mice (n = 5 mice/group) were treated every other day for 2 weeks with control Ig or rIL-37. Naïve T-cells were purified, RNA isolated, and qPCR analysis was performed to ascertain the steady-state levels of genes involved in T-cell activation (Cd3e, Cd28, Prf1, Lat, Il12rb1, Stat4) and inhibition (Pdcd1). Significance was determined using a one-way ANOVA with Tukey's post-test with *p < 0.05, **p < 0.01, ***p < 0.001, and ****p < 0.0001

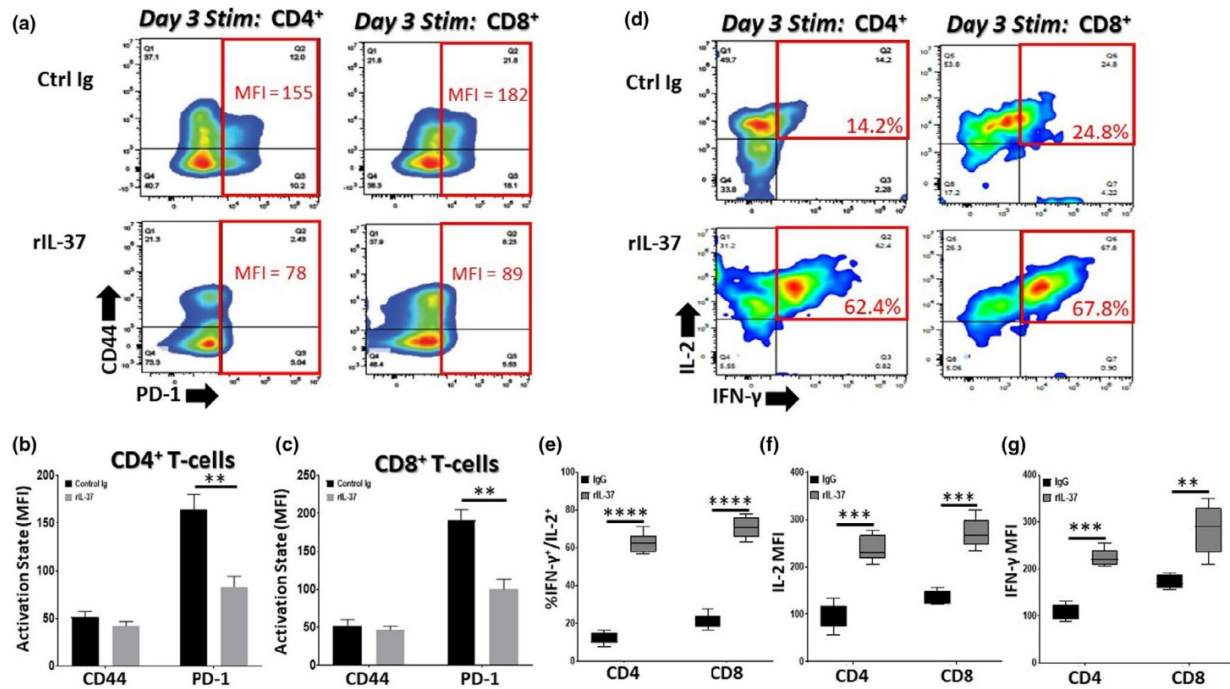


FIGURE 3 Recombinant IL-37 treatment reduces PD-1 surface expression and improves the function of aged T-cells. Aged (24 months old) C57BL/6 mice were treated with control immunoglobulin (Control Ig) or recombinant IL-37 (rIL-37) every other day for 2 weeks. Naïve CD4⁺ T-cells and CD8⁺ T-cells were purified from treated mice using MACs selection and stimulated *in vitro* with α CD3/ α CD28. On day 3 post-stimulation, (a–c) the mean surface expression of CD44 and PD1 (mean fluorescence intensity [MFI]) and (d–g) the percentage and MFI of IL-2/IFN- γ -producing T-cells were determined using flow cytometric analysis. Means \pm SD are shown in (b, c, e, f, and g) with ** $p < 0.01$, *** $p < 0.001$, and **** $p < 0.0001$ determined using a Student's t test relative to aged T-cell responses from Control Ig treated mice. $n = 9$ mice/group with 3 independent experiments conducted. The red boxes in (a) and (d) denote functional parameters of interest.

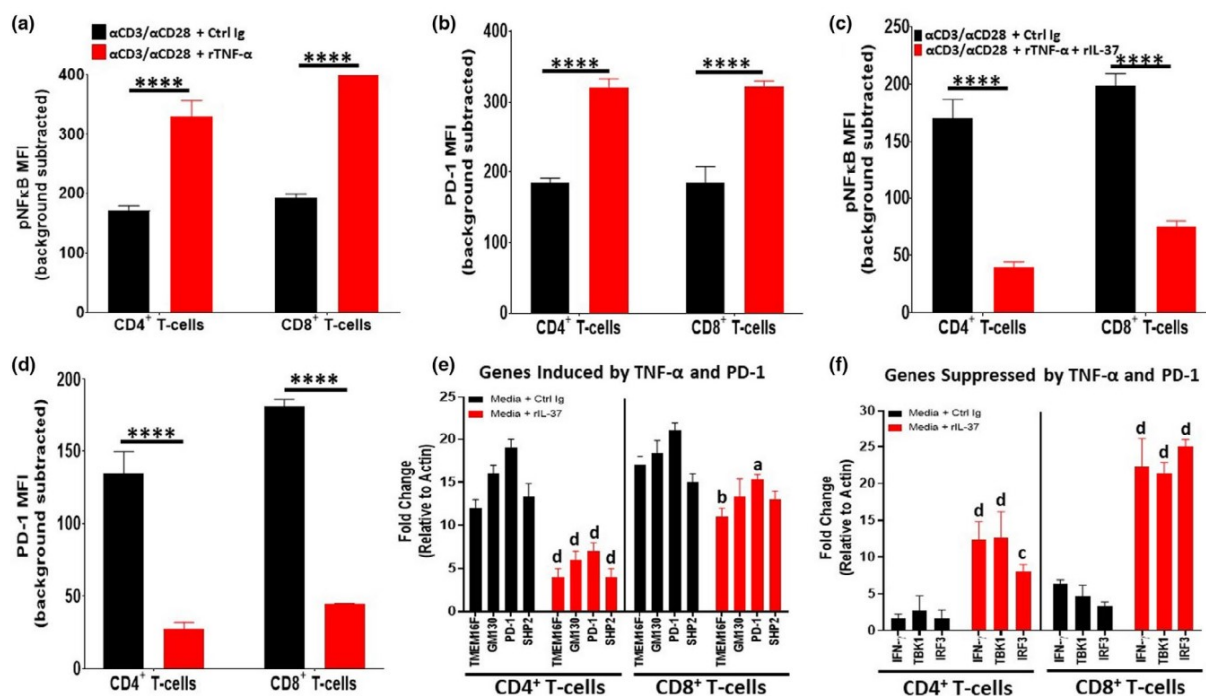


FIGURE 4 Recombinant IL-37 treatment opposes TNF-α signaling in aged

T-cells. Naïve CD4⁺ and CD8⁺ T-cells were purified from aged (24 months old) C57BL/6

mice via MACs selection and stimulated in vitro with αCD3/αCD28 in the presence of

Control Ig, rTNF-α, or rTNF-α + rIL-37. (a, c) After 10' of stimulation, phospho-flow

cytometry was performed to determine NF-κB activation. (b, d) After 3 days of

stimulation, the surface expression of PD-1 on aged T-cells was determined using flow

cytometric analysis. (e, f) Naïve T-cells were purified as described above and stimulated

with Control Ig or rIL-37 for 4 h. After the stimulation period, qPCR analysis was

performed to ascertain the expression levels of genes involved in T-cell activation (IFN-γ,

TBK1, IRF3) and inhibition (TMEM16F, GM130, SHP2, and PD1). Importantly, the genes

chosen for assessment are regulated by TNF-α and PD-1 signaling. Significance was

determined using a Student's t test relative to αCD3/αCD28 + Control Ig (a–d) and media

+Control Ig (e, f) treated groups. For a–d, means ± SD are shown with ****p < 0.0001.

For (e) and (f), a=*p < 0.05, b=**p < 0.01, c=***p < 0.001, and d=****p < 0.0001 where

gene expression levels observed in Control Ig-treated aged T-cells were used as the positive control for each gene tested. n = 9 mice/group with 3 independent experiments conducted

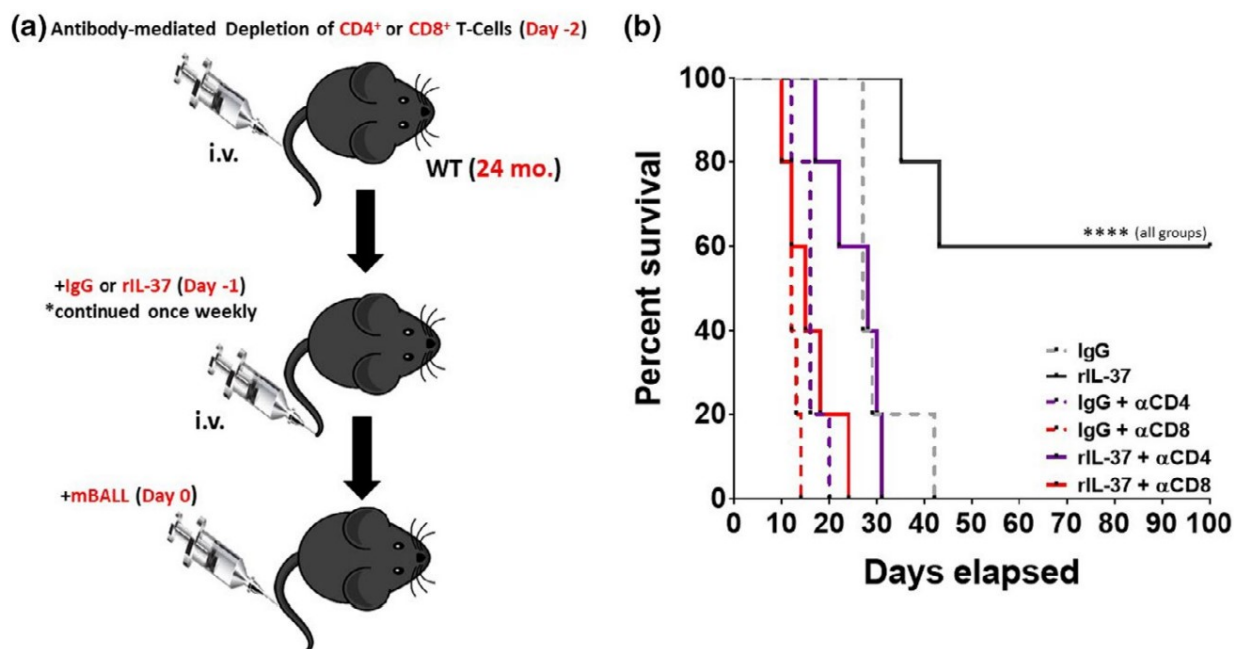


FIGURE 5 Recombinant IL-37 treatment protects aged mice from B-ALL pathogenesis in a T-cell dependent manner. (a) Aged (24 months old) C57BL/6 mice were treated with T-cell depleting antibodies (α CD4 and α CD8) 2 days prior to intravenous challenge with BCR-ABL+ Arf^{-/-} murine B-ALL cells (mB-ALL). Mice were also treated with Control Ig or rIL-37 1 day prior to the injection of mB-ALL cells, and this treatment continued throughout the experiment. (b) Survival was monitored for over 3 months. Significance was determined using log-rank test with ****p < 0.0001 indicating a significant extension of survival in aged mice treated with rIL-37 relative to each experimental group tested. n = 5 mice/group

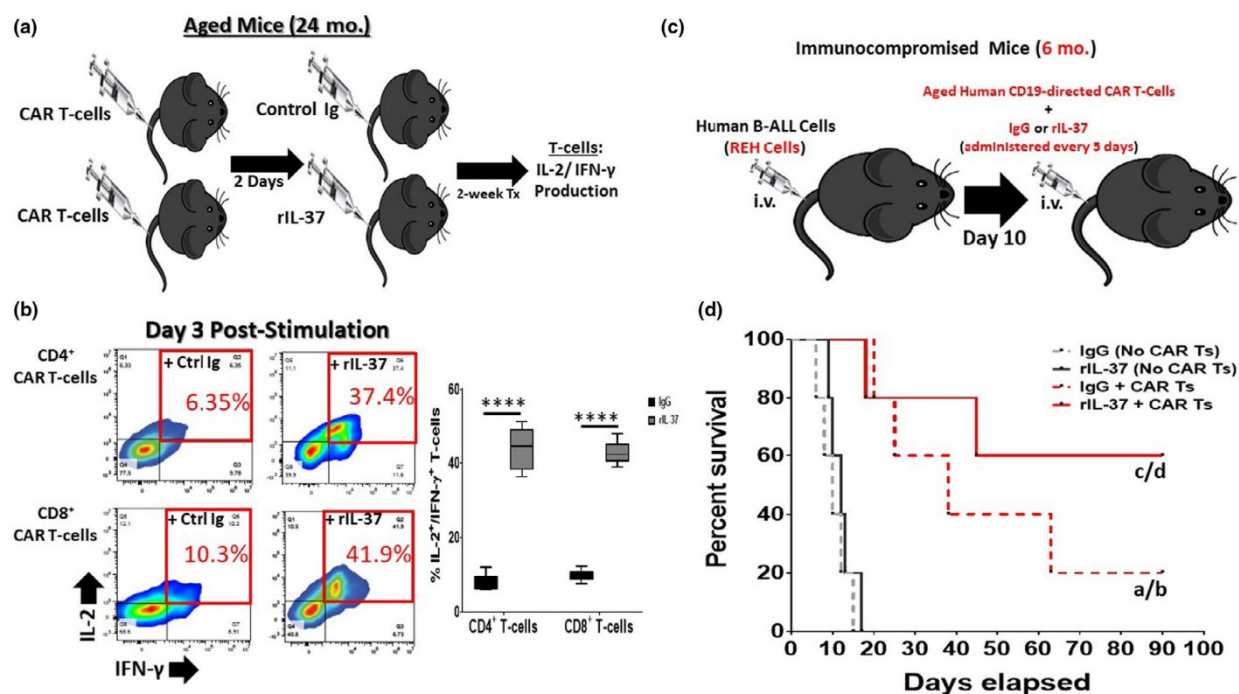


FIGURE 6 Recombinant IL-37 Treatment Improves the Efficacy of Aged CAR T-cells. (a) Murine CD3⁺ T-cells were purified from aged (24 months old) C57BL/6 wild-type mice and transduced to express CD19-directed CARs (transduced cells express GFP). Aged CAR T-cells were then injected into aged wild-type mice which were then treated with control immunoglobulin (Control Ig) or recombinant IL-37 (rIL-37) once weekly for 2 weeks. After 2 weeks of treatment, GFP⁺ CAR T-cells were sorted from mice and stimulated in vitro with CD19-expressing murine BALL cells. On day 3 of culture, IL-2 and IFN- γ production from aged CAR T-cells was assessed by flow cytometric analysis. (b) Representative flow cytometry and quantitative data showing the percentage of IL-2 and IFN- γ producing aged CAR T-cells. Means \pm SD are shown in (c) with ****p < 0.0001 determined using a Student's t test. n = 9 mice/group with 3 independent experiments conducted. (c) NOG immunocompromised (6 months old) mice were intravenously challenged with human B-ALL cells (REH cells). On day 10 post-transplantation (when

signs of morbidity were observed in all mice), mice were injected with CD19-directed CAR T-cells from an aged donor (67 years old). Mice were simultaneously injected with Control Ig or rIL-37 and this treatment was continued every 5 days until the experiment was terminated. (d) Survival was monitored for over 3 months. Significance was determined using log-rank test with “a” denoting significance between IgG + CAR Ts and IgG (No CAR Ts) treated groups, “b” denoting significance between IgG + CAR Ts and rIL-37 (No CAR Ts) treated groups, “c” denoting significance between the rIL-37 + CAR Ts and IgG (No CAR Ts) treated groups, and “d” denoting significance between the rIL-37 + CAR Ts and rIL-37 (No CAR Ts) treated groups. n = 5 mice/group

2.6 Figures, Supplemental Figures, Tables CONTINUED :

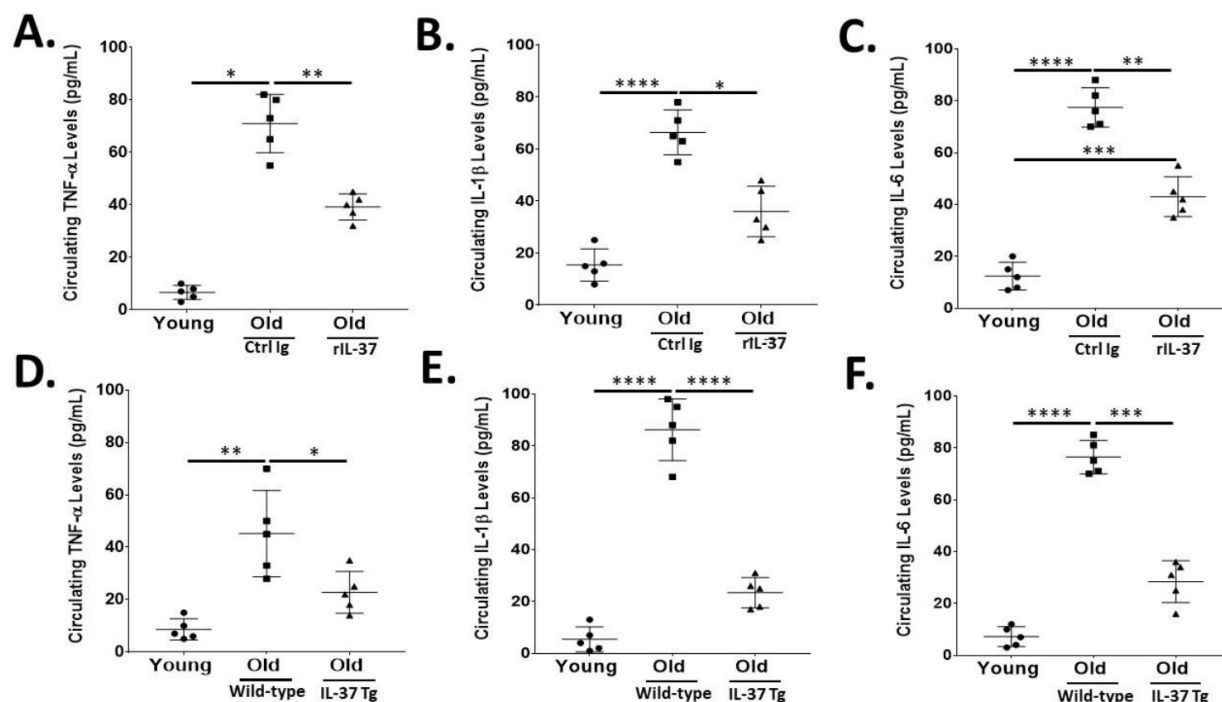


Figure S1. Transgenic Expression of and Treating Aged Mice with Interleukin-37 Abrogates Aging-associated Chronic Inflammation. (A-C) Aged (24 months old) mice were treated with Ctrl Ig and rIL-37 intravenously every 2 days for 2 weeks. Serum was collected from mice and circulating levels of TNF-α, IL-1β, and IL-6 were determined via ELISA analysis. (D-F) Serum was collected from aged (24 months old) wild-type and IL-37tg mice, and ELISA analysis was performed to determine the circulating levels of TNF-α, IL-1β, and IL-6. Means + s.d. are shown with * $p < 0.05$, ** $p < 0.01$, *** $p < 0.001$, and **** $p < 0.0001$ determined using a one-way ANOVA with Tukey's post-test. $n = 5$ mice/group.

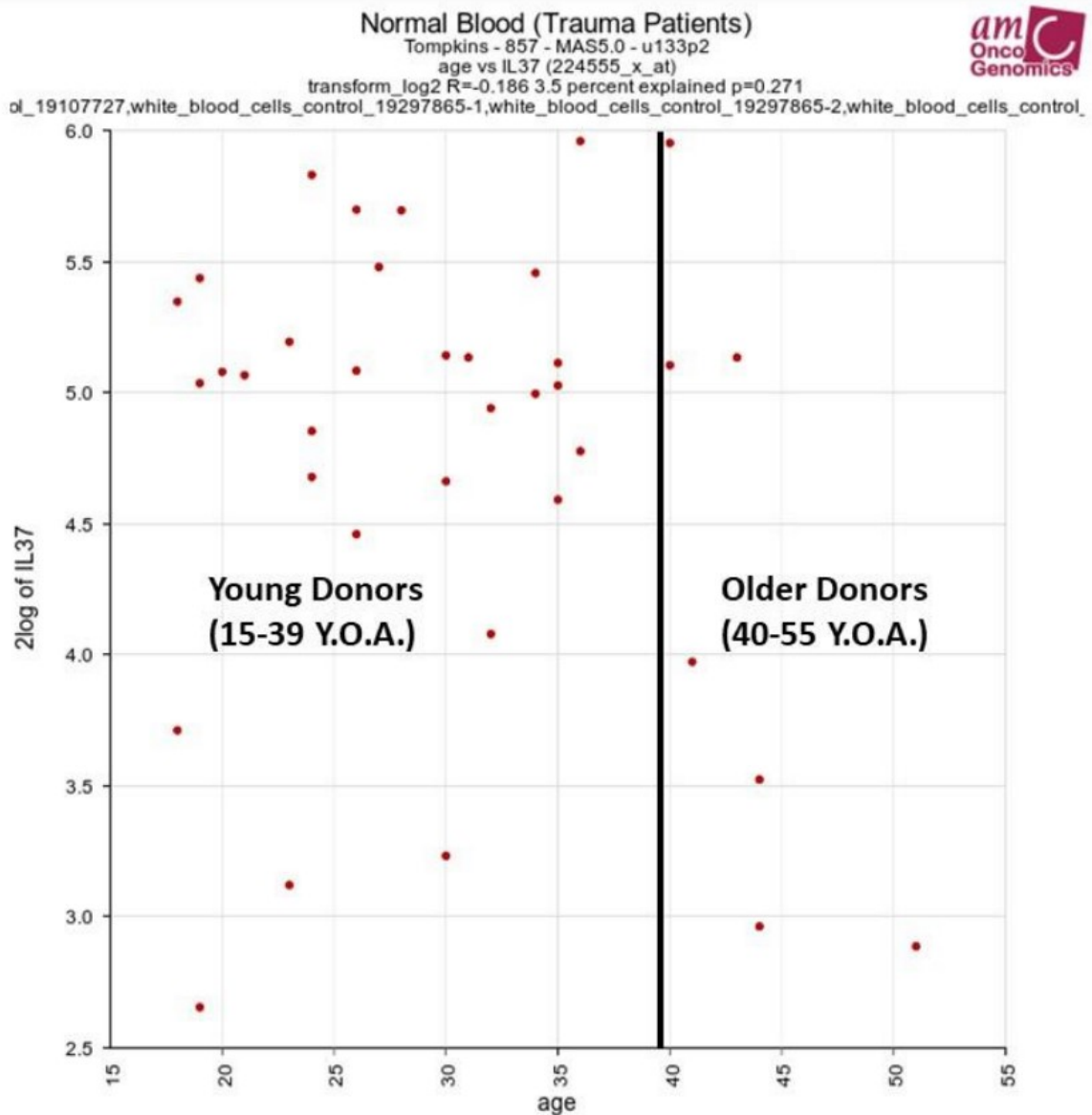


Figure S2. IL-37 gene expression levels in leukocytes isolated from young and middle-aged healthy donors. The R2 Database was utilized to determine the gene expression levels of IL-37 across age ranges. The database used was from Tompkin's study, where 37 healthy control samples were used to determine the gene expression levels of IL-37 in leukocytes. The GEO ID of the Tompkins study is gse36809.

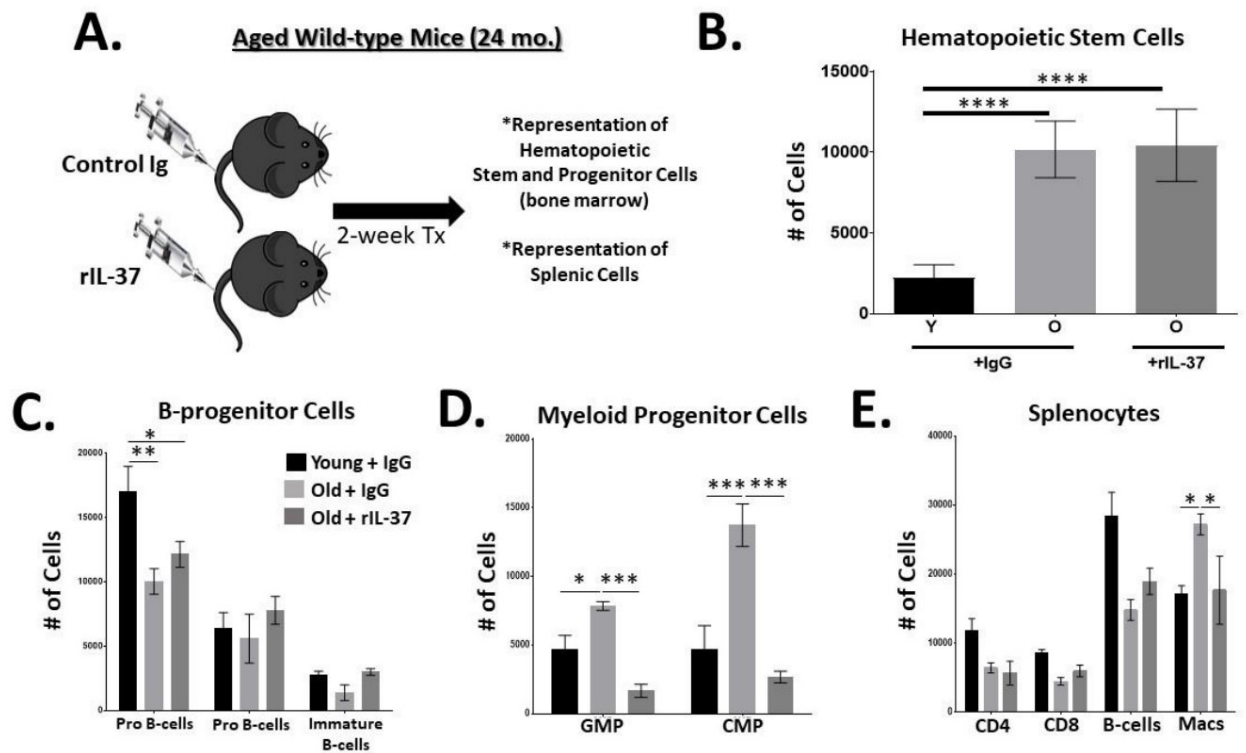


Figure S3. Treating aged mice with recombinant Interleukin-37 suppresses aging-associated increases in myelopoiesis. (A) Aged (24 months old) C57BL/6 wild-type mice were treated with control immunoglobulin (Control Ig) or recombinant IL-37 (rIL-37) every other day for 2 weeks to assess global changes in immunity. (B-D) Bone marrow was isolated from sacrificed mice to determine the representation of hematopoietic stem cells, Bprogenitor cells, and myeloid progenitor cells [GMP: Granulocyte-monocyte progenitors/CMP: Common myeloid progenitors] using flow cytometric analysis. (E) Spleens were isolated to determine the representation of T-cells (CD4⁺ and CD8⁺), B-cells, and macrophages (Macs) using flow cytometric analysis. Means + s.d. are shown with *p<0.05, **p<0.01, ***p<0.001, and ****p<0.0001 determined using a one-way ANOVA with Tukey's post-test in B-E. n=5 mice/group.

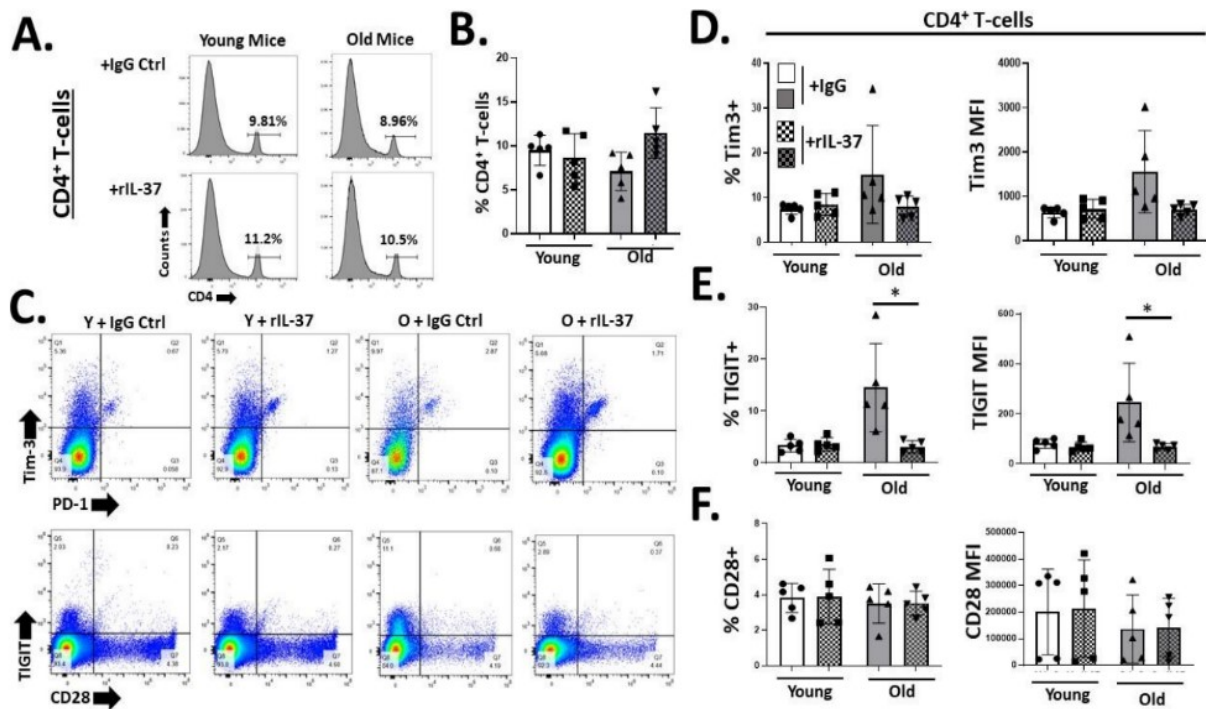


Figure S4. Recombinant IL-37 treatment of aged mice reduces TIGIT expression on naïve CD4⁺ T-cells. Aged (24 months old) C57BL/6 wild-type mice were treated with control immunoglobulin (Control Ig) or recombinant IL-37 (rIL-37) every other day for 2 weeks to assess global changes in immunity. (A-B) Splenocytes were harvested from treated mice and stained to enumerate the percent of T-helper cells via flow cytometric analysis. (C-F) Naïve T-helper cells were also stained to assess their surface expression of immunoinhibitory (Tim-3, PD-1, and TIGIT) and costimulatory (CD28) receptors. The percent and MFI of these receptors in D-F are shown as means + s.d. with * $p < 0.05$. Significance was determined using the Student's t-test relative to young +IgG or old+IgG controls with $n=5$ mice/group.

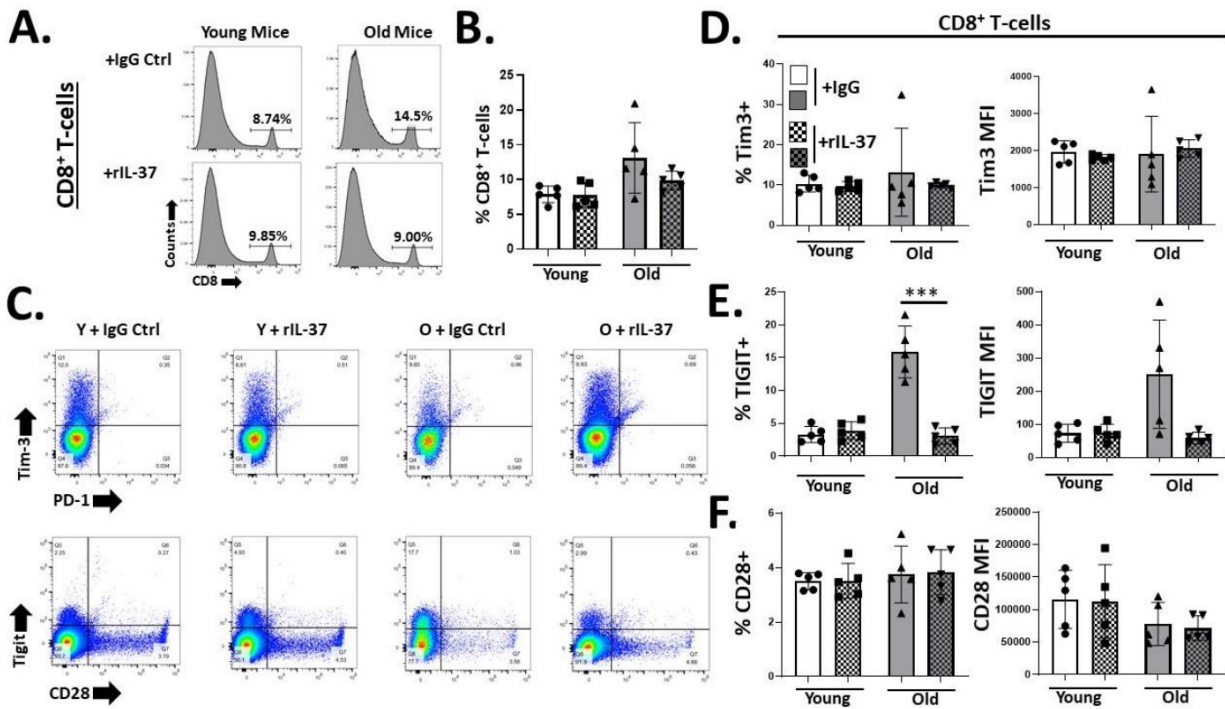


Figure S5. Recombinant IL-37 treatment of aged mice reduces TIGIT expression on naïve CD8⁺ T-cells. Aged (24 months old) C57BL/6 wild-type mice were treated with control immunoglobulin (Control Ig) or recombinant IL-37 (rIL-37) every other day for 2 weeks to assess global changes in immunity. (A-B) Splenocytes were harvested from treated mice and stained to enumerate the percent of cytotoxic lymphocytes cells via flow cytometric analysis. (C-F) Naïve cytotoxic lymphocytes were also stained to assess their surface expression of immunoinhibitory (Tim-3, PD-1, and TIGIT) and costimulatory (CD28) receptors. The percent and MFI of these receptors in D-F are shown as means + s.d. with * $p < 0.05$. Significance was determined using the Student's t-test relative to young +IgG or old+IgG controls with $n = 5$ mice/group.

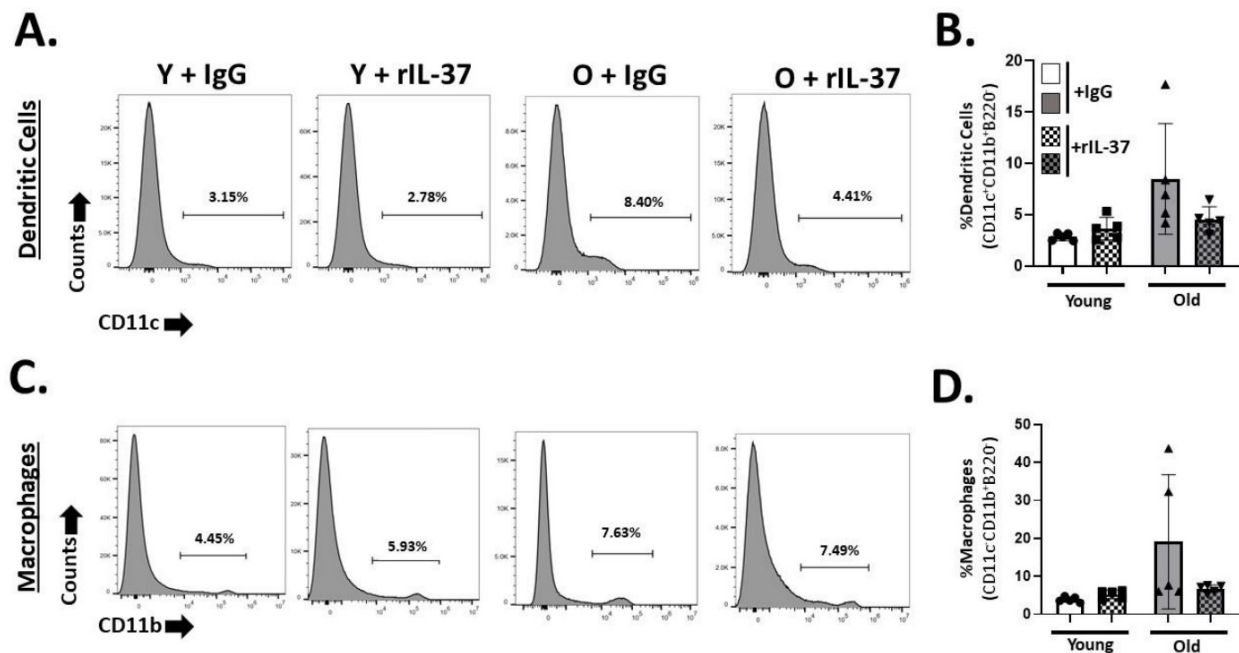


Figure S6. Recombinant IL-37 treatment of aged mice reduces the percentage of splenic-derived myeloid cells. Aged (24 months old) C57BL/6 wild-type mice were treated with control immunoglobulin (Control Ig) or recombinant IL-37 (rIL-37) every other day for 2 weeks to assess global changes in immunity. (A-B) Splenocytes were harvested from treated mice and stained to enumerate the percent of conventional dendritic cells (CD11c⁺ /CD11b⁺ /B220⁻ , A and B) and macrophages (CD11c⁻ /CD11b⁺ /B220⁻ , C and D) via flow cytometric analysis. The means + s.d. are shown in B and D with n=5 mice/group.

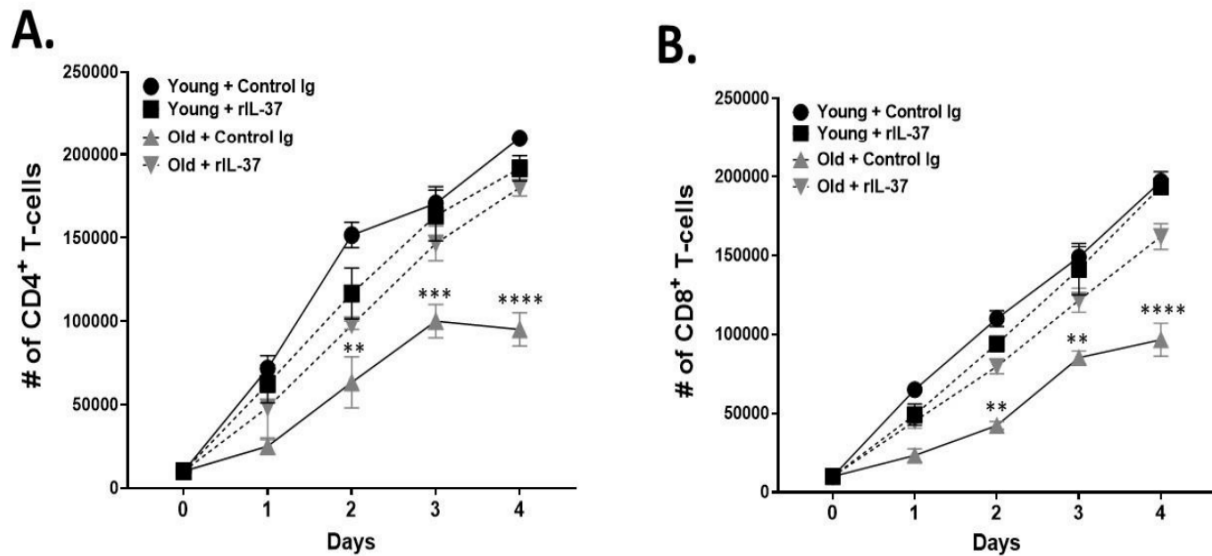


Figure S7. Recombinant IL-37 treatment abrogates aged T-cell exhaustion leading to a youthful proliferative capacity. Aged (24 months old) C57BL/6 wild-type mice were treated with control immunoglobulin (Control Ig) or recombinant IL-37 (rIL-37) every other day for 2 weeks. Purified T-cells were stimulated ex vivo with α CD3/ α CD28 antibody stimulation. T-cells were plated at 2×10^4 cells/well on Day 0, and the total number of cells were enumerated each day for 4 days via trypan blue exclusion assays. The means + s.d. are shown for each time point. Significance was determined using the Student's t-test relative to young + control Ig group with $n=5$ mice/group.

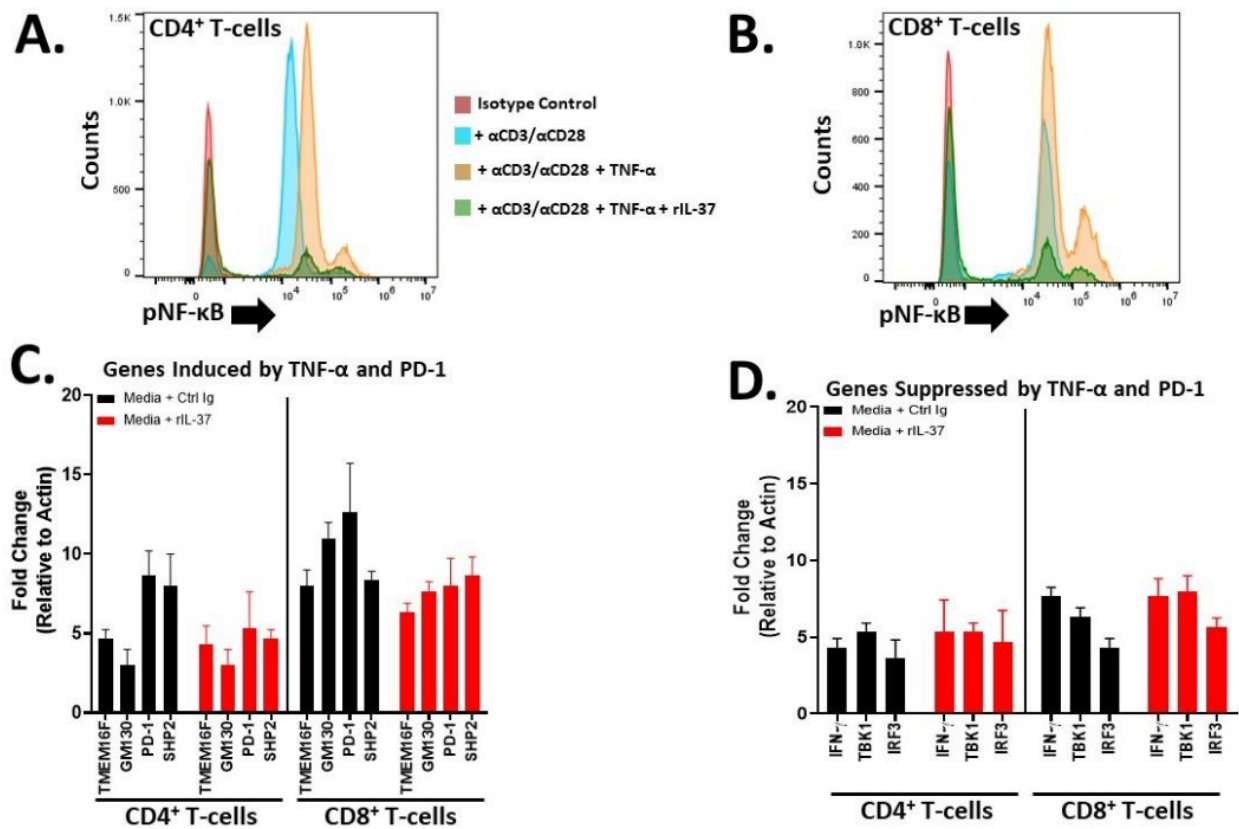


Figure S8. Recombinant IL-37 treatment opposes TNF- α signaling in aged, but not young, T-cells. Naïve CD4⁺ and CD8⁺ T-cells were purified from aged (24 months old) C57BL/6 mice via MACs selection and stimulated in vitro with α CD3/ α CD28 in the presence Control Ig, rTNF- α , or rTNF- α + rIL-37. (A and B) After 10' of stimulation, phospho-flow cytometry was performed to determine NF- κ B activation. Representative data are shown. (C and D) The experiment described above was performed on naïve T-cells purified from young (2 months old) C57BL/6 mice. Naïve T-cells were stimulated with Control Ig or rIL-37 for 4 hours. After the stimulation period, qPCR analysis was performed to ascertain the expression levels of genes involved in T-cell activation (IFN- γ , TBK1, IRF3) and inhibition (TMEM16F, GM130, SHP2, and PD1). Means + s.d. are shown with n=9 mice/group (3 independent experiments were conducted).

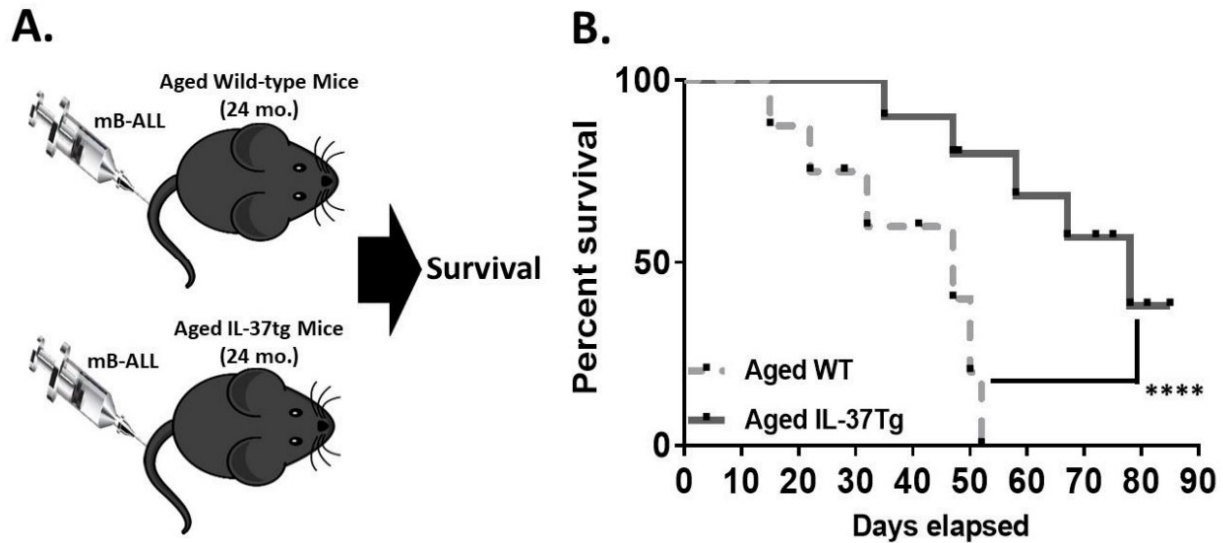


Figure S9. Interleukin-37 protects against B-cell acute lymphoblastic leukemia pathogenesis. (A) C57BL/6 wildtype and IL-37 transgenic mice were aged for 24 months, inoculated intravenously with BCR-ABL1+ Arf-/- murine B-ALL cells (mB-ALL) and (B) survival was monitored. Significance in B was determined using the log-rank test with **** $p < 0.0001$. $n = 10$ mice/group.

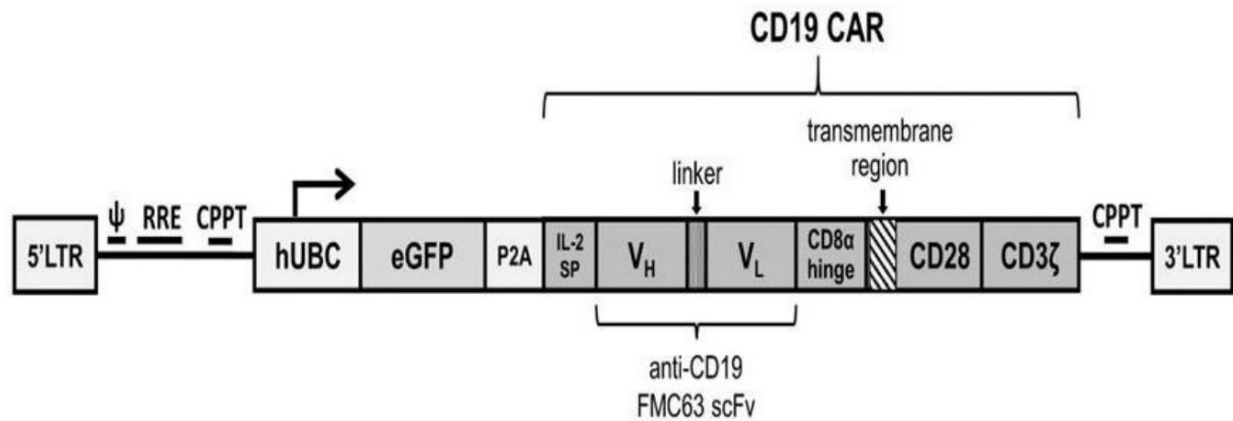


Figure S10. Schematic of the bicistronic construct encoding enhanced green fluorescent protein (eGFP) and the CD19-CAR. The transgene includes a 5' long terminal repeat (LTR), human ubiquitin C promoter (hUGC), eGFP, a P2A sequence, the CD19-CAR and a 3' LTR. Our second generation CD19-CAR consists of an interleukin-2 signal peptide (IL-2 SP), the anti-CD19 FMC63 single chain variable fragment (scFv), a CD8 alpha hinge region, the transmembrane and intracellular domains of CD28, and the CD3-ζ intracellular signaling domain.

**Chapter 3: Adipocyte-secreted IL-9
promotes B-cell acute lymphoblastic
leukemia progression**

3.1 Abstract

Increased adiposity associated with obesity is now recognized as a driver of many cancers. Indeed, recent studies have demonstrated that patients with B-cell acute lymphoblastic leukemia (**B-ALL**) presenting with high adiposity levels have inferior overall survival outcomes compared to lean patients. This relationship has been attributed to adipocyte-mediated sequestration of chemotherapies and the secretion of amino acids that protect leukemia cells from death; however, additional factors in the adipocyte secretome likely impact B-ALL pathogenesis. We have discovered that the cytokine interleukin-9 (IL-9) is secreted by murine and human adipocytes. Furthermore, we found that circulating IL-9 levels are elevated in patients with obesity and B-ALL and that human B-ALL cells exposed to the adipocyte-secretome upregulate the IL-9 receptor (IL-9R). Additionally, we found that IL-9 stimulation of human B-ALL cell increases phosphorylated retinoblastoma and E2F, while decreasing pro-apoptotic Bim protein levels. These molecular changes coincided with increased proliferation and the induction of chemoresistance in leukemia cells. In xenograft experiments we observed that loss of the IL-9R on human B-ALL cells did not impact disease kinetics in lean mice, whereas IL-9R-deficient B-ALL cells were more indolent in obese mice. These findings demonstrate that IL-9 is produced by adipocytes and promotes B-ALL pathogenesis.

3.1 Introduction

The United States Center for Disease Control reports that obesity rates in children and adolescents have more than tripled since the 1970's (Committee on Accelerating Progress in Obesity, Food et al. 2012, Fatima, Doi et al. 2015). Current forecast estimate that by 2030, 51% and 20% of the U.S. and global population, respectively, will be classified as presenting with obesity (Kelly, Yang et al. 2008, Finkelstein, Khavjou et al. 2012, Hruby and Hu 2015).

Leukemia is the most common cancer of children and adolescents, with B-cell acute lymphoblastic leukemia (B-ALL) being the most common subtype (Mullighan 2013, Whitehead, Metayer et al. 2016, Rajkumar and Vijay 2017, Brayley, Stanton et al. 2019). Recently, obesity has been identified as a risk factor in leukemia patients with obesity and is associated with poor survival outcomes (Butturini, Dorey et al. 2007, Eissa, Zhou et al. 2017), due to increased levels of residual disease after initial treatment protocols (Orgel, Tucci et al. 2014).

The obesity phenotype is not only an increase in the body mass index (BMI) of an individual, but there are also several molecular characteristics of obesity to consider. Obese individuals have higher circulating levels of proinflammatory cytokines and chemokines (IL-2, IL-6, TNF- α , MCP-1) inducing a chronic low grade inflammatory state (Indulekha, Surendar et al. 2015, Ellulu, Patimah et al. 2017, Kochumon, Al Madhoun et al. 2020). The abundance of adipocytes found in obese individuals supports chronic inflammation as well as promoting chemoresistance in ovarian cancer and breast cancer (Lehuédé, Li et al. 2019, Yang, Zaman et al. 2019). Studies from Mittelman et. al have found that adipocytes can act as chemotherapeutic depots promoting chemoresistance and disrupting the pharmacokinetics of chemotherapies (Behan, Avramis et al. 2010,

Pramanik, Sheng et al. 2013, Sheng, Parmentier et al. 2017). In a previous study, our lab found that the adipocyte secretome upregulated the surface expression of Galectin-9 on human B-ALL cells and promoted chemoresistance to multiple frontline chemotherapies (Lee, Hamilton et al. 2022).

Given the pleiotropic impact of adipocyte-secreted factors on B-ALL cells, we wanted to identify soluble factors that could promote B-ALL pathogenesis in addition to previously published soluble drivers. Given our recent findings that the adipocyte, but not the bone marrow stromal cell secretome, induced B-ALL chemoresistance, we mined our Luminex data to identify soluble factors differentially secreted by these cell types (Lee, Hamilton et al. 2022). Among differentially secreted soluble factors, we identified interleukin-9 (IL-9) as a candidate of interest due to its high level of secretion by adipocytes relative to stromal cells.

Interleukin-9 is a pleiotropic cytokine in the IL2R γ chain family that is produced by several cell types including Th9 cells, Tc9 cells, Mast cells and V δ 2 T cells (Goswami and Kaplan 2011, Chakraborty, Kubatzky et al. 2019, Do-Thi, Lee et al. 2020, Wan, Wu et al. 2020). Interleukin-9 receptor signaling activates the STAT and the MAPK pathway and IL-9 has been shown to promote proliferation and survival of non-malignant cells (Yang, Ricciardi et al. 1989, Goswami and Kaplan 2011, Lin and Leonard 2018, Leonard, Lin et al. 2019, Do-Thi, Lee et al. 2020). Although the role of IL-9 has been explored in both innate and adaptive non-malignant cells, the impact of IL-9 on the function of malignant B-ALL cells is unknown (Vink, Warnier et al. 1999, Veldhoen, Uyttenhove et al. 2008, Elyaman, Bradshaw et al. 2009, Thomas, Targan et al. 2017, Takatsuka, Yamada et al. 2018, Do-Thi, Lee et al. 2020). In chronic lymphocytic leukemia, elevated levels of IL-9 are correlated with a poor prognosis and promotion of the CLL tumor microenvironment

(Chen, Lv et al. 2014, Patrussi, Capitani et al. 2021). In acute myeloblastic leukemia (AML), IL-9 stimulation increases the colony formation ability and the proportion of AML cells in S-phase (Lemoli, Fortuna et al. 1996). Furthermore, recombinant IL-9 treatment of human diffuse large B-cell lymphoma (DLBCL) cell lines promotes proliferation and chemoresistance *in vitro* (Lv, Feng et al. 2013, Lv, Feng et al. 2016). In our study, we present data demonstrating that the IL-9R is expressed on the surface of B-ALL cells and can be found expressed across different B-ALL subtypes. Furthermore, we have found that B-ALL cells respond to IL-9 addition by increasing proliferation and induction of chemoresistance to frontline chemotherapies. This study also demonstrates the secretion of IL-9 from adipocytes, a previously undescribed phenotype.

3.2 Materials & Methods

ELISA and Luminex Analyses

To obtain a comprehensive profile of cytokine and chemokine production by bone marrow stromal cells and adipocytes, we performed a Luminex analysis using the Milliplex 32-plex cytokine/chemokine assay kit (Millipore Sigma, cat# MCYTMAG-70K-PX32). To validate our Luminex results we performed ELISA analysis of adipocyte and stromal cell supernatants, murine peripheral blood, and human plasma to detect IL-9 levels (Thermofisher, cat#88-8092-88) (Thermofisher, cat# BMS2081), per the manufacturers' protocols.

Patient IL-9 IHC Analysis

10 paraffin embedded adipose tissue samples from bariatric surgery patients, were stained for IL-9 (LSBio, cat#LS-C348950) at a 1:100 dilution. These samples were

processed by the Winship Cancer Tissue and Pathology core. Images were taken at 20x magnification using the BioTek Lionheart FX microscope. Blinded image quantification conducted using the Klein scoring technique [101].

St. Jude Pecan Database

The gene expression FPKM of the IL-9R across B-ALL subtypes accessed from the St. Jude Pecan Database. The baseline level of IL-9R from healthy PBMC's are from the GTEx portal.

Immunofluorescence

0.1% Poly-L-lysine (cat# P8920, Sigma-Aldrich) was added to each well of a μ -Slide 8 well chambered coverslip (cat# 80826, Ibidi) for 2 hours at 4°C. The μ -Slide 8 well chambered coverslip was washed with 1X PBS without Mg²⁺ and Ca²⁺ 535 (cat# 536 SH30378.02, HyClone). B-ALL cells were cultured for 3 days in 10% RPMI1640 or 50ng rIL-9 in the Poly-L-lysine coated μ 537 Slide 8 well chambered coverslips. Cells were fixed using 4% Paraformaldehyde in PBS (cat# J91899, Alfa Aesar), and permeabilized by adding 0.1% NP-40 (cat# ab142227, Abcam). Three washes were conducted using 1X PBS without Mg²⁺ 538 and Ca²⁺ 539. Cells were then incubated at room temperature in 10% Normal Goat Serum (cat# 50062Z, Life Technologies) in order to block nonspecific binding sites. Human B-ALL cell lines were stained overnight with a primary antibody against IL-9R (cat#NBP2-61701, Novus Biologics, 1:100) α Tubulin (cat#2144S, Cell Signaling, 1:50). After 24 hours of primary antibody incubation, cells were incubated with secondary antibodies (AlexaFluor-488, cat# A11034, Invitrogen/ AlexaFluor-568, cat# A11057, Invitrogen/ AlexaFluor-635, cat# A31574, 544 Invitrogen) each at a 1:100 dilution. Cells were then washed with 1X PBS, followed by 3 washes with 1X Tris Buffer Saline (TBS).

After washing, cells were mounted with ProLong Gold mounting media containing DAPI (cat# P36941, Invitrogen). Images captured using the Olympus FV1000 microscope.

Flow Cytometry, Annexin-V/PI and EdU Staining

Annexin-V-FITC/PI staining was performed to measure apoptosis per the manufacturer's protocol (cat# BMS500FI-300, eBioscience). Cell cycle analysis was performed using the Click-iT EdU AlexaFluor 488 Flow Cytometry Kit (cat#C10425, Invitrogen) per the manufacturer's instructions. After EdU labeling, 5 μ L of Propidium iodide (20 μ g/mL) was used to stain for DNA content in each sample. B-ALL cells were stained with the IL-9R Antibody (cat#310404, Biolegend) for flow cytometry. All flow samples were acquired using the Beckman Coulter CytoFLEX flow and analyzed by using Flowjo software.

MTT-proliferation kit

To determine the ability of IL-9 to promote proliferation of B-ALL cells, the CellTiter 96 Non-Radioactive Cell Proliferation Assay (MTT) (cat#G4000, Promega) was used per the manufacturer's protocol.

Western Blot & qPCR

Western Blot's and qPCRs conducted using the same protocols in Lee et al., *Obesity-induced galectin-9 is a therapeutic target in B-cell acute lymphoblastic leukemia*, 2022.

Primary anti-human antibodies used: IL-9R (cat#NBP2-61701, Novus Bio), phosphoRb (cat#9308S, Cell Signaling), Total Rb (cat#9309s, Cell Signaling), E2F1 (cat#sc-56661, Santa Cruz), GAPDH (cat#97166S, Cell Signaling), Bcl-xL (cat#5082764S, Cell Signaling), BIM (cat#2933S, Cell Signaling), β -tubulin (cat#2144S, Cell Signaling), Bax (cat#5023S, Cell Signaling), BID (cat#2002S, Cell Signaling), MCL-1 (cat#5453S, Cell

Signaling), and BCL-w (cat#2724S, Cell Signaling). All primary antibodies used at dilutions of 1:1000 and all-secondary antibodies used at dilutions of 1:5000. Secondary Antibodies used: IRDye-800CW Goat anti-Rabbit (cat#926-32211, Li-Cor) and IRDye-680RD Goat anti-Mouse (cat#926-68070, Li-Cor). Protein signals were detected using the Li-Cor Odyssey CLx. Protein quantification via signal intensity performed using ImageJ software (NIH).

Murine diet induced obesity

C57BL/6 mice or NOG mice (NOD.Cg-Prkdc Il2rg/JicTac) were fed control (10% fat calories) or high-fat (60% fat calories) diets for two to four months prior to experimentation. The obese phenotype was verified in mice prior to experimentation based on previous published studies (Lee et al., *Obesity-induced galectin-9 is a therapeutic target in B-cell acute lymphoblastic leukemia*, 2022). Murine diet was purchased from Bio-Serv (cat# F4031 for control diets and cat# S3282 for high-fat diets) and sterilized by irradiation prior to usage.

***In vivo* experiments**

Male and female, lean and obese mice were challenged with mB-ALL i.v. ($1-2 \times 10^5$ BAML-MiG cells/ mouse) and (5×10^5 IL9R^{-/-} human REH B-ALL cells). Once signs of leukemia manifested such as lethargy, ruffled fur, labored breathing, and hunched posture then mice were humanely euthanized. Survival was monitored pre- and during treatment.

B-ALL cell lines

Human B-cell acute lymphoblastic leukemia (B-ALL) cells were gifted from Dr. Graham and Dr. Porter laboratories (The Department of Pediatrics at Emory University School of Medicine). Nalm6 cells were grown in RPMI1640 media (cat# 10-393040-CV, Corning) supplemented with 10% fetal bovine serum (FBS, cat# S11550, Atlanta Biologicals). REH, SEM, RCH-AcV, 697 cells were grown in RPMI1640 media supplemented with 20% FBS. GFP-expressing murine OP-9 bone marrow stromal cells were maintained in Alpha-Minimum Essential Medium (α MEM, cat# 15-012-CV, Corning) supplemented with 20% FBS.

IL-9R Knockout B-ALL cells

The company Synthego conducted the development of an IL-9R deficient B-ALL cell line. They utilize CRISPR to develop a knockout cell pool approach using REH B-ALL cells. This resulted in a cell pool with 52% of the cells containing the IL-9RKO. The Emory Flow Core then sorted these cells based on positive surface expression of the IL-9R.

Guide RNA sequence: CUUGGGAGUCUCUGUCACAG

Transcript ID: ENST00000244174.11

Statistical Analysis

Statistics were conducted utilizing the GraphPad prism software.

3.3 Results

Interleukin-9 is produced and secreted by murine and human adipocytes

Adipocytes play a role in progression and the induction of chemoresistance in many cancers [102-104], however the factors mediating these responses are still being elucidated. To this end, we conducted a cytokine and chemokine Luminex assay on supernatant from differentiated adipocytes and stromal cells and found that interleukin-9 (**IL-9**) was secreted by adipocytes. IL-9 levels were measured from the supernatant after three days of conditioning, which resulted in an average of 30 pg/mL in the adipocyte supernatant contrasting with an average of 0 pg/mL in the stromal supernatant (Fig. 1A). To our knowledge we are the first group to report the secretion of IL-9 by adipocytes. To validate this finding, we conducted an enzyme-linked immunosorbent assay (ELISA) analysis (Fig. 1B) and found IL-9 can be found in stromal conditioned media but is at significantly higher levels in adipocyte conditioned media. Given the importance of this finding in murine-derived adipocytes, we wanted to confirm IL-9 production from human adipocytes.

Visceral human adipose tissue was sectioned and a blinded histological examination on adipose tissue was conducted to ascertain IL-9 production (Fig. 1D). Importantly, this experiment was conducted on adipose tissue derived from lean and obese donors undergoing bariatric surgery. We found significantly higher levels of IL-9 in the adipose tissue of the patients with obesity compared with lean patients. The results from these experiments conclusively demonstrate that both murine and human adipocytes produce IL-9.

Circulating IL-9 levels are elevated in obese female and male mice

We used the diet induced obesity (**DIO**) murine model to ascertain how increases in adiposity impacted circulating IL-9 levels. Female and male C57BL/6 mice were placed on control (10%kcal/gm fat) and high-fat (60%kcal/gm fat) diets for a minimum of 2 months to induce obesity. We then recorded the weights of female and male mice on both diets and assessed circulating IL-9 levels via ELISA analysis. Linear regression analysis was then performed to compare the relationship between mouse weight and serum IL-9 levels. Correlation coefficient calculations demonstrated a significant positive correlation between increasing mouse weights and circulating IL-9 levels in both sexes of mice (Fig.1 C). Collectively these data demonstrate the secretion of a novel adipokine, IL-9, by adipocytes and demonstrate a dosing effect whereby circulating levels of IL-9 increase with weight gain.

The IL-9R is expressed on human B-ALL cells and is upregulated in response to the adipocyte secretome

The IL-9R is expressed on the surface of adaptive immune cells including T-cells and B-cells [105, 106]; however, to our knowledge, it's expression has not been assessed on B-ALL cells in the absence and presence of the adipocyte secretome. We first mined the St. Jude Pecan Cloud Database to assess IL-9R gene expression levels in primary patient samples relative to levels found in healthy peripheral blood mononuclear cells (PBMCs) reported in the Genotype-Tissue Expression (GTEx). We found IL-9R expression across B-ALL subtypes with notable increases in aggressive subtypes including Ph-like and infant ALL(INF) (Fig.2A).

To further confirm the expression of the IL-9R on human B-ALL cells we performed flow cytometric analysis to stain for its surface expression on multiple human B-ALL cell lines. From this experiment, we observed substantial IL-9R surface expression on all human B-ALL cell lines tested (Fig.2B). Interleukin-9 receptor protein expression in human B-ALL cells was also confirmed by confocal analysis and revealed that treating these leukemia cells with recombinant human IL-9 (**rh IL-9**) resulted in more punctate staining or aggregation of the IL-9R indicative of activation of the IL-9R (Fig. 2C). As a result of this response, we also determined how the gene and protein expression of the IL-9R on human B-ALL cells was impacted by the soluble microenvironment. We performed qPCR analysis to ascertain *IL-9R* gene expression levels in 6 human B-ALL cell lines cultured for 3 days in stromal and adipocyte conditioned media (Fig, 2D).

After normalizing to IL-9R gene expression levels found in leukemia cells cultured in unconditioned media, we observed that culturing B-ALL in SCM did not modulate IL-9R gene expression levels in most of the human B-ALL cell lines tested, with the exception of Nalm6 leukemia cells. In contrast, 5 out of the 6 human B-ALL cell lines test exhibited increased IL-9R expression when cultured in ACM, with the most pronounced responses observed in Nalm6, REH, and 697 cell lines. In contrast to the gene expression of the IL-9R on human B-ALL cells conditioned in adipocyte conditioned media; direct addition of rhIL-9 did not result in a significant protein upregulation in human REH cells (Fig.2E). These results demonstrate that human B-ALL cells express the IL-9R, it is responsive to IL-9 stimulation, and it is upregulated on leukemia cells in response to the adipocyte secretome.

IL-9 induces proliferation in human B-ALL cells

To determine the functional consequence of stimulating human B-ALL cells with rhIL-9, we first assessed how proliferation was impacted due documented reports of IL-9 mediated activation of STAT5 in non-malignant lymphocytes [107, 108] and proliferative responses induced in IL-9 stimulated AML and DLBCL cells [109, 110]. For these experiments, 4 human B-ALL cell lines were plated at the same density and left untreated or treated with rhIL-9 and the number of leukemia cells in culture was assessed every 12 hours using nonradioactive MTT assays. Notably, all human B-ALL cells responded to rhIL-9 stimulation, with significant increases in proliferation observed in RCH-AcV and SEM cells (Fig. 3A). Cell cycle analysis of rhIL-9-treated B-ALL cells confirmed that IL-9 stimulation increased B-ALL cycling and demonstrated that this effect could be achieved with doses as low as 100 picograms (Fig. 3B).

To determine how IL-9 induced human B-ALL proliferation, we assessed total and activated levels of proteins which regulate proliferation in leukemia cells. Of the candidates assessed, we observed a dose-dependent increase in phospho- and total retinoblastoma (**Rb**) protein levels, which coincided with increased E2F protein levels in rhIL-9 stimulated human B-ALL cells (Fig. 3C & 3D). Mechanistically, the phosphorylation of Rb releases E2F1 from the Rb-E2F1 complex, which then induces G1-S cell cycle progression. Based on our results, we speculate that this pathway is activated in human B-ALL cells exposed to IL-9-secreting adipocytes (Fig. 3E).

IL-9 protects human B-ALL from chemotherapy-mediated cytotoxicity

In addition to assessing the protein levels of regulators of cellular proliferation in human B-ALL cells stimulated with rhIL-9, we also determine how regulators of apoptosis were affected by this treatment. Notably, we found that the treating human B-ALL cells with increasing doses of rhIL-9 resulted a dose-dependent decrease in pro-apoptotic Bim protein levels (Fig. 4A and Supp 1). The IL-9-mediated downregulation of Bim_L and Bim_S in B-ALL was larger than the downregulation of the largest isoform Bim_{EL} (Fig. 4A and Supp 1). This is noteworthy because while all three isoforms are associated with induction of apoptosis, Bim_L and Bim_S are the more cytotoxic isoforms[111]. Given the importance of these findings, these results were corroborated with confocal analysis, we observed significantly lower Bim levels in human B-ALL cells treated with rhIL-9 (Fig. 4B).

Given these results, and published data demonstrating that IL-9 promotes chemoresistance in DLBCL cells [110], we next assessed how rhIL-9 stimulation impacted how human B-ALL cells respond to chemotherapy treatment. In these experiments, human B-ALL cells were pre-treated with rhIL-9 for 24 hours prior to chemotherapy treatment to better recapitulate what happens in a clinical setting. Treating human B-ALL cells with rhIL-9 resulted in a dose-dependent increase in chemoresistance to methotrexate (Fig. 4C). Similarly, IL-9 also significantly reduced the cytotoxic effects of doxorubicin at doses of 10 and 25 nanograms (Supp 1). In all, these results demonstrate that IL-9 promotes chemoresistance in human B-ALL cells to multiple frontline chemotherapies.

Interleukin-9 promotes human B-ALL progression

Noting the ability of IL-9 to promote B-ALL proliferation and chemoresistance *in vitro*, we sought to determine how IL-9 affects B-ALL progression *in vivo*. We utilized the previously mentioned DIO model and challenged wild type mice and IL-9 knockout mice with a murine B-ALL (GFP-expressing, BCR-ABL1+ /Arf-null). These experiments revealed that there was significant difference in survival in between lean and obese wild-type mice (Fig. 5A). Notably, there was also a significant extension in survival for obese IL9KO mice compared with the obese wild type mice. This highlights the potential for a reduction in global IL-9 levels to improve the survival of B-ALL patients with obesity. To further interrogate the relationship between IL-9 & B-ALL an IL-9RKO B-ALL cell line (REH parental) was developing by Synthego using a CRISPR-Cas9 based methodology. This IL-9R^{-/-} B-ALL cell line was found to not respond to IL-9 in the context of proliferation, cell cycle changes and chemoresistance (Fig. 5B & 5C, Supp 3A). These results demonstrate that the IL-9R is functionally inactive in these cells, preventing the cells from responding to exogenous rhIL-9.

Immunodeficient mice (NOD.Cg-Prkdc^{scid} Il2rg^{tm1Sug}/JicTac) were then placed on the high fat or control diet until the obesity phenotype was established; these mice were then challenged with the IL9R^{-/-} human B-ALL cells (Fig.5D, Supp 3B, Supp 3C). Although there was not a significant improvement in the survival of mice challenged with the IL9R deficient B-ALL cells, there was a delay in the kinetics of disease progression in these mice. Collectively these data demonstrates that IL-9 promotes B-cell acute lymphoblastic leukemia.

IL-9 plasma levels are positively correlated with BMI in pediatric patients with B-ALL

Similar to results found in mice (Figure 1C), we wanted to determine if circulating IL-9 levels correlated with BMI in pediatric patients with B-ALL. In the healthy pediatric donors, there was a positive, yet insignificant, correlation between BMI and plasma IL-9 levels (Fig6A). Conversely, in patients with B-ALL, there was both a positive and statistically significant correlation between BMI and plasma IL-9 levels, suggesting that IL-9 could promote disease progression in obese patients with B-ALL and could serve as a biomarker for disease severity (Fig 6B). In summary, the data presented here demonstrates that adipocytes secrete IL-9 which binds to B-ALL cells, driving pro-survival and pro-proliferative pathways leading to a more aggressive B-ALL (Fig 6C.).

3.4 Discussion

Patients with obesity have a higher concentration of adipocytes, and these adipocytes have been shown to be inflammatory and promote poor outcomes in solid and hematological cancers [112-114]. In leukemia patients with obesity there are higher levels of chemoresistance and poor survival outcomes [115-117]. The molecular mechanisms driving poor outcomes for patients with obesity remain understudied, highlighting the need for additional research into how adipokines promote or antagonize cancer cells, how the different adipose tissue depots interact with cancer cells, and how adipokines could be used as predictive markers of patient's response or outcomes.

In these studies, we present data demonstrating that IL-9 is secreted by adipocytes and circulating IL-9 can be found at higher levels in mice fed a high-fat diet compared to mice on a control diet. Immunohistochemistry of adipose tissue from patients with obesity showed higher levels of IL-9 expression when compared with lean patients. To our knowledge we are the first group to show the secretion of IL-9 from adipocytes and expression of IL-9 in patient adipose tissue.

Interleukin-9 has been shown in nonmalignant and malignant cells to promote cell growth and colony formation [118, 119]. However, the relationship between IL-9 and B-ALL remains understudied. Our findings demonstrate that the IL-9R is expressed across numerous human B-ALL subtypes and expressed in human B-ALL cell lines. This receptor is upregulated when B-ALL cells are cultured in adipocyte conditioned media, illustrating a relationship between a high adipose environment and B-ALL. Furthermore, the addition of rIL-9 to leukemia cells increases the percentage of cells in S-phase and subsequently increases proliferation of those cells. The protein Rb when phosphorylated

(pRb) serves as a checkpoint in the cell cycle, and an increase in the expression of pRb can release the cell cycle promoter E2F1[120, 121]. Western blot analysis revealed that upon addition of rIL9 to human B-ALL cells there was an increase in pRb levels and the cell cycle promoter E2F1 highlighting a novel proliferative mechanism. Thus, we propose the novel mechanism that IL-9 drives proliferation through the upregulation of E2F1 in human B-ALL cells.

Chemoresistance is a common issue in cancer patients with obesity [122-124]. Therefore, how adipocytes impact pharmacokinetics and pharmacodynamics is an area of increasing biomedical research. Notably, adipocytes have been shown to sequester chemotherapy and release of cancer promoting fatty acids and metabolites which antagonize the cytotoxic/cytostatic actions of multiple classes of chemotherapies [125-129]. We have found that addition of rIL9 to B-ALL cells induced chemoresistance to both methotrexate and doxorubicin. Upon treatment with rIL9 human B-ALL cells reduce the expression of the cytotoxic isoforms of the pro-apoptotic Bim protein, notably all three isoforms are induced in pre-B acute lymphoblastic leukemia cells treated with glucocorticoids [130]. Furthermore, when the IL-9R is knocked out this chemoresistance is ablated. To our knowledge we are the first group to illustrate the ability of IL-9 to induce chemoresistance to methotrexate and doxorubicin in B-ALL.

When an immunocompetent murine model is challenged with a murine B-ALL, the IL-9KO mice exhibited significantly improved survival when compared to their wild-type counterparts. Furthermore, NOG mice challenged with an IL-9R null human B-ALL did have delayed disease kinetics despite not seeing a significant difference in survival. These *in vivo* studies highlight the importance of IL-9 to the progression of B-ALL in high

adipose environments. Importantly, in human B-ALL patients but not healthy patients we found there is a positive correlation with obesity and IL-9 levels in the plasma, suggesting that in high BMI patients, IL-9 may be utilized as a biomarker. This study provides evidence that IL-9 is secreted by adipose tissue, can be found at higher levels in patients with obesity and is able to induce proliferation, chemoresistance and cell cycle progression.

3.5 Figures, Supplemental Figures & Tables

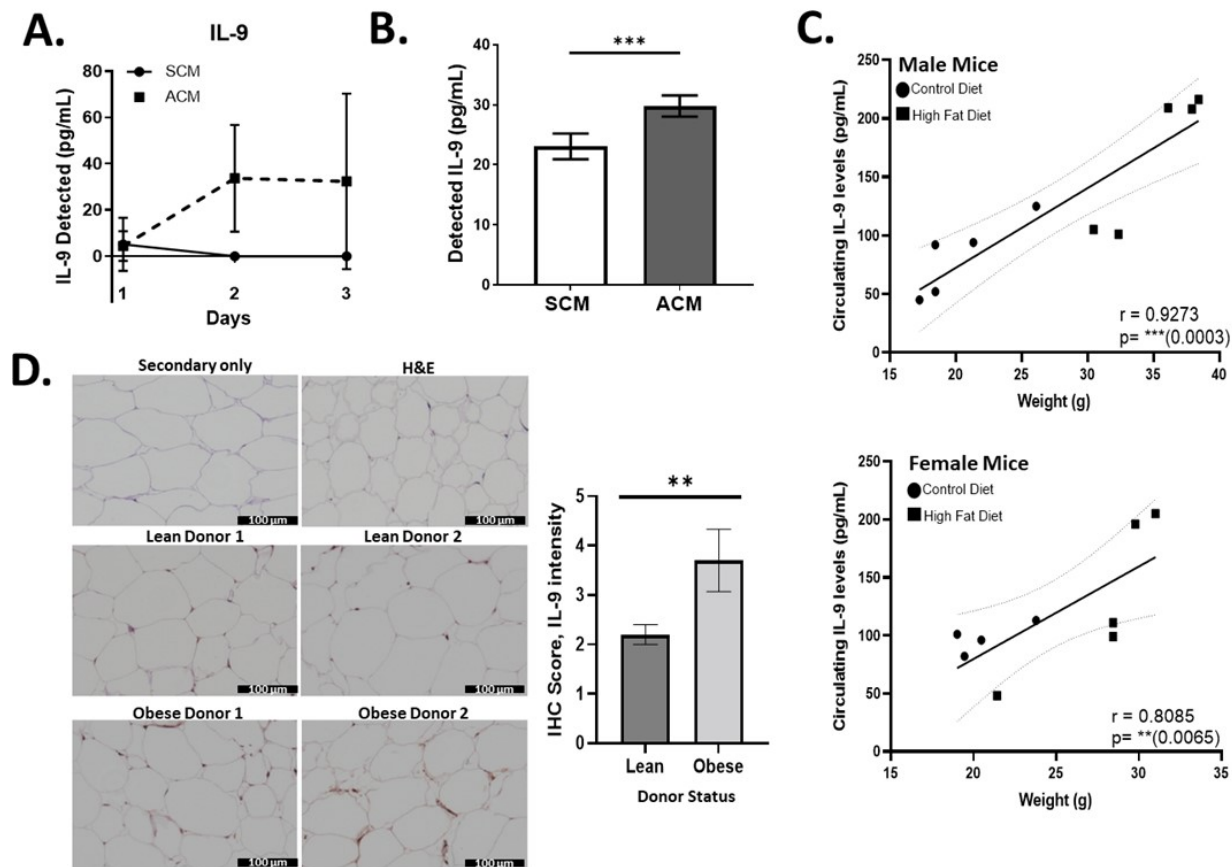


Figure 1: Interleukin-9 is secreted by adipocytes and is elevated in obese mice. **A.** Luminex assay of adipocyte and stromal supernatant at day 1,2 and 3. **B.** ELISA assay of adipocyte supernatant and stromal supernatant(n=3). **C.** Correlation between weight and circulating IL-9 levels from ELISA assay, male and female mice. **D.** IHC for IL-9 in adipose tissue from human donors, blinded IHC quantification by DKG.

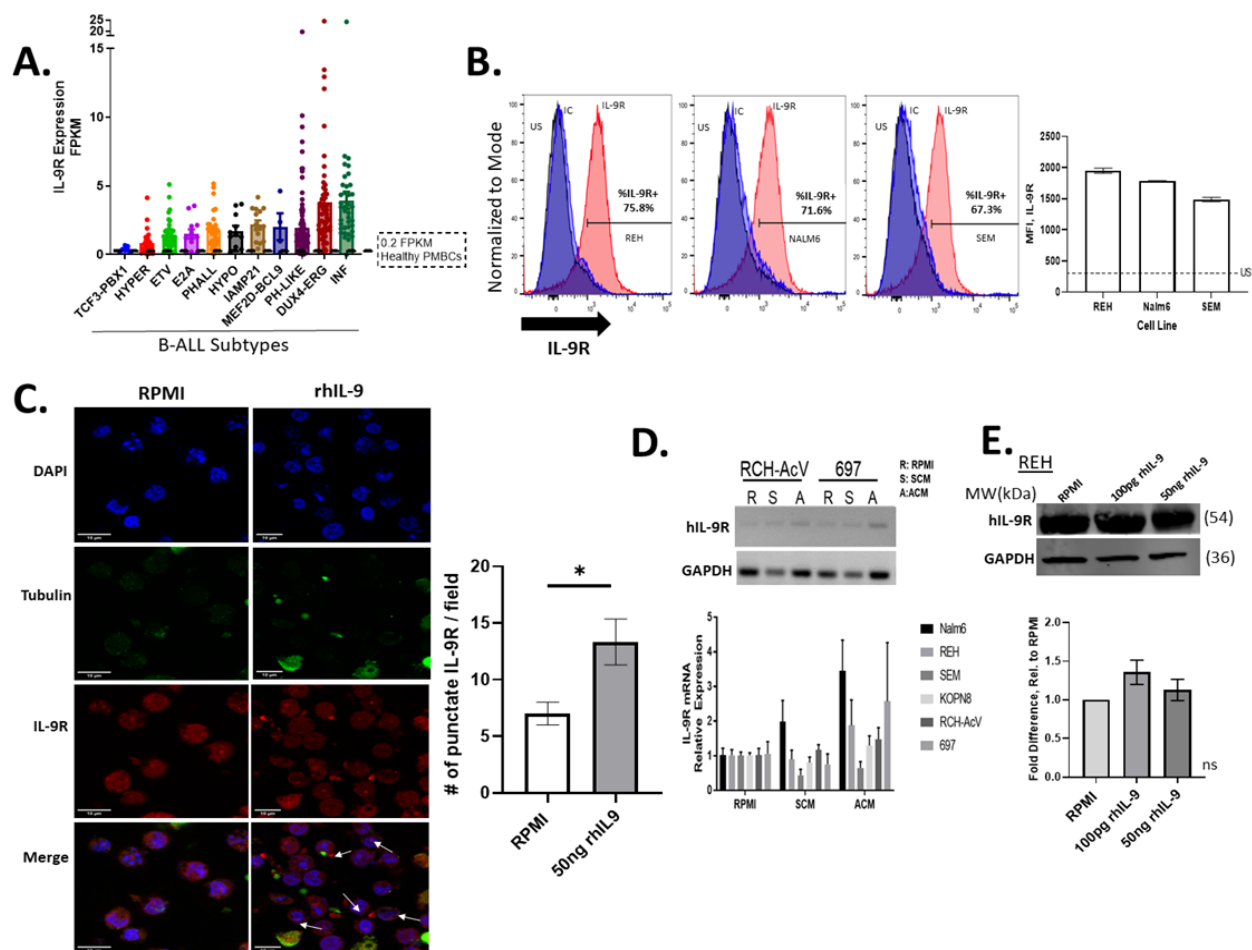


Figure 2: Interleukin-9 Receptor is expressed on human B-ALL cells and is upregulated in adipocyte secretome. **A.** IL-9R gene expression data from St. Jude Pecan Database and GTex database. **B.** Flow cytometry of IL-9R, US-unstained, IC-Isotype control. Mean fluorescent intensity (MFI) of IL-9R. **C.** Confocal microscopy of REH cell line for IL-9R, DAPI (blue), Tubulin (Green), IL-9R (Red) 60x magnification. Quantification, # of punctate IL-9R across three fields. **D.** qPCR of IL-9R after 3 days of conditioning in adipocyte or stromal conditioned media. **E.** Western Blot of IL-9R after addition of rIL9 with quantification.

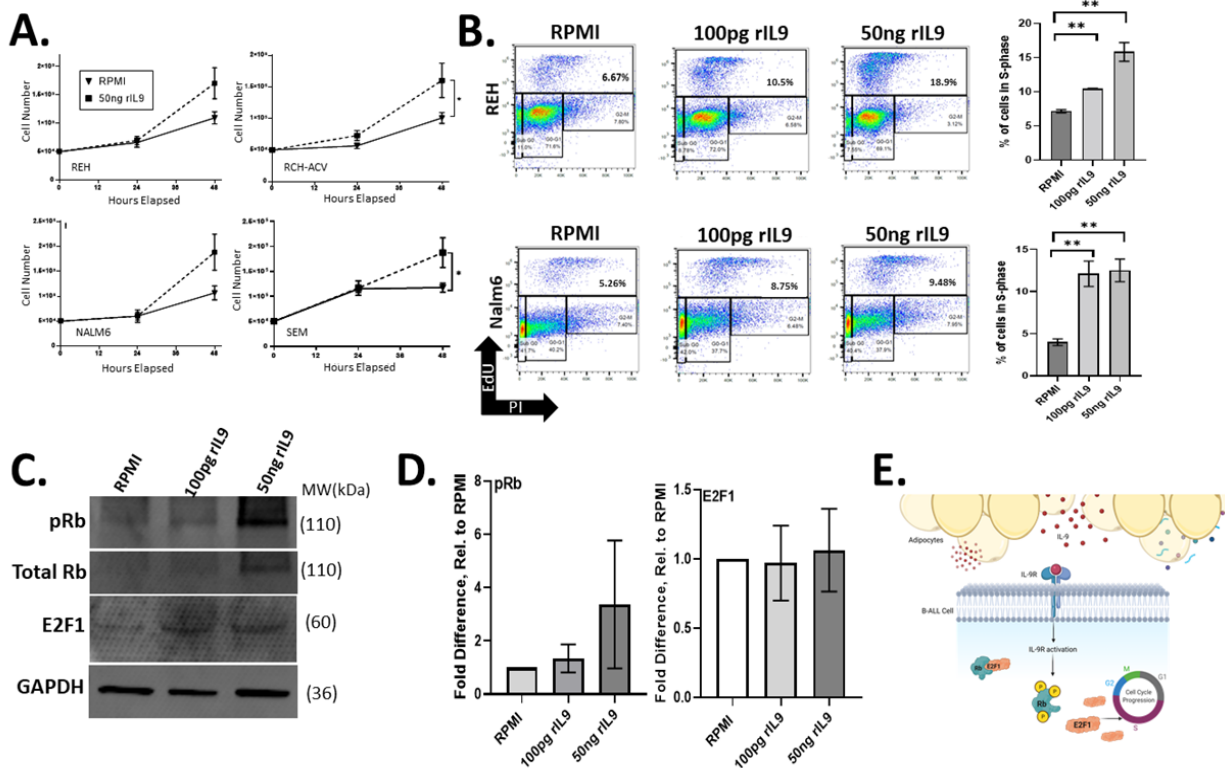


Figure 3: Interleukin-9 induces proliferation in human B-ALL cells. A. Proliferation of human B-ALL cell lines measured using MTT non-radioactive proliferation assay, untreated cells vs. 50ng rIL9 treated cells. **B.** EdU flow cytometry results to determine cell cycle differences between untreated and recombinant human IL-9 treated cells at a low dose (100pg) and high dose (50ng). **C.** Western Blot of human B-ALL cells (REH) after 24 hours of conditioning with 100pg and 50ng rIL9. **D.** Quantification of Western Blot in C, with the fold difference relative to RPMI. **E.** Graphical illustration created in Biorender of postulated mechanism of IL-9 promoting cell cycle progression.

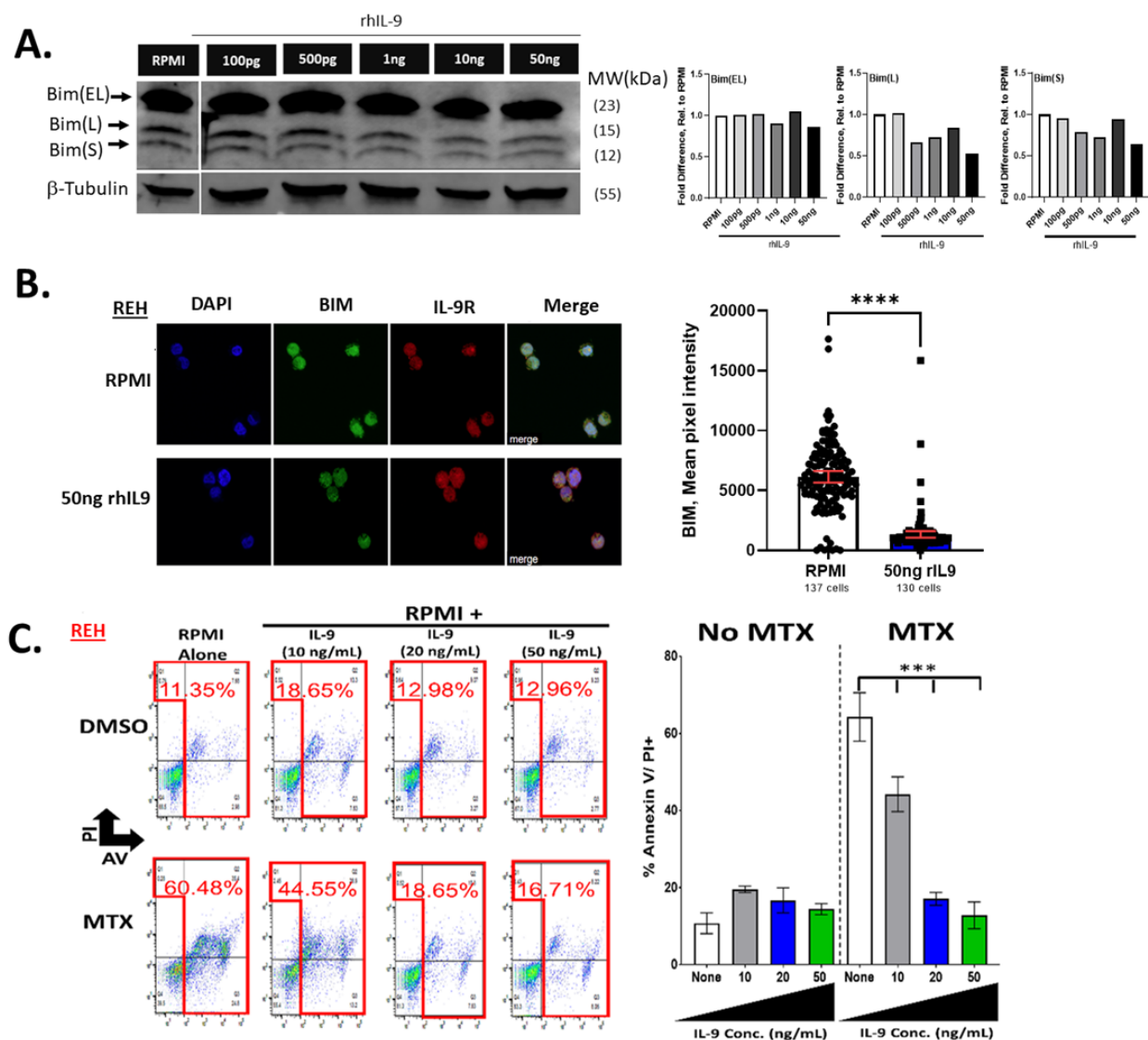


Figure 4: Interleukin-9 protects human B-ALL cells from chemotherapy-mediated cytotoxicity. **A.** Western Blot of BIM protein levels in human B-ALL cells (REH) after 24 hours of conditioning with increasing doses of rIL9. **B.** Confocal microscopy of REH cells, top panel: untreated cells, bottom panel: rIL9 treated cells. Images taken 24 hours post treatment. Quantification conducted using Lionheart FX software. DAPI(Blue), BIM(Green), IL-9R(Red) **C.** Annexin-5/PI assay on REH cells after 24 hours of conditioning with rIL9 and a subsequent 48 hours with methotrexate (MTX). Top panel: untreated, Bottom panel: treated with increasing doses of rIL9.

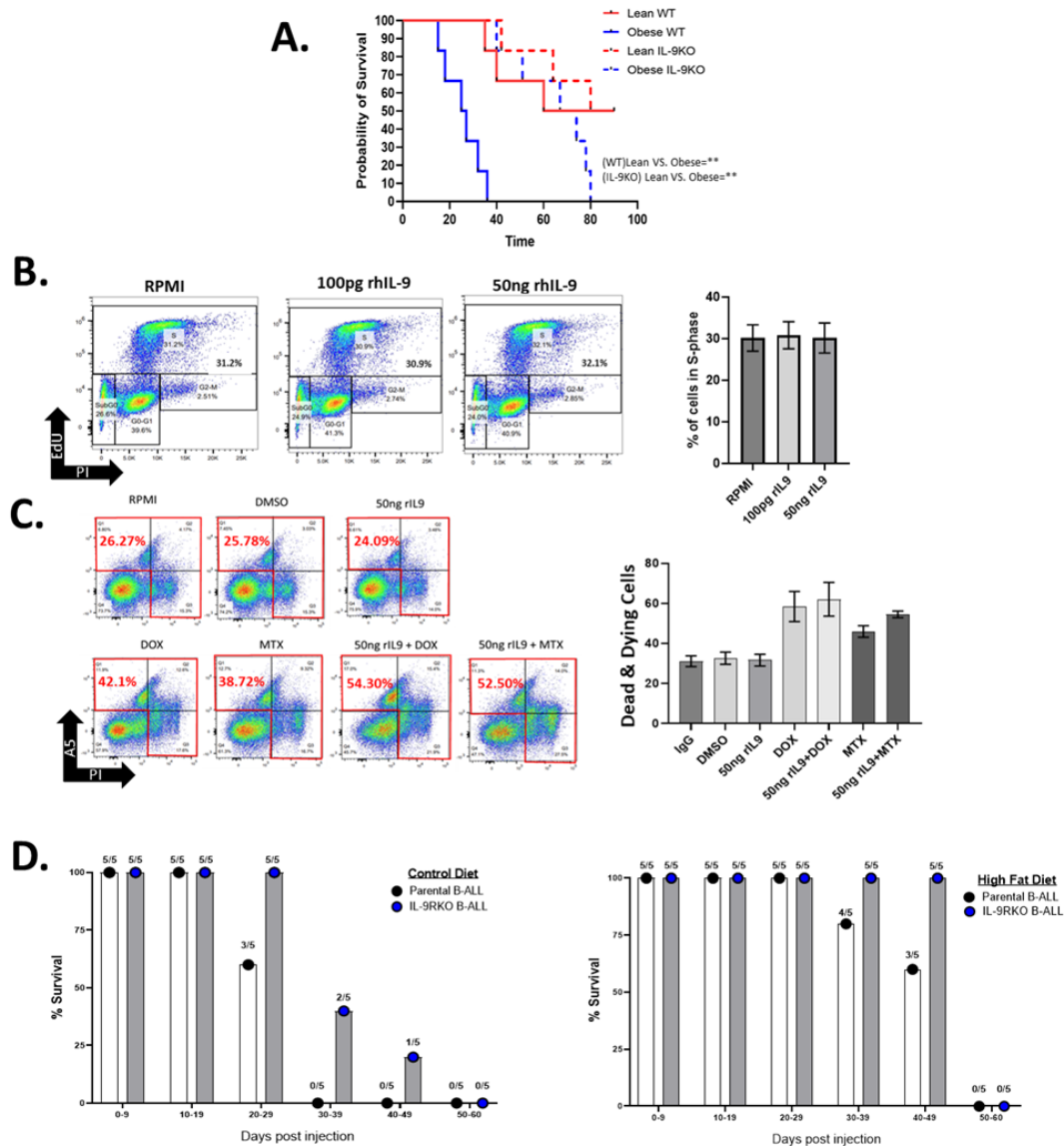


Figure 5: Interleukin-9 promotes B-ALL progression. **A.** Kaplan Meier Survival curve of IL-9 global KO mice, challenged with murine BAML-MiG leukemia (i.v. $1-2 \times 10^5$ cells/injection) **B.** EdU flow cytometry results of IL-9R^{-/-} B-ALL cell line, REH, to determine cell cycle differences between untreated and recombinant human IL-9 treated cells at a low dose (100pg) and high dose (50ng) **C.** Annexin-5/PI assay on IL-9R^{-/-} cells after 24 hours of conditioning with rIL9 and a subsequent 48 hours with methotrexate(MTX) or doxorubicin(DOX). **D.** Survival of NOG/NODscid mice post injection with IL-9R null B-ALL or parental REH cells (i.v. 5×10^5 cells/injection).

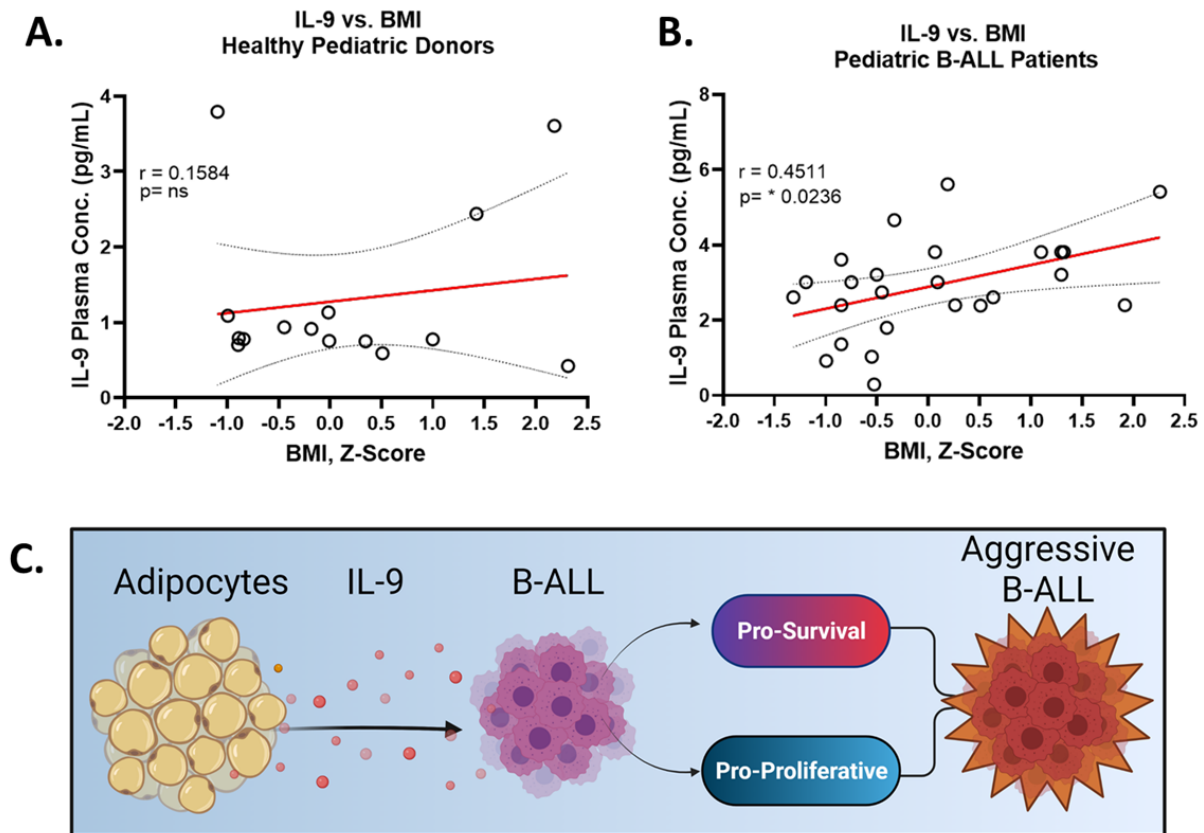
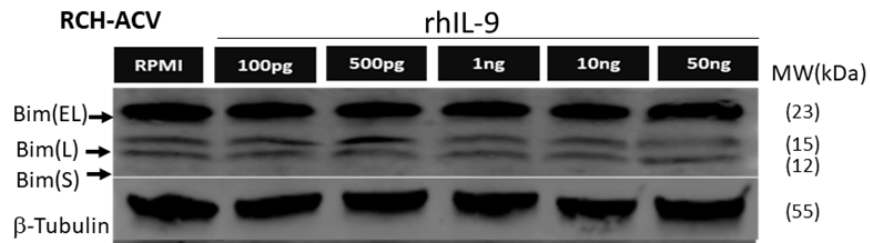
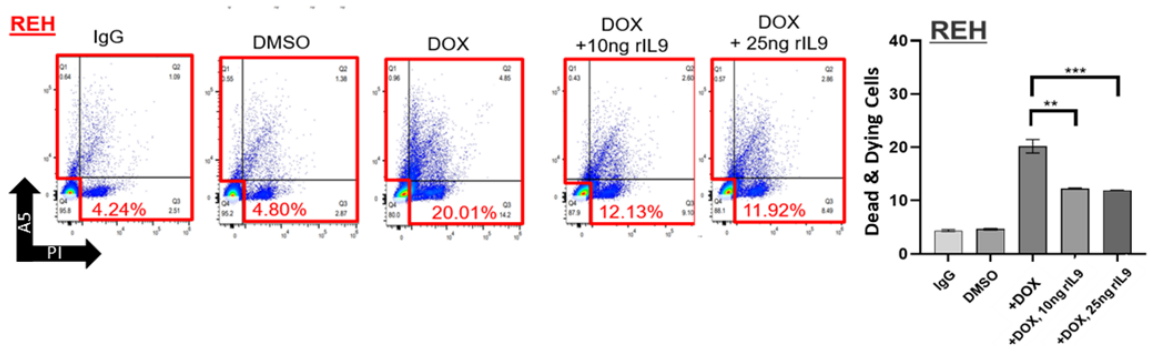
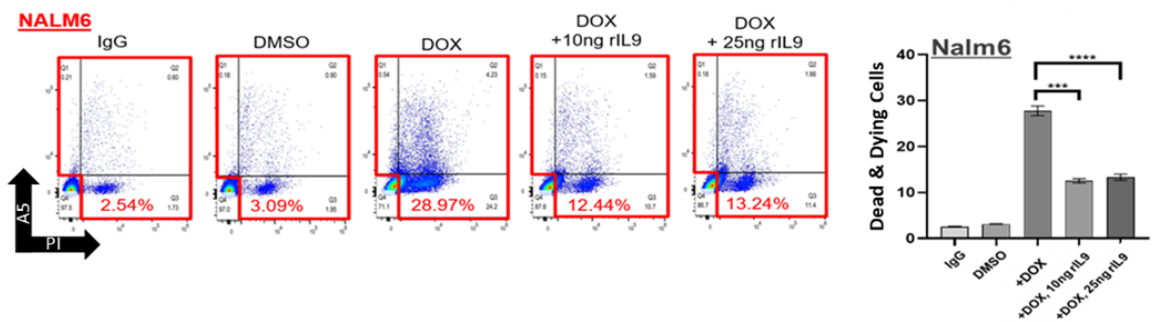
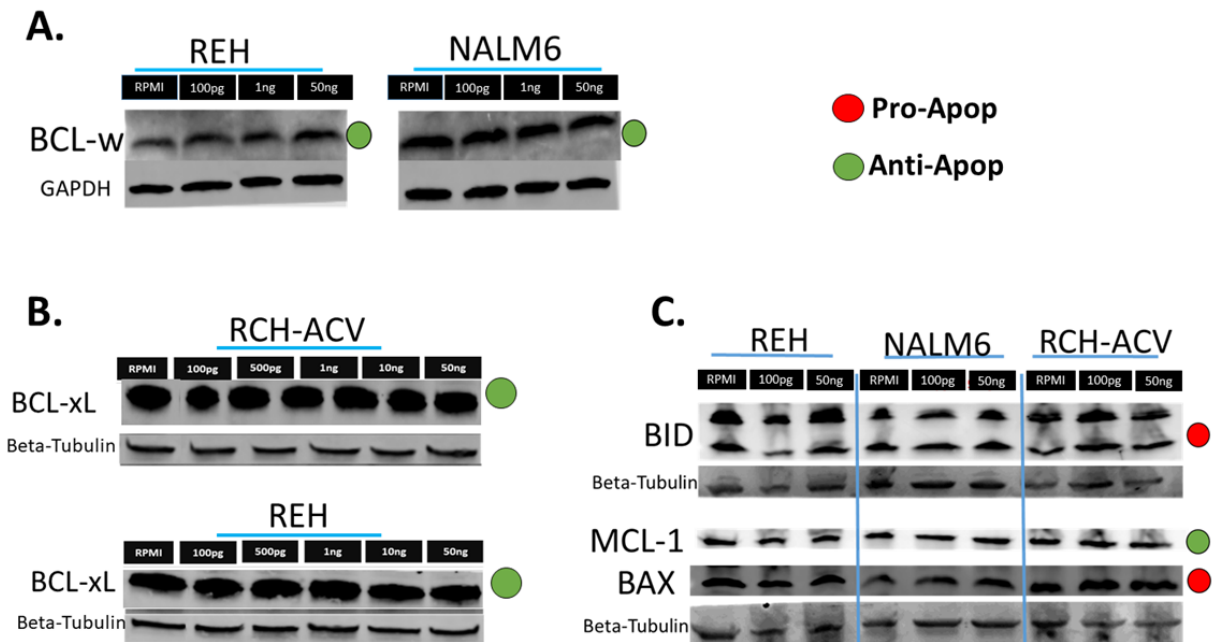


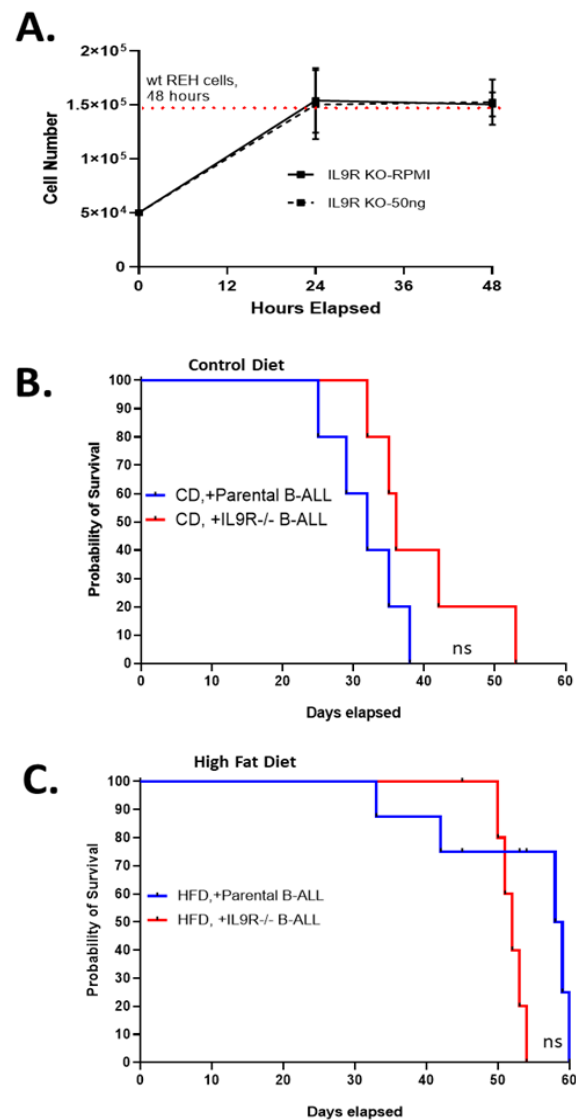
Figure 6: Interleukin-9 plasma levels are positively correlated with BMI in patients with B-ALL. **A.** Plasma levels of IL-9 via ELISA from healthy pediatric donors vs. BMI of the donors. **B.** Plasma levels of IL-9 via ELISA from pediatric B-ALL patients vs. BMI of the pediatric patients. **C.** Graphical demonstration of how secretion of IL-9 by adipocytes can drive an aggressive B-ALL phenotype.

A.**B.****C.**

Supplemental Figure 1: IL-9 promotes chemoresistance to frontline chemotherapies. **A.** Western Blot of BIM protein levels in human B-ALL cells (REH) after 24 hours of conditioning with increasing doses of rIL9. **B.** Annexin-5/PI assay on REH cells after 24 hours of conditioning with rIL9 and a subsequent 48 hours with doxorubicin (DOX). **C.** Annexin-5/PI assay on Nalm6 cells after 24 hours of conditioning with rIL9 and a subsequent 48 hours with doxorubicin (DOX).



Supplemental Figure 2: IL-9 does not significantly alter expression of apoptotic mediators. **A.** Western Blot of BCL-w protein levels in human B-ALL cells (REH, NALM6) after 24 hours of conditioning with increasing doses of rIL9. **B.** Western Blot of BCL-xL protein levels in human B-ALL cells (REH, RCH-ACV) after 24 hours of conditioning with increasing doses of rIL9. **C.** Western Blot of BID, MCL-1, and BAX protein levels in human B-ALL cells (REH, NALM6, RCH-ACV) after 24 hours of conditioning with increasing doses of rIL9.



Supplemental Figure 3: IL-9 does not extend the survival of mice transplanted with human B-ALL. **A.** Proliferation of human IL-9R^{-/-} B-ALL cell lines measured using MTT non-radioactive proliferation assay, untreated cells vs. 50ng rIL9 treated cells. **B.** Survival of NOG/NODscid mice on control diet, post injection with IL-9R null B-ALL or parental REH cells (i.v. 5x10⁵ cells/injection). **C.** Survival of NOG/NODscid mice on high fat diet, post injection with IL-9R null B-ALL or parental REH cells (i.v. 5x10⁵ cells/injection).

A.

Adipose Tissue Donors, Fig 1D		
	(n=2)	(n=8)
Age (years)		
Median	51.5	30
Range	48,55	19-52
Gender(n)		
Female	2	6
Male	0	2
Body Mass Index (BMI)		
Median	22.9	48.6
Range	20,25	40-64

Supplemental Figure 4: Patient characteristics from adipose tissue donors.

A.

Healthy Pediatric Donors, Fig 6A	
Pediatric Donors (n=15)	
Age (years)	
Median	7
Range	2.0-16.0
Gender(n)	
Female	6
Male	9
Body Mass Index, BMI	
Median	23.2
Range	15.2-40.5

B.

Pediatric Leukemia Patients, Fig 6B	
Leukemia Patients (n=25)	
Age (years)	
Median	6.9
Range	2.2-17.4
Gender(n)	
Female	10
Male	15
Body Mass Index, BMI	
Median	16.7
Range	12.7-27.2
ETV6 RUNX1 n(% positive)	
	4/25 (16%)
BCR-ABL1 n(%positive)	
	1/25 (4%)
Trisomy 4 n(%positive)	
	11/25 (44%)
Trisomy 10 n(%positive)	
	9/25 (36%)
Double Trisomy n(%positive)	
	11/25 (44%)

Supplemental Figure 5: Patient characteristics of pediatric donors and B-ALL patients.

Chapter 4: Discussion

4.1 Summary and implications of results

The research presented in this dissertation seeks to help two aggrieved patient populations who will experience sustained growth in the future. The “silver tsunami” of aged individuals is already affecting our woefully unprepared healthcare system as aged individuals are on track to outpace the younger generation within the United States. Furthermore, the obese population has tripled since the 70’s and is estimated to continue to grow at a sustained rate.

In the last two decades, survival rates in patients with leukemia have significantly improved [131, 132]. However, in patients that survive, issues persist including those associated with toxicity. Furthermore, in patients with relapsed and refractory disease effective treatment options were limited until the revolutionary breakthrough of immunotherapies [133, 134]. Despite their unquestionable success, the efficacy of immunotherapies can be limited by mutations in target antigens, an immunosuppressive microenvironment, manufacturing and cost concerns, and adverse events such as cytokine storms. Within this dissertation we highlight novel cytokines which may be targeted to treat patients with obesity (IL-9) and aged patients (IL-37) which may improve the efficacy of chemotherapy and immunotherapy treatments, respectively.

Importantly, we demonstrate that recombinant IL-37 treatment can improve T-cell-mediated immunity in aged backgrounds, reduce the effects of chronic inflammation and increase the efficacy of aged CAR T-cells. These results demonstrate that components of aging-associated immune senescence are reversible and further support emerging literature demonstrating the effectiveness of targeting the inflammatory microenvironment to improve the efficacy of immunotherapies (Bouchlaka et al., 2013;

Maude, Barrett, et al., 2014). This study will be vital as the aged population increases and the use of immunotherapies become more prevalent in this growing demographic.

Notably, our studies on the impact of obesity on B-ALL development demonstrated that murine adipocytes secrete IL-9, which was also found at higher levels in adipose tissue from patients with obesity relative to their lean counterparts. We discovered that human B-ALL express the IL-9 receptor and can respond to stimulation by this cytokine. Notable phenotypes observed in IL-9 stimulated human B-ALL cells included increased proliferation, cell cycle progression, and the induction of chemoresistance. Molecular changes in IL-9-stimulated human B-ALL cells included phosphorylation of retinoblastoma (**Rb**) and E2F1 (which likely drove the increased proliferation observed) and the downregulation of potent pro-apoptotic forms of Bim (which likely promoted chemoresistance). In murine studies we found that challenging immunocompromised mice with human IL-9R-deficient B-ALL cells delayed disease kinetics, which highlights the possibility of utilizing neutralizing antibodies as a novel treatment approach during the maintenance phase of therapy. These results were corroborated by our syngeneic studies which demonstrated a significant extension in the survival of IL-9KO relative to wild-type mice after transplanting murine B-ALL cells. These results present a novel mechanism for a cytokine that has primarily been studied in the realm of allergic inflammation.

4.2 Limitations and Future Directions

Questions frequently remain unanswered in scientific research due to the lack of analytical tools, time, and fiscal resources. As scientists, we do our best to both answer and ask critical questions and produce results despite these limitations.

In our aging studies, barriers included our inability to conduct a longitudinal study of IL-37 in aged human individuals (with and without leukemia) due to sample limitations. Furthermore, we still need to determine how IL-37 impacts chemotherapy treatment, and vice versa. The addition of these studies are important research directions for this project.

The next steps for our obesity study should include, when human donor samples become available, conducting IL-9 ELISAs on secretomes collected from human adipocytes (non-diseases and patients with B-ALL). For the latter, it would be interesting to perform this assay at various disease stages including at diagnosis, induction, maintenance, remission, and relapse. Furthermore, it is important to identify the endogenous stimuli which induces IL-9 production from adipocytes, and we need to develop a more comprehensive understanding of what pathways are activated or suppressed in IL-9-stimulated B-ALL cells. Additionally, there are numerous adipocyte anatomical depots: visceral, bone-marrow and subcutaneous adipocytes; each of which are also morphologically distinct, being comprised of either brown, white or beige adipocytes. The determination of which population of adipocytes is driving the secretion of IL-9 would be valuable, given that the dominant population fluctuates based on a person's age (e.g., brown adipose tissue is higher in pediatric populations). These studies could help future researchers determine which population could benefit from the use of

an IL-9 neutralizing antibody treatment, which has already been explored clinically as a treatment for asthma[135].

It is my sincere hope that the scientific community will utilize this research as a framework for the development of future projects which aim to target the inflammatory milieu to improve treatment outcomes in high-risk patients with ALL.

REFERENCES

1. Kanasi, E., S. Ayilavarapu, and J. Jones, *The aging population: demographics and the biology of aging*. Periodontol 2000, 2016. **72**(1): p. 13-8.
2. Bluethmann, S.M., A.B. Mariotto, and J.H. Rowland, *Anticipating the "Silver Tsunami": Prevalence Trajectories and Comorbidity Burden among Older Cancer Survivors in the United States*. Cancer Epidemiol Biomarkers Prev, 2016. **25**(7): p. 1029-36.
3. Rappuoli, R., et al., *Vaccines, new opportunities for a new society*. Proc Natl Acad Sci U S A, 2014. **111**(34): p. 12288-93.
4. Ventola, C.L., *The antibiotic resistance crisis: part 1: causes and threats*. P t, 2015. **40**(4): p. 277-83.
5. Bae, J., Y.Y. Kim, and J.S. Lee, *Factors Associated With Subjective Life Expectancy: Comparison With Actuarial Life Expectancy*. J Prev Med Public Health, 2017. **50**(4): p. 240-250.
6. Lunenfeld, B. and P. Stratton, *The clinical consequences of an ageing world and preventive strategies*. Best Pract Res Clin Obstet Gynaecol, 2013. **27**(5): p. 643-59.
7. Henry, C.J., A. Marusyk, and J. DeGregori, *Aging-associated changes in hematopoiesis and leukemogenesis: what's the connection?* Aging (Albany NY), 2011. **3**(6): p. 643-56.
8. Weinberger, B., *Vaccines for the elderly: current use and future challenges*. Immun Ageing, 2018. **15**: p. 3.
9. Lord, J.M., *The effect of ageing of the immune system on vaccination responses*. Hum Vaccin Immunother, 2013. **9**(6): p. 1364-7.
10. Fulop, T., et al., *Aging, immunity, and cancer*. Discov Med, 2011. **11**(61): p. 537-50.
11. Cheryl D. Fryar, M.D.C., and Joseph Afful, *Prevalence of overweight, obesity, and severe obesity among children and adolescents aged 2–19 years: United States, 1963–1965 through 2017–2018*. NCHS Health E-Stats, 2020.
12. Hruby, A. and F.B. Hu, *The Epidemiology of Obesity: A Big Picture*. Pharmacoeconomics, 2015. **33**(7): p. 673-89.
13. Conway, B. and A. Rene, *Obesity as a disease: no lightweight matter*. Obes Rev, 2004. **5**(3): p. 145-51.
14. Bastard, J.P., et al., *Recent advances in the relationship between obesity, inflammation, and insulin resistance*. Eur Cytokine Netw, 2006. **17**(1): p. 4-12.
15. Kawai, T., M.V. Autieri, and R. Scalia, *Adipose tissue inflammation and metabolic dysfunction in obesity*. Am J Physiol Cell Physiol, 2021. **320**(3): p. C375-c391.
16. de Heredia, F.P., S. Gómez-Martínez, and A. Marcos, *Obesity, inflammation and the immune system*. Proc Nutr Soc, 2012. **71**(2): p. 332-8.
17. Galic, S., J.S. Oakhill, and G.R. Steinberg, *Adipose tissue as an endocrine organ*. Mol Cell Endocrinol, 2010. **316**(2): p. 129-39.
18. Bai, Y. and Q. Sun, *Macrophage recruitment in obese adipose tissue*. Obes Rev, 2015. **16**(2): p. 127-36.
19. Ghosh, A.R., et al., *Adipose Recruitment and Activation of Plasmacytoid Dendritic Cells Fuel Metaflammation*. Diabetes, 2016. **65**(11): p. 3440-3452.
20. Frasca, D., et al., *Obesity induces pro-inflammatory B cells and impairs B cell function in old mice*. Mech Ageing Dev, 2017. **162**: p. 91-99.
21. Rozhok, A. and J. DeGregori, *A generalized theory of age-dependent carcinogenesis*. Elife, 2019. **8**.

22. Evans, E.J., Jr. and J. DeGregori, *Cells with Cancer-associated Mutations Overtake Our Tissues as We Age*. *Aging Cancer*, 2021. **2**(3): p. 82-97.
23. DePinho, R.A., *The age of cancer*. *Nature*, 2000. **408**(6809): p. 248-54.
24. Herrera, A.P., et al., *Disparate inclusion of older adults in clinical trials: priorities and opportunities for policy and practice change*. *Am J Public Health*, 2010. **100** **Suppl 1**(Suppl 1): p. S105-12.
25. Aapro, M.S., et al., *Never too old? Age should not be a barrier to enrollment in cancer clinical trials*. *Oncologist*, 2005. **10**(3): p. 198-204.
26. Ruiter, R., J. Burggraaf, and R. Rissmann, *Under-representation of elderly in clinical trials: An analysis of the initial approval documents in the Food and Drug Administration database*. *Br J Clin Pharmacol*, 2019. **85**(4): p. 838-844.
27. Scher, K.S. and A. Hurria, *Under-representation of older adults in cancer registration trials: known problem, little progress*. *J Clin Oncol*, 2012. **30**(17): p. 2036-8.
28. Burd, C.E., et al., *Barriers to the Preclinical Development of Therapeutics that Target Aging Mechanisms*. *J Gerontol A Biol Sci Med Sci*, 2016. **71**(11): p. 1388-1394.
29. Fane, M. and A.T. Weeraratna, *How the ageing microenvironment influences tumour progression*. *Nat Rev Cancer*, 2020. **20**(2): p. 89-106.
30. Mangoni, A.A. and S.H. Jackson, *Age-related changes in pharmacokinetics and pharmacodynamics: basic principles and practical applications*. *Br J Clin Pharmacol*, 2004. **57**(1): p. 6-14.
31. Huizer-Pajkos, A., et al., *Adverse Geriatric Outcomes Secondary to Polypharmacy in a Mouse Model: The Influence of Aging*. *J Gerontol A Biol Sci Med Sci*, 2016. **71**(5): p. 571-7.
32. Amlacher, R., et al., *Influence of age on antileukemic action, subacute toxicity and tissue distribution of ambazone in B6D2F1 mice*. *Arch Geschwulstforsch*, 1990. **60**(1): p. 11-8.
33. von Moltke, L.L., et al., *Cognitive toxicity of drugs used in the elderly*. *Dialogues Clin Neurosci*, 2001. **3**(3): p. 181-90.
34. Ritz, P. and B. Vellas, *Pharmacokinetics and drug toxicity in elderly patients: a case for geriatric core data in clinical trials*. *J Nutr Health Aging*, 2007. **11**(3): p. 261-4.
35. Manna, P. and S.K. Jain, *Obesity, Oxidative Stress, Adipose Tissue Dysfunction, and the Associated Health Risks: Causes and Therapeutic Strategies*. *Metab Syndr Relat Disord*, 2015. **13**(10): p. 423-44.
36. Savini, I., et al., *Obesity-associated oxidative stress: strategies finalized to improve redox state*. *Int J Mol Sci*, 2013. **14**(5): p. 10497-538.
37. Crujeiras, A.B., et al., *Oxidative stress associated to dysfunctional adipose tissue: a potential link between obesity, type 2 diabetes mellitus and breast cancer*. *Free Radic Res*, 2013. **47**(4): p. 243-56.
38. Makki, K., P. Froguel, and I. Wolowczuk, *Adipose tissue in obesity-related inflammation and insulin resistance: cells, cytokines, and chemokines*. *ISRN Inflamm*, 2013. **2013**: p. 139239.
39. Siegel, R.L., et al., *Cancer statistics, 2022*. *CA Cancer J Clin*, 2022. **72**(1): p. 7-33.
40. Puckett, Y. and O. Chan, *Acute Lymphocytic Leukemia*, in *StatPearls*. 2022, StatPearls Publishing

Copyright © 2022, StatPearls Publishing LLC.: Treasure Island (FL).

41. Terwilliger, T. and M. Abdul-Hay, *Acute lymphoblastic leukemia: a comprehensive review and 2017 update*. *Blood Cancer J*, 2017. **7**(6): p. e577.
42. Woo, J.S., M.O. Alberti, and C.A. Tirado, *Childhood B-acute lymphoblastic leukemia: a genetic update*. *Exp Hematol Oncol*, 2014. **3**: p. 16.
43. Kimura, S. and C.G. Mullighan, *Molecular markers in ALL: Clinical implications*. *Best Pract Res Clin Haematol*, 2020. **33**(3): p. 101193.

44. Loghavi, S., J.L. Kutok, and J.L. Jorgensen, *B-acute lymphoblastic leukemia/lymphoblastic lymphoma*. *Am J Clin Pathol*, 2015. **144**(3): p. 393-410.
45. Kaseb, H., M.A. Tariq, and G. Gupta, *Lymphoblastic Lymphoma*, in *StatPearls*. 2022, StatPearls Publishing

Copyright © 2022, StatPearls Publishing LLC.: Treasure Island (FL).

46. Inaba, H. and C.G. Mullighan, *Pediatric acute lymphoblastic leukemia*. *Haematologica*, 2020. **105**(11): p. 2524-2539.
47. Chiaretti, S., G. Zini, and R. Bassan, *Diagnosis and subclassification of acute lymphoblastic leukemia*. *Mediterr J Hematol Infect Dis*, 2014. **6**(1): p. e2014073.
48. Chang, H.Y., et al., *Causes of death in adults with acute leukemia*. *Medicine (Baltimore)*, 1976. **55**(3): p. 259-68.
49. Loh, M.L., et al., *Tyrosine kinome sequencing of pediatric acute lymphoblastic leukemia: a report from the Children's Oncology Group TARGET Project*. *Blood*, 2013. **121**(3): p. 485-8.
50. Pieters, R., et al., *A treatment protocol for infants younger than 1 year with acute lymphoblastic leukaemia (Interfant-99): an observational study and a multicentre randomised trial*. *Lancet*, 2007. **370**(9583): p. 240-250.
51. Brown, P., *Treatment of infant leukemias: challenge and promise*. *Hematology Am Soc Hematol Educ Program*, 2013. **2013**: p. 596-600.
52. Gröbner, S.N., et al., *The landscape of genomic alterations across childhood cancers*. *Nature*, 2018. **555**(7696): p. 321-327.
53. Iacobucci, I. and C.G. Mullighan, *Genetic Basis of Acute Lymphoblastic Leukemia*. *J Clin Oncol*, 2017. **35**(9): p. 975-983.
54. Belson, M., B. Kingsley, and A. Holmes, *Risk factors for acute leukemia in children: a review*. *Environ Health Perspect*, 2007. **115**(1): p. 138-45.
55. Menegaux, F., et al., *Household exposure to pesticides and risk of childhood acute leukaemia*. *Occup Environ Med*, 2006. **63**(2): p. 131-4.
56. Jabbour, E., et al., *New insights into the pathophysiology and therapy of adult acute lymphoblastic leukemia*. *Cancer*, 2015. **121**(15): p. 2517-28.
57. Chan, E.S. and B.N. Cronstein, *Methotrexate--how does it really work?* *Nat Rev Rheumatol*, 2010. **6**(3): p. 175-8.
58. Toksvang, L.N., et al., *Maintenance therapy for acute lymphoblastic leukemia: basic science and clinical translations*. *Leukemia*, 2022. **36**(7): p. 1749-1758.
59. Winick, N., et al., *Intensive oral methotrexate protects against lymphoid marrow relapse in childhood B-precursor acute lymphoblastic leukemia*. *J Clin Oncol*, 1996. **14**(10): p. 2803-11.
60. Salazar, J., et al., *Methotrexate consolidation treatment according to pharmacogenetics of MTHFR ameliorates event-free survival in childhood acute lymphoblastic leukaemia*. *Pharmacogenomics J*, 2012. **12**(5): p. 379-85.
61. Thorn, C.F., et al., *Doxorubicin pathways: pharmacodynamics and adverse effects*. *Pharmacogenet Genomics*, 2011. **21**(7): p. 440-6.
62. Martino, E., et al., *Vinca alkaloids and analogues as anti-cancer agents: Looking back, peering ahead*. *Bioorg Med Chem Lett*, 2018. **28**(17): p. 2816-2826.
63. Herradón, E., et al., *Cardiovascular Toxicity Induced by Chronic Vincristine Treatment*. *Front Pharmacol*, 2021. **12**: p. 692970.
64. van de Velde, M.E., et al., *Vincristine-induced peripheral neuropathy in children with cancer: A systematic review*. *Crit Rev Oncol Hematol*, 2017. **114**: p. 114-130.
65. Topp, M.S., et al., *Long-term follow-up of hematologic relapse-free survival in a phase 2 study of blinatumomab in patients with MRD in B-lineage ALL*. *Blood*, 2012. **120**(26): p. 5185-7.

66. Buie, L.W., et al., *Blinatumomab: A First-in-Class Bispecific T-Cell Engager for Precursor B-Cell Acute Lymphoblastic Leukemia*. *Ann Pharmacother*, 2015. **49**(9): p. 1057-67.
67. Sedykh, S.E., et al., *Bispecific antibodies: design, therapy, perspectives*. *Drug Des Devel Ther*, 2018. **12**: p. 195-208.
68. Wu, J., et al., *Blinatumomab: a bispecific T cell engager (BiTE) antibody against CD19/CD3 for refractory acute lymphoid leukemia*. *J Hematol Oncol*, 2015. **8**: p. 104.
69. Segal, D.M., G.J. Weiner, and L.M. Weiner, *Bispecific antibodies in cancer therapy*. *Curr Opin Immunol*, 1999. **11**(5): p. 558-62.
70. Miliotou, A.N. and L.C. Papadopoulou, *CAR T-cell Therapy: A New Era in Cancer Immunotherapy*. *Curr Pharm Biotechnol*, 2018. **19**(1): p. 5-18.
71. Curran, K.J., H.J. Pegram, and R.J. Brentjens, *Chimeric antigen receptors for T cell immunotherapy: current understanding and future directions*. *J Gene Med*, 2012. **14**(6): p. 405-15.
72. Singh, N., et al., *CAR T Cell Therapy in Acute Lymphoblastic Leukemia and Potential for Chronic Lymphocytic Leukemia*. *Curr Treat Options Oncol*, 2016. **17**(6): p. 28.
73. Shah, N.N. and T.J. Fry, *Mechanisms of resistance to CAR T cell therapy*. *Nat Rev Clin Oncol*, 2019. **16**(6): p. 372-385.
74. Xu, X., et al., *Mechanisms of Relapse After CD19 CAR T-Cell Therapy for Acute Lymphoblastic Leukemia and Its Prevention and Treatment Strategies*. *Front Immunol*, 2019. **10**: p. 2664.
75. Shang, Y. and F. Zhou, *Current Advances in Immunotherapy for Acute Leukemia: An Overview of Antibody, Chimeric Antigen Receptor, Immune Checkpoint, and Natural Killer*. *Front Oncol*, 2019. **9**: p. 917.
76. Kantarjian, H., et al., *Monoclonal antibody-based therapies: a new dawn in the treatment of acute lymphoblastic leukemia*. *J Clin Oncol*, 2012. **30**(31): p. 3876-83.
77. Ai, J. and A. Advani, *Current status of antibody therapy in ALL*. *Br J Haematol*, 2015. **168**(4): p. 471-80.
78. Tsui, C.K., et al., *CRISPR-Cas9 screens identify regulators of antibody-drug conjugate toxicity*. *Nat Chem Biol*, 2019. **15**(10): p. 949-958.
79. Maury, S., et al., *Rituximab in B-Lineage Adult Acute Lymphoblastic Leukemia*. *N Engl J Med*, 2016. **375**(11): p. 1044-53.
80. Salles, G., et al., *Rituximab in B-Cell Hematologic Malignancies: A Review of 20 Years of Clinical Experience*. *Adv Ther*, 2017. **34**(10): p. 2232-2273.
81. Feugier, P., *A review of rituximab, the first anti-CD20 monoclonal antibody used in the treatment of B non-Hodgkin's lymphomas*. *Future Oncol*, 2015. **11**(9): p. 1327-42.
82. DiJoseph, J.F., et al., *Antibody-targeted chemotherapy with CMC-544: a CD22-targeted immunoconjugate of calicheamicin for the treatment of B-lymphoid malignancies*. *Blood*, 2004. **103**(5): p. 1807-14.
83. Piccaluga, P.P., et al., *Surface antigens analysis reveals significant expression of candidate targets for immunotherapy in adult acute lymphoid leukemia*. *Leuk Lymphoma*, 2011. **52**(2): p. 325-7.
84. Inaba, H. and C.H. Pui, *Immunotherapy in pediatric acute lymphoblastic leukemia*. *Cancer Metastasis Rev*, 2019. **38**(4): p. 595-610.
85. Thorsson, V., et al., *The Immune Landscape of Cancer*. *Immunity*, 2018. **48**(4): p. 812-830.e14.
86. Bagchi, S., R. Yuan, and E.G. Engleman, *Immune Checkpoint Inhibitors for the Treatment of Cancer: Clinical Impact and Mechanisms of Response and Resistance*. *Annu Rev Pathol*, 2021. **16**: p. 223-249.
87. Iwai, Y., et al., *Involvement of PD-L1 on tumor cells in the escape from host immune system and tumor immunotherapy by PD-L1 blockade*. *Proc Natl Acad Sci U S A*, 2002. **99**(19): p. 12293-7.

88. He, X. and C. Xu, *Immune checkpoint signaling and cancer immunotherapy*. Cell Research, 2020. **30**(8): p. 660-669.
89. McGranahan, N., et al., *Allele-Specific HLA Loss and Immune Escape in Lung Cancer Evolution*. Cell, 2017. **171**(6): p. 1259-1271.e11.
90. Kaushik, I., et al., *The evolutionary legacy of immune checkpoint inhibitors*. Semin Cancer Biol, 2022.
91. Labani-Motlagh, A., M. Ashja-Mahdavi, and A. Loskog, *The Tumor Microenvironment: A Milieu Hindering and Obstructing Antitumor Immune Responses*. Front Immunol, 2020. **11**: p. 940.
92. Chen, L., et al., *FAP positive fibroblasts induce immune checkpoint blockade resistance in colorectal cancer via promoting immunosuppression*. Biochem Biophys Res Commun, 2017. **487**(1): p. 8-14.
93. Piali, L., et al., *Endothelial vascular cell adhesion molecule 1 expression is suppressed by melanoma and carcinoma*. J Exp Med, 1995. **181**(2): p. 811-6.
94. Zhao, Y., et al., *Fibroblast activation protein in the tumor microenvironment predicts outcomes of PD-1 blockade therapy in advanced non-small cell lung cancer*. J Cancer Res Clin Oncol, 2022.
95. Thommen, D.S., et al., *Progression of Lung Cancer Is Associated with Increased Dysfunction of T Cells Defined by Coexpression of Multiple Inhibitory Receptors*. Cancer Immunol Res, 2015. **3**(12): p. 1344-55.
96. Lamplugh, Z. and Y. Fan, *Vascular Microenvironment, Tumor Immunity and Immunotherapy*. Front Immunol, 2021. **12**: p. 811485.
97. Wherry, E.J., *T cell exhaustion*. Nat Immunol, 2011. **12**(6): p. 492-9.
98. Dolina, J.S., et al., *CD8(+) T Cell Exhaustion in Cancer*. Front Immunol, 2021. **12**: p. 715234.
99. Porsche, C.E., et al., *Obesity results in adipose tissue T cell exhaustion*. JCI Insight, 2021. **6**(8).
100. Minato, N., M. Hattori, and Y. Hamazaki, *Physiology and pathology of T-cell aging*. Int Immunol, 2020. **32**(4): p. 223-231.
101. Fedchenko, N. and J. Reifenrath, *Different approaches for interpretation and reporting of immunohistochemistry analysis results in the bone tissue - a review*. Diagn Pathol, 2014. **9**: p. 221.
102. Lehuédé, C., et al., *Adipocytes promote breast cancer resistance to chemotherapy, a process amplified by obesity: role of the major vault protein (MVP)*. Breast Cancer Res, 2019. **21**(1): p. 7.
103. Yang, J., et al., *Adipocytes promote ovarian cancer chemoresistance*. Scientific Reports, 2019. **9**(1): p. 13316.
104. Lengyel, E., et al., *Cancer as a Matter of Fat: The Crosstalk between Adipose Tissue and Tumors*. Trends Cancer, 2018. **4**(5): p. 374-384.
105. Wan, J., et al., *IL-9 and IL-9-producing cells in tumor immunity*. Cell Communication and Signaling, 2020. **18**(1): p. 50.
106. Tong, H., et al., *Identification of Interleukin-9 Producing Immune Cells in Endometrial Carcinoma and Establishment of a Prognostic Nomogram*. Front Immunol, 2020. **11**: p. 544248.
107. Demoulin, J.B. and J.C. Renaud, *Interleukin 9 and its receptor: an overview of structure and function*. Int Rev Immunol, 1998. **16**(3-4): p. 345-64.
108. Elyaman, W., et al., *IL-9 induces differentiation of TH17 cells and enhances function of FoxP3+ natural regulatory T cells*. Proc Natl Acad Sci U S A, 2009. **106**(31): p. 12885-90.
109. Lemoli, R.M., et al., *Interleukin-9 stimulates the proliferation of human myeloid leukemic cells*. Blood, 1996. **87**(9): p. 3852-9.
110. Lv, X., et al., *Interleukin-9 promotes cell survival and drug resistance in diffuse large B-cell lymphoma*. J Exp Clin Cancer Res, 2016. **35**(1): p. 106.
111. Sionov, R.V., S.A. Vlahopoulos, and Z. Granot, *Regulation of Bim in Health and Disease*. Oncotarget, 2015. **6**(27): p. 23058-134.

112. Wang, Y., et al., *Fat mass and obesity-associated protein (FTO) mediates signal transducer and activator of transcription 3 (STAT3)-driven resistance of breast cancer to doxorubicin*. *Bioengineered*, 2021. **12**(1): p. 1874-1889.
113. Kolb, R., F.S. Sutterwala, and W. Zhang, *Obesity and cancer: inflammation bridges the two*. *Curr Opin Pharmacol*, 2016. **29**: p. 77-89.
114. Avgerinos, K.I., et al., *Obesity and cancer risk: Emerging biological mechanisms and perspectives*. *Metabolism*, 2019. **92**: p. 121-135.
115. Liu, Q., et al., *The Impact of Obesity on the Outcomes of Adult Patients with Acute Lymphoblastic Leukemia - A Single Center Retrospective Study*. *Blood Lymphat Cancer*, 2021. **11**: p. 1-9.
116. Butturini, A.M., et al., *Obesity and outcome in pediatric acute lymphoblastic leukemia*. *J Clin Oncol*, 2007. **25**(15): p. 2063-9.
117. Eissa, H.M., et al., *The effect of body mass index at diagnosis on clinical outcome in children with newly diagnosed acute lymphoblastic leukemia*. *Blood Cancer J*, 2017. **7**(2): p. e531.
118. Goswami, R. and M.H. Kaplan, *A brief history of IL-9*. *J Immunol*, 2011. **186**(6): p. 3283-8.
119. Lei, R.E., et al., *IL-9 promotes proliferation and metastasis of hepatocellular cancer cells by activating JAK2/STAT3 pathway*. *Int J Clin Exp Pathol*, 2017. **10**(7): p. 7940-7946.
120. Dyson, N., *The regulation of E2F by pRB-family proteins*. *Genes Dev*, 1998. **12**(15): p. 2245-62.
121. Meng, P. and R. Ghosh, *Transcription addiction: can we garner the Yin and Yang functions of E2F1 for cancer therapy?* *Cell Death Dis*, 2014. **5**(8): p. e1360.
122. Vaysse, C., C. Muller, and F. Fallone, *Obesity: an heavyweight player in breast cancer's chemoresistance*. *Oncotarget*, 2019. **10**(35): p. 3207-3208.
123. Bouleftour, W., et al., *Obesity and chemotherapy administration: between empiric and mathematic method review*. *Acta Oncologica*, 2019. **58**(6): p. 880-887.
124. Muller, C., *Tumour-surrounding adipocytes are active players in breast cancer progression*. *Ann Endocrinol (Paris)*, 2013. **74**(2): p. 108-10.
125. Sheng, X., et al., *Adipocytes cause leukemia cell resistance to daunorubicin via oxidative stress response*. *Oncotarget*, 2016. **7**(45): p. 73147-73159.
126. Sheng, X., et al., *Adipocytes Sequester and Metabolize the Chemotherapeutic Daunorubicin*. *Mol Cancer Res*, 2017. **15**(12): p. 1704-1713.
127. Samimi, A., et al., *Role of bone marrow adipocytes in leukemia and chemotherapy challenges*. *Cell Mol Life Sci*, 2019. **76**(13): p. 2489-2497.
128. Ehsanipour, E.A., et al., *Adipocytes cause leukemia cell resistance to L-asparaginase via release of glutamine*. *Cancer Res*, 2013. **73**(10): p. 2998-3006.
129. Tucci, J., et al., *Adipocytes Provide Fatty Acids to Acute Lymphoblastic Leukemia Cells*. *Front Oncol*, 2021. **11**: p. 665763.
130. Abrams, M.T., et al., *Inhibition of glucocorticoid-induced apoptosis by targeting the major splice variants of BIM mRNA with small interfering RNA and short hairpin RNA*. *J Biol Chem*, 2004. **279**(53): p. 55809-17.
131. Imai, K. and H. Akiyama, *[Acute lymphoblastic leukemia (ALL)]*. *Gan To Kagaku Ryoho*, 2007. **34**(13): p. 2180-4.
132. Smith, M.A., et al., *Outcomes for children and adolescents with cancer: challenges for the twenty-first century*. *J Clin Oncol*, 2010. **28**(15): p. 2625-34.
133. Al-Mahayri, Z.N., M.M. AlAhmad, and B.R. Ali, *Long-Term Effects of Pediatric Acute Lymphoblastic Leukemia Chemotherapy: Can Recent Findings Inform Old Strategies?* *Front Oncol*, 2021. **11**: p. 710163.
134. Silverman, L.B., *Balancing cure and long-term risks in acute lymphoblastic leukemia*. *Hematology Am Soc Hematol Educ Program*, 2014. **2014**(1): p. 190-7.

135. Antoniu, S.A., *MEDI-528, an anti-IL-9 humanized antibody for the treatment of asthma*. *Curr Opin Mol Ther*, 2010. **12**(2): p. 233-9.